
TECHNISCHE UNIVERSITÄT MÜNCHEN

Fachgebiet Forstgenetik

Analysis of protein abundances in
Fagus sylvatica L. and *Cenococcum geophilum* Fr.
following biotic and abiotic stresses

René C. Kerner

Vollständiger Abdruck der vom Wissenschaftszentrum Weihenstephan für Ernährung, Landnutzung und Umwelt der Technischen Universität München zur Erlangung des akademischen Grades eines Doktors der Naturwissenschaften (Dr. rer. nat.) genehmigten Dissertation.

Vorsitzender: Univ. Prof. Dr. B. Küster

Prüfer der Dissertation:

1. Univ. Prof. Dr. G. Müller-Starck (i.R.)
2. Univ. Prof. Dr. R. Matyssek

Die Dissertation wurde am 21.09.2011 bei der Technischen Universität München eingereicht und durch die Fakultät Wissenschaftszentrum Weihenstephan für Ernährung, Landnutzung und Umwelt am 17.01.2012 angenommen.

*This thesis is dedicated to my parents and my sister,
for all the advice and
love they have given me over the years.*

Erklärung

Ich erkläre an Eides statt, dass ich die der Fakultät für Ernährung, Landnutzung und Umwelt der Technischen Universität München zur Promotionsprüfung vorgelegte Arbeit mit dem Titel:

Analysis of protein abundances in
Fagus sylvatica L. and *Cenococcum geophilum* Fr.
following biotic and abiotic stresses

in Weihenstephan am Fachgebiet Forstgenetik, unter der Anleitung und Betreuung durch Univ. Prof. Dr. Gerhard Müller-Starck ohne sonstige Hilfe erstellt und bei der Abfassung nur die gemäß § 6 Abs. 5 angegebenen Hilfsmittel benutzt habe.

Ich habe die Dissertation in dieser oder ähnlicher Form in keinem anderen Prüfungsverfahren als Prüfungsleistung vorgelegt.

Die Fakultät für Ernährung, Landnutzung und Umwelt hat der Vorveröffentlichung Teile der Dissertation zugestimmt.

Ich habe den angestrebten Doktorgrad noch nicht erworben und bin nicht in einem früheren Promotionsverfahren für den angestrebten Doktorgrad endgültig gescheitert.

Die Promotionsordnung der Technischen Universität München ist mir bekannt.

München, den 21.09.2011

René Kerner

Content

ACKNOWLEDGMENT	6
LIST OF PUBLICATIONS	7
SUMMARY	8
COMMON ABBREVIATIONS	11
1 INTRODUCTION	13
1.1 THE IMPORTANCE OF <i>FAGUS SYLVATICA</i> L.	14
1.2 THE IMPORTANCE OF <i>CENOCOCCUM GEOPHILUM</i> FR.	15
1.3 ABIOTIC AND BIOTIC STRESSORS IN PLANTS	16
1.3.1 OZONE	16
1.3.2 ELEVATED CO ₂	19
1.3.3 <i>PHYTOPHTHORA PLURIVORA</i> SP. NOV.	21
1.3.4 PLANT DEFENSE STRATEGIES AGAINST PATHOGENS	23
1.4 DROUGHT AS AN ABIOTIC STRESSOR FOR <i>C. GEOPHILUM</i>	24
1.5 PROTEOMICS AS A TOOL TO MONITOR MOLECULAR CHANGES	26
1.6 SPECIFIC OBJECTIVES OF THE PRESENT WORK	29
2 MATERIAL AND METHODS	31
2.1 EUROPEAN BEECH UNDER THE INFLUENCE OF ABIOTIC AND BIOTIC STRESS	32
2.1.1 EXPOSURE TO FREE AIR OZONE FUMIGATION AND INOCULATION WITH <i>P. PLURIVORA</i>	32
2.1.2 EXPOSURE TO ELEVATED CO ₂ AND FURTHER INFESTATION WITH <i>P. PLURIVORA</i>	34
2.2 <i>C. GEOPHILUM</i> EXPOSED TO WATER DEPRIVATION	37
2.3 PROTEOMIC ANALYSES	40
2.3.1 IMPROVEMENT OF THE 2-DE PROTOCOL	40
2.3.2 2-D DIGE EXPERIMENTAL DESIGN	42
2.3.3 RELATIVE MASS SPECTROMETRY	47

3	RESULTS AND DISCUSSION	49
3.1	IMPROVEMENT OF THE 2-D ELECTROPHORESIS PROTOCOL	50
3.2	LEAF INJURY AND PROTEOMIC CHANGES IN JUVENILE EUROPEAN BEECH FOLLOWING THREE YEAR EXPOSURE TO FREE-AIR ELEVATED OZONE AND INOCULATION WITH THE ROOT PATHOGEN <i>P. PLURIVORA</i>	57
3.2.1	VISUAL OZONE DAMAGE IN LEAVES	57
3.2.2	OZONE RESPONSIVE PROTEINS DETECTED BY 2-D DIGE IN JUVENILE BEECH TREES AROUND THE LYSIMETERS	59
3.2.3	JUVENILE BEECH TREES FUMIGATED WITH FREE-AIR ELEVATED OZONE AND POST INFECTED WITH THE ROOT PATHOGEN <i>P. PLURIVORA</i>	78
3.3	CHANGES IN THE PROTEOME OF BEECH SAPLINGS UPON PATHOGEN INOCULATION AND ELEVATED CO₂ CONCENTRATIONS	80
3.4	<i>C. GEOPHILUM</i> FACING DROUGHT STRESS	84
4	CONCLUSIONS AND OUTLOOK	90
4.1	OPTIMIZATION OF THE PROTEIN SEPARATION PROTOCOL	91
4.2	EXPOSURE TO FREE-AIR OZONE FUMIGATION AND INOCULATION WITH <i>P. PLURIVORA</i>	92
4.3	EXPOSURE TO ELEVATED CO₂ CONCENTRATIONS AND INOCULATION WITH <i>P. PLURIVORA</i>	93
4.4	<i>C. GEOPHILUM</i> FACING DROUGHT STRESS	94
4.5	OUTLOOK	95
5	REFERENCES	97
6	APPENDIX	111

Acknowledgment

I would sincerely like to thank all those people who made this thesis possible and who guide me and helped me from the initial to the final stage of my work. Without their support and encouragement, this thesis would not have been possible.

I owe my deepest gratitude to my supervisor Prof. Gerhard Müller-Starck and Dr. habil Dieter Ernst who gave me the opportunity to carry out the exciting and challenging work presented in this thesis. Their encouragement, guidance, support and patience throughout my research definitively enabled me to evolve as a scientist and as a person. I am sincerely thankful to Dr. Karin Pritsch for giving me the opportunity to work within the EU-funded Network of Excellence, for all her understanding, critical suggestions on my work and for being an important motivator. I would like to thank Prof. Rainer Matyssek for his acceptance as second supervisor and Prof. Bernhard Küster for his acceptance as chairman of my thesis.

I am grateful to Edgar Delgado-Eckert who inspired, encouraged and helped me with his mathematical knowledge. His statistical help and critical comments have indeed enhanced the quality of my thesis. I wish to express my gratitude to Holger Paetsch for offering his help at any time. Special thanks to Sarah Sturm for her excellent technical assistance and being extremely helpful in the second part of my thesis. We were a great team Sarah! I would like to thank my present and past colleagues from the Helmholtz Zentrum, specially Christian Lindermayr, Maren Jürgensen, Andreas Fröhlich, Christian Holzmeister and Laura Arango, who gave me good advice on proteomics and other molecular fields. They helped me with any problems I had and made me feel very welcome and well integrated at the Helmholtz Zentrum. Thanks to William Dupuy and Estela del Castillo for building the right foundation concerning the mass spectrometric approach.

Many thanks to my parents and my sister Cordula for all their love and making me believe in my potential. Lastly, I would like to thank all my friends, for being an important part of my life and for cheering me up during the course of my work.

List of publications

Abril N, Gion JM, **Kerner R**, Müller-Starck G, Cerrillo RMN, Plomion C, Renaut J, Valledor L and Jorrin-Novo JV (2011). "Proteomics research on forest trees, the most recalcitrant and orphan plant species". Phytochemistry **72**(10): 1219-1242.

Kerner R, Delgado-Eckert E, Del Castillo E, Peter M, Müller-Starck G and Pritsch K. "Proteome analysis of water deprived *Cenococcum geophilum* cultures". Paper in preparation.

Kerner R, Delgado E, Dupuy J, Winkler JB, Grams T, Jürgensen M, Lindermayr C, Ernst D and Müller-Starck G. "Responses of European beech saplings following four vegetation periods of ozone exposure: an integrative study". Paper in preparation.

Kerner R, Winkler J, Dupuy J, Jürgensen M, Lindermayr C, Ernst D and Müller-Starck G (2011). "Changes in the proteome of juvenile European beech following three years exposure to free-air elevated ozone". iForest - Biogeosciences and Forestry **4**(1): 69-76.

Summary

The initial focus of this thesis was the optimization of a protein separation procedure for leaves of *Fagus sylvatica* L. (European beech), a highly recalcitrant plant material for two-dimensional gel electrophoresis (2-DE). Based on the previous protein separation protocols of Vâlcu et al. (2006a, b) different parameters were changed in order to achieve the best spot resolution possible. Performing isoelectric focusing with rehydration loading instead of cuploading, and using lower starting voltages and prolonged separation times significantly meliorate the quality of separated proteins on the 2-D gel. Another step in optimizing the 2-DE protocol was to preclude errors resulting from technical variability, an obstacle that must be overcome in order to reliably determine quantitative changes in protein abundances. By using technical triplicates it was possible to select protein spots with low variation. In addition, six different types of statistical normalization methods were used to improve the accuracy and reliability of significantly different proteins for the following comparative analyses.

Using this optimized protocol, the main focus of this study was the quantitative analysis of differentially protein abundances of European beech after long-term treatment with elevated ozone and CO₂ concentrations. For this purpose, sublethal fumigation doses of two-fold ambient concentrations were applied, which can be expected in the near future as a consequence of antropogenic activity and climate change. Depending on the treatment, beech trees from different ontogenic scales were investigated under exposure chambers or under field conditions at the lysimeter free-air fumigation site from the Helmholtz Zentrum München. Moreover, following abiotic treatment, beech trees were inoculated with the root pathogen *Phytophthora plurivora* in order to examine pathogen-induced responses under both ambient and twice-ambient ozone/CO₂ exposure.

Under elevated ozone exposure, juvenile beech trees clearly demonstrate a differential response of proteins. In contrast, 43 days after re-shifting beech trees to control conditions, beech leaves showed only one spot to be significantly different. Some of the identified proteins have been previously described in the context of short-term ozone responses in plants. These findings indicate the congruence, at least for certain cellular functions, of plant reactions following short-

and long-term ozone exposure. In particular, a large number of identified proteins involved in the Calvin cycle and photosynthesis were down-regulated. In contrast, proteins from the mitochondrial electron transport, carbon metabolism/catabolism, stress/defense response, and some enzymes associated with the detoxification system were up-regulated. Furthermore, the present proteomic time line analyses have been linked to responses at the transcript, metabolite and morphological level previously reported for the same experimental setup. Results from the global comparison revealed that molecular events took place in the harvested tissue well before visible symptoms were manifested. These results indicate that first generated molecular responses aimed to counteract deleterious effect of sublethal ozone concentrations. Later, when plant cells were not capable of supporting cell integrity, a hypersensitive response was likely induced to prevent the spread of leaf lesions, which then manifested visually as brownish patches on the leaves. In contrast to the ozone analysis, *P. plurivora* showed no statistically significant differences in beech leaves, possibly because the low number of biological replicates used specifically for this study masked the effect of the treatment.

Beech saplings exposed under elevated CO₂ exhibited 11 differentially abundant proteins. These results demonstrated a clear down-regulation of two isoforms of the RuBisCO protein, most likely indicating the acclimation of beech leaves to elevated CO₂. Furthermore it is presumed that the enzymes putative lactoylglutathione lyase, putative minor allergen Alt a, chloroplastic protein ycf2, and cysteine synthase were up-regulated under the condition of elevated CO₂. The last named enzyme indicates enhanced biosynthesis of cysteine as a consequence of reduced plant N content, which is a prominent response in plants grown under elevated CO₂. Furthermore, beech saplings inoculated with the root pathogen *P. plurivora* showed increasing abundance levels of two protein spots. Despite this fact, it was not possible to detect those proteins by mass spectrometry.

Finally, a relative mass spectrometry approach was carried out to identify proteomic signatures in water deprived *Cenococcum geophilum* isolates, as it represents an important element of forest ecosystems and it is generally considered to better protect plants from drought stress than other mycorrhizal fungi. The results indicate that 9 proteins related to stress response and tolerance, carbon metabolism and the transport and signaling machinery showed statistically significant differences compared to the controls. Interestingly, the activated LEA (late embryogenesis abundant) domain containing protein has been identified in different tolerant plant species

growing under the effect of drought stress. Thus, one of the main questions arising here was whether or not *C. geophilum* expressing this protein could have an effect on the drought tolerance of its symbiotic partner. Furthermore, these results uncovered evidence that differentially abundant proteins were involved in repair and defense reactions commonly induced by multiple stresses such as reactive oxygen species. Overall, the predominance of regulated proteins related to stress response, as well as transport and signaling machinery reflect the importance of cells in dealing with both osmotic control and increased levels of damaging compounds such as reactive oxygen species for adaptation and survival to drought stress.

Common abbreviations

2-D DIGE	two dimensional fluorescence difference gel electrophoresis
2-D	two dimension
2-DE	two dimensional gel electrophoresis
2ME	2-mercaptoethanol
ABA	abscisic acid
ACN	acetonitrile
ADK	adenosine kinase
ANOVA	analysis of variance
ATP	adenosine triphosphate
BSA	bovine serum albumin
CBB	coomassie brilliant blue
DMF	N,N-dimethylformamide
DTT	dithiothreitol
ECM	ectomycorrhiza
EPA	environmental protection agency
ESI	electro spray ionization
ESTs	expressed sequence tags
ET	ethylene
ETI	effector triggered immunity
FA	formic acid
FACE	free-air CO ₂ enrichment
FDR	false discovery rate
GA	gibberellic
GS	glutamine synthetase
GSH	glutathione
H ₂ O ₂	hydrogen peroxide
ICAT	isotope coded affinity tag
IEF	isoelectric focusing
iTRAQ	isobaric tags of relative and absolute quantification
ITS	internal transcribed spacer
JA	jasmonic acid
LC-MS/MS	liquid chromatographic- tandem mass spectrometry
m/z	mass-to-charge
MALDI	matrix assisted laser desorption
MAPK	mitogen-activated protein kinase
MS	mass spectrometry
MS/MS	tandem mass spectrometry

NADP	nicotinamide adenine dinucleotide phosphate
NASF	normalized spectral abundance factor
NO _x	nitrogen oxides
O ₂ • ⁻	superoxide radicals
n.s.	not specified
OG	octyl-β-D-glucopyranoside
OH• ⁻	hydroxyl radical
PAMP	pathogen-associated molecular patterns
PAO	polyamine oxidase
PC	polycarbonate
PCR	polymerase chain reaction
PHGDH	D-3-phosphoglycerate dehydrogenase
PK	pyruvate kinase
PMF	peptide mass fingerprinting
POD	peroxidase
PPO	polyphenoloxidase
PR	pathogenesis related
PTMs	posttranslational modifications
PVPP	polyvinyl polypyrrolidone
R proteins	resistance proteins
RGR	relative growth rate
RIPs	ribosome inactivating proteins
ROS	reactive oxygen species
RuBisCO	ribulose-1,5-bisphosphate carboxylase/oxygenase
SA	salicylic acid
SAM	S-adenosyl-methionine
SBP1	selenium-binding protein 1
SD	standard deviation
SDS-PAGE	sodium dodecyl sulfate polyacrylamide gel electrophoresis
SILAC	stable isotope labeling in cell culture
TCA	trichloroacetic acid
TEMED	N,N,N',N'-tetramethylethylenediamine
TMT	tandem mass tag
VOCs	volatile organic compound

1 Introduction

- 1.1 The importance of *Fagus sylvatica* L.
- 1.2 The importance of *Cenococcum geophilum* Fr.
- 1.3 Abiotic and biotic stressors in plants
 - 1.3.1 Ozone
 - 1.3.2 Elevated CO₂
 - 1.3.3 *Phytophthora plurivora* sp. nov.
 - 1.3.4 Plant defense strategies against pathogens
- 1.4 Drought as an abiotic stressor for *C. geophilum*
- 1.5 Proteomics as a tool to monitor molecular changes
- 1.6 Specific objectives of the present work

1.1 The importance of *Fagus sylvatica* L.

Fagus sylvatica (European beech) is one of the eleven species of deciduous trees belonging to the genus *Fagus*. It has naturally expanded throughout Europe during the last postglacial era about 10.000 years ago. Today it covers a broad ecological spectrum of site conditions in regard to climate, soil type and soil pH (Ellenberg et al. 1988; Ellenberg 1996; Leuschner et al. 2006). Thereby European beech is an essential element of forest ecosystems in central, eastern and the southeastern Europe, ranging from the temperate to warm-temperate climates (Kramer 1988).

Morphologically, European beech is characterized by their alternate, simple, toothed leaves and by having a smooth, grey bark. Usually they reach heights of about 25-35 m and 1.5 m trunk diameter. It has a typical lifespan of 150 to 200 years and is associated with ectomycorrhizal (ECM) fungi as symbiont partner. After approximately 30 years it begins to flower with monoecious (male and female) units by building small catkins, which appear shortly after the leaves in spring. The seeds are small triangular nuts maturing in the autumn five to six months after pollination. Mast production is irregularly among years. Quantities are particularly abundant in years following warm temperatures and low precipitation during the summer.

In forest systems, European beech has been replaced in past decades by Norway spruce, which has higher growth performance and yields 40% more biomass compared to European beech (Rössler et al. 2006). Today it is being re-introduced in mixed forest plantations in order to overcome the problems and risks of monocultures (Dittmar et al. 2003). Its economical role has been recognized and there has been increased attempts to enlarge its population (Dertz 1996). European beech is mainly used in USA, Europe and New Zealand as ornamental trees in parks and large gardens. The wood of European beech is especially used as firewood due to its relatively high energy content. Furthermore, the wood material is very important in the furniture industry for flooring and staircase construction.

Several studies have also focused on beech trees at the molecular level. Genetic variability has been well studied with isoenzymes and molecular markers (Müller-Starck et al. 1992; Müller-Starck et al. 1993; Sander et al. 2000). It is documented that the genetic variation within populations is higher than differentiation among populations (Borghetti et al. 1993; Wolf et al. 1996). So far, very little is known about the proteome of European beech. According to the

literature, only four studies were published in these fields, two of them presenting significant methodological work (Vâlcu et al. 2006a, b). The same authors in 2009 reported defense responses of beech seedlings elicited by infection with the root pathogen *Phytophthora plurivora* and root or leaf wounding using 2-DE followed by mass spectrometric identification of proteins (Vâlcu et al. 2009). Pawlowski (2007) analyzed mechanisms of dormancy breaking in beech seeds and the role of abscisic and gibberellic acid (ABA and GA) in this process.

1.2 The importance of *Cenococcum geophilum* Fr.

Cenococcum geophilum Fr. is the most widespread ectomycorrhizal fungus within the phylum *Ascomycota* (Horton et al. 2001). This species lives in symbiotic interaction with an extraordinary large variety of autotrophic partners (Molina et al. 1982). Trappe (1964) reported its association to 150 species within 40 different plant genera. It can be found growing in different pH ranges, moisture contents and climate conditions. As such it is able to colonize wide habitats, ranging within the arctic, temperate and subtropical environment (Trappe 1964). As a cosmopolitan fungus, *C. geophilum* is best known for its unambiguously black tip, and beaded surface. The beads are large and pronounced, like a blackberry. Its hyphae are wiry and black, very thick and they visibly project in all directions (InvestigadoresACG 2011). Its sterile mycelium lacks sexual or asexual spores, thus its reproduction undergoes cleaving and transport of sclerotia or fragmentation of hyphae (LoBuglio et al. 1996). Despite the process previously termed as Muller's Ratchet, which described the relentless decay of genome information encountered by asexual populations, worldwide surveys of *C. geophilum* isolates revealed an unexpected high genetic diversity for an asexual fungus (LoBuglio et al. 1991; Shinohara et al. 1999; Chen et al. 2007). Jany et al. (2002) suggest occurrence of a high rate of mitotic or meiotic recombination and an effect of stand features on population structure.

Mycorrhizae are probably the most common symbiotic relationship between fungi and higher plants. They are well known to improve plants access to soil water and nutrients, tolerance to environmental extremes such as drought stress. Specifically *C. geophilum* is generally considered to be more resilient to drought stress than other ECM fungi (Mexal et al. 1973; Coleman et al. 1989). However, despite the overall beneficial effect of the symbiosis between this fungus and

their autotrophic hosts, its role in various mechanisms such as drought resistance is poorly understood.

1.3 Abiotic and biotic stressors in plants

1.3.1 Ozone

Tropospheric ozone is an indirectly emitted gas formed by the reaction of sunlight with mostly anthropogenic caused air pollutants such as nitrogen oxides (NO_x), hydrocarbons, volatile organic compound (VOCs) and, to a lesser but still significant extent, methane and carbon monoxide. Fig. 1 illustrates the formation of ozone based on NO_x and VOCs.

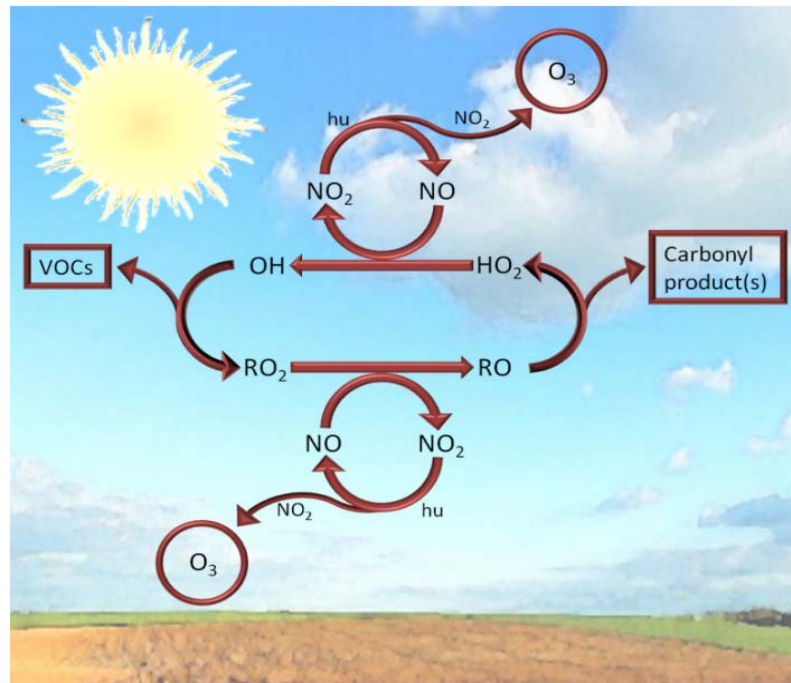


Fig. 1 - Schematic representation of the tropospheric ozone formation in the presence of volatile organic compounds (VOCs) and nitrogen oxides (NO_x). Modified after Jenkin and Hayman (1999).

Ozone plays a critically important role in the stratosphere, which benefits us as humans, but the formation of ozone closer to earth has multiple adverse effects. In the lower atmosphere, high concentrations are toxic and have harmful effect on humans, animals and plants. The U.S. Environmental Protection Agency (EPA) has identified ozone as the most difficult air pollutant to control. Ozone chemistry is complex, making it difficult to quantify ozone's contributions to poor local air quality (NASA 2004). Changes in the ozone concentration are mainly due to anthropogenic pollutants such as biomass and fossil fuel burning, which have resulted in large increases in ground level ozone concentrations over the last 100 years (Hough et al. 1990; Marengo et al. 1994).

Due to the powerful oxidizing properties, and consequently its capability of damaging organic molecules, ozone has been well known to be detrimental for plants. Type and severity of damage/reaction can vary depending on concentration, weather conditions, length of exposure, age and genetic predisposition of plants.

In leaves, ozone enters through the stomata into apoplast spaces, where it decomposes rapidly in the presence of water. Its destruction is followed by the formation of superoxide radicals ($O_2^{\bullet-}$), hydrogen peroxide (H_2O_2) and hydroxyl radical (OH^{\bullet}), which consequently triggers a cellular oxidative burst (Laisk et al. 1989; Pell et al. 1997), thus generating a signal cascade within plant cells. Although the mechanism of reactive oxygen species (ROS) production is not well understood, four main enzymatic sources have been proposed: (i) activation of NAD(P)H oxidase and cell wall peroxidase (PODs), (ii) induction of extracellular pH-dependent polyamine oxidase (PAO), (iii) expression of oxalate oxidase and/or (iv) diamine and polyamine oxidases (Langebartels et al. 2002).

The increase of apoplastic ROS concentrations over a threshold limit induces changes in the guard cells, thereby a secondary endogenous ROS accumulation and activation of mitogen-activated protein kinase (MAPK) is propagated (Kangasjärvi et al. 2005). MAPK activation, in turn, seems to be involved in the up-regulation of the synthesis of ethylene (ET) which, together with salicylic acid (SA), is needed to induce ozone related lesions. In contrast to this mechanism jasmonic acid (JA) acts antagonistically to contain the spread of cell death (Overmyer et al. 2000; Castagna et al. 2009). Depending on the fine tuning of those counteracting compounds, plants will induce cell death or defense signals.

Plants use enzymatic components and low molecular weight antioxidants in order to detoxify cells from ozone or any of its derivatives (Kangasjärvi et al. 1994; Langebartels et al. 2002). A few examples of enzymatic antioxidants are superoxide dismutase, catalase and peroxidase, all of which are catalyzers of reactions that eliminate ROS. Low molecular antioxidants such as ascorbic acid, tocoferol and thiol (SH) compounds interact with radicals and peroxides to form weak reactive products (Roshchina et al. 2003). In addition to antioxidants, plants may induce pathogenesis related (PR) proteins as a consequence of the hypersensitive response and the systemic acquired resistance. Recently it was shown, at the transcript level, that several expressed sequence tags (ESTs) related to cell structure, stress response and cell walls, signal transduction, as well as disease and defense were induced in beech upon ozone fumigation (Olbrich et al. 2009).

Of the above-mentioned responses, the most affected pathways during elevated ozone are: the xanthophyll cycle and β -carotenethe, the phenylpropanoid metabolism and oxidation-reduction of ascorbate in the apoplast and symplast. Furthermore elevated ozone have been shown to decrease gas exchange (Kronfuß et al. 1998) and to inhibit carboxylation efficiency and net photosynthesis (Dizengremel 2001; Agrawal et al. 2002; Bohler et al. 2007; Ryang et al. 2009). Different studies have also shown an induction of glucose catabolism, dark respiration, as well as activation of detoxification and repair processes (Bohler et al. 2007; He et al. 2007).

Much research has been done on proteomics in plants (Jorrín-Novo et al. 2009), however, there is still very little information available in terms of proteomic analysis after long-term exposure to ozone under controlled conditions, and even less information on woody plants in the field under similar conditions.

1.3.2 Elevated CO₂

Although carbon dioxide (CO₂) levels are relatively constant over the past 6500 centuries (180-300 ppm), sharp increases in CO₂ are being observed since the beginning of industrialization (Solomon et al. 2007). Due to the anthropogenic activities, including the burning of fossil fuels and deforestation, present (March, 2011) global atmospheric CO₂ levels are reaching concentrations of 391.55 ppm (Conway et al. 2011) and are expected to surpass 550 ppm by the middle of this century (Prentice 2001).

Increased levels of CO₂ will have substantial direct and indirect effects on the biosphere. Changes in CO₂ concentration will represent an upsurge of an essential resource for plants. It has sometimes been argued that plants may have the capacity to sequester much of the increased CO₂ in the atmosphere. This effect is known as “CO₂ fertilization” because, in the envisioned scenario, higher ambient CO₂ concentrations in the atmosphere literally “fertilize” plant growth (Schmidt et al. 2004). However, it is important to note that the effects of elevated CO₂ are much more than increasing plant-available carbon. It is also a longwave-radiation trapping gas, with consequences for surface temperature and precipitation, climatic variables that in turn affect plant ecology. For instance, rising CO₂ levels have caused an increase of globally averaged surface temperatures, thus causing shifts in precipitation patterns around the world (Levin et al. 2009; IPCC 2011). Therefore, rising temperatures and changes in precipitation will have a strong ecological pressure on plant community composition (Langley et al. 2010). In some areas, elevated CO₂ and their indirect effects will shift species composition, thus reducing biodiversity (Smith et al. 2000). Although elevated CO₂ alone tend to increase plant productivity, indirect effects such as predicted warmer temperatures should be taken into account in order to determine net primary production and crop productivity.

One of the most consistent effects of plants grown under elevated CO₂ is the reduction of stomatal conductance followed by a decline in transpiration (Wullschleger et al. 2002; Ainsworth et al. 2007). Despite this decrease, a higher photosynthetic CO₂ uptake was observed in different species (Garcia et al. 1998; Leakey et al. 2004; James I.L. et al. 2007). This increase is associated with the fact that CO₂ is a limiting factor for all plant species with a C₃ pathway of CO₂ assimilation. Higher CO₂ concentrations enables the enzyme ribulose-1,5-bisphosphat-carboxylase/-oxygenase

(RuBisCO) to carboxylate more CO₂ molecules, thus resulting in depletion of photorespiration (Ziska et al. 2007). As a consequence, plants may experience a higher relative growth rate (RGR), biomass and yield production (Kimball 1982; Lambers et al. 1998). Previous reports demonstrated that plants grown under elevated CO₂ had increased leaf area and leaf thickness (Bowes 1993; Bray et al. 2002), which is partly related to the accumulation of non-structural carbohydrates (Lambers et al. 1998). However, rapid growth alters the plant ontogenetic stages, which ultimately lead to accelerated leaf senescence (Heineke et al. 1999). In some cases it was shown that the accelerated growth may not be uniformly distributed throughout the plants (Norby 1994; Jongen et al. 1995; Kimball et al. 2002).

Acclimation of plants after long-term CO₂ exposure has been observed in different studies. Those mechanism can be accompanied by the general depletion of RuBisCO activity, decreased photosynthesis and adjustment of carbohydrate (Singh 2009). Nevertheless, long-term CO₂ exposure using modern free-air CO₂ enrichment (FACE) technique showed a stimulation of photosynthetic carbon gain and net primary production despite down regulation of the RuBisCO activity (Leahey et al. 2009).

Another general response of plants to elevated CO₂ is the reduction of N content (Curtis et al. 1998; Norby et al. 1999; Taub et al. 2008). Although the mechanism responsible for this reduction is not completely understood, it is believed that a dilution of N in plant tissues and decreases in root specific uptake are the predominant mechanisms by which elevated CO₂ affects N limitation in plants (Taub et al. 2008). Further variations in plants responses upon exposure to elevated CO₂ concerns dark respiration, which is elevated in some species while in others decreased (Poorter et al. 1997; Wang et al. 2001). Elevated CO₂ may also affect the hormone status by altering the regulation of ACC oxidase and ethylene, which in turn can affect the plant developmental stage (Sisler et al. 1988; Smith et al. 1993).

Although a large number of studies to date have been dedicated to the effects of elevated CO₂ on plants, the associated responses of proteins have been reported only in two proteomic approaches (Bae et al. 2004; Graham 2008).

1.3.3 *Phytophthora plurivora* sp. nov.

The species *Phytophthora plurivora*, is a cosmopolitan hemibiotrophic root pathogen that was first described by Sawada in 1927 when it was isolated from orange trees (Bunny 1996). This species causes disease on a wide variety of plants. Especially for European beech, *P. plurivora* has been reported to be a particular aggressive root pathogen, which affects the root system as well as trunk cortex (Werres 1995; Jung 2004). The life cycle of *Phytophthora* species equips them to build up infective units very rapidly in the soil when conditions favor infection and to subsist in long-term survival structures when conditions prevent infections. Propagules important for their dispersal include mycelia (vegetative structures), the asexual chlamidospore, sporangia and zoospore, and the sexual oospore. Using sexual and asexual reproductive structures, they are able to use both r and K selected strategies to maximize their survival. r strategies are represented by the production of high quantities of short live sporangia and zoospores while K strategies entail the production of fewer, but longer surviving oospores. The life cycle of *P. plurivora* is shown in Fig. 2. Zoospores are the most important propagules involved in the infection of its host. Damp earth and water stress are factors predisposing zoospore release and therefore infection of the host (Bunny 1996; Jung 2004). The infection itself takes place in the root crown and lower trunk. As the infection develops, *Phytophthora* cankers are usually produced at or below ground level, but can found higher up if wounding has occurred (Dreistadt 2008). The lesion infects the inner bark and outer layer of wood, killing cambium and phloem (Dreistadt 2008).

Within the oomycetes group of pathogens, most molecular research has been made on *Phytophthora* species. Few studies, however, have evaluated molecular and physiological reactions of woody plants upon infection with the hemibiotrophic root pathogen *P. plurivora*. Fleischmann et al. (2002) demonstrated that beech saplings were severely affected after inoculation with *P. plurivora* and *P. cambivora*. A few days after inoculation, photosynthesis and transpiration were strongly reduced and 60% of the root system was destroyed compared to the controls. Similar results were observed using proteomics after inoculation of beech seedlings with the root pathogen *P. plurivora* (Vâlcu et al. 2009). Here root tip necroses were observed after 4-6 days. The infection resulted in weakened rhizosphere activity and nutrient uptake, which was accompanied by a severe reduction of photosynthesis and transpiration. Plants were also shown to suffer from severe drought and displayed symptoms of oxidative stress. Schlink (2010) showed

a massive shift in gene expression patterns after beech saplings were inoculated with *P. plurivora*. Reactions consisted of down-regulation of SA responsive genes in roots and leaves while some JA responsive genes showed a very late up-regulation only in leaves, probably caused by the desiccation shortly before plant death.

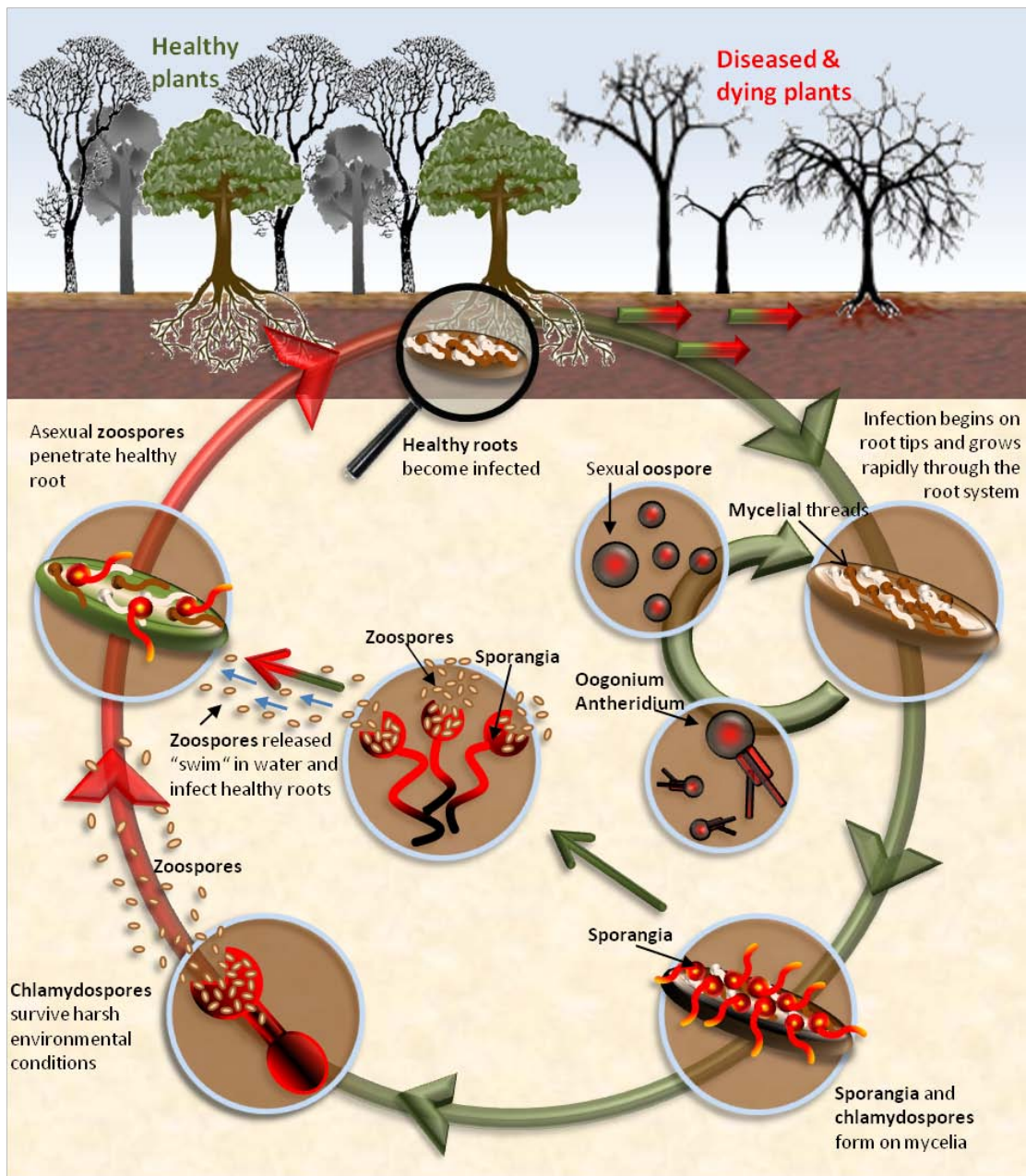


Fig. 2 - Life cycle of *Phytophthora* species. Modified from <http://www.dwg.org.au/>.

1.3.4 Plant defense strategies against pathogens

The ability of plants to survive pathogen attack is due to their arsenal of defense systems at their disposal together with the ability to compensate for the loss of tissue (Walters 2010).

When plants are attacked by pathogens, the defense reactions can be generally classified as preexisting or inducible defense. These barriers can once again be divided into physical or chemical in nature (Walters 2010). Passive or preexisting defenses are always present in the plant and build a general barrier for intruders. Physical barriers largely involve modification of surface structures, for example the thickening of cuticle and epidermal cell wall. Within the roots, plants can enhance the production of suberin, which is deposited in the cell walls, thus acting as a barrier to harmful solutes and pathogens.

Preexisting chemical barriers are established by antimicrobial secondary compounds called phytoanticipins. Examples of such compounds are phenols and quinones that have antimicrobial functions in specific tissues and organs. Other compounds, for example glucosinolates, are produced in an inactive and harmless form. After pathogen attack, they are transformed into the active form aimed at damaging the pathogen. In contrast to this defensive response, plant resistance genes may encode an enzyme that converts pathogen toxins into a non-toxic derivate or modify the affinity of plant receptors to specific toxins. Additionally, plants can contain ribosome inactivating proteins (RIPs). Such compounds inactivate protein synthesis at the ribosome which blocks viral growth.

When pathogens successfully enter the host, plants elicit defense mechanisms called active or inducible defenses. In such cases, rapid recognition of the pathogen and mobilization of defenses are needed. Plants use two types of immune receptors to detect non-self molecules. First, plants detect infection with a general pathogen recognition system that targets conserved microbial molecules called pathogen-associated molecular patterns (PAMP). The result of this interaction is a PAMP-triggered immunity (Jones et al. 2006). Second, plants possess resistance proteins (R proteins) that detect specific pathogen effector proteins. This pathogen recognition is called effector triggered immunity (ETI) (Pieterse et al. 2007).

After pathogens reception, rapid local and delayed systemic responses are developed in the host plant (Scheel 1998). **Rapid active defenses** compile fluxes in ions such as K^+ , H^+ , Ca^{2+} which subsequently induce extracellular production of ROS and nitric oxides. These compounds act as secondary messenger for defense responses and further hyper sensitive cell death, thus preventing further spread of the pathogen (Hayat et al. 2009). The oxidative burst also triggers cross-linking of the host cell wall, thereby reinforcing this physical barrier. Another rapid activated response is the production of phytoalexins antibiotic compounds that inhibit the growth of bacteria and fungi.

Plants can induce **delayed active defenses** in systems where the attack is not immediately fatal (School of Biological Sciences 2003). In terms of physical defenses, plants might repair wounds by producing thick cork cells in the secondary meristem. In this way plants prevent further infection of opportunistic pathogens. Pathogenesis related proteins, a group of low molecular weight proteins induced by PAMP, can attenuate the progression of diseases caused by several pathogens. Many of them have β -glucanase, chitinase or lysozyme activity and are such able to dissolve fungal and bacterial cell wall. Lastly systemic acquired resistance is a mechanism that develops resistance throughout the whole plant following an early localized exposure to a pathogen.

1.4 Drought as an abiotic stressor for *C. geophilum*

In times of climate change, prolonged drought periods are among the major stresses that adversely affect plant growth, crop yield and in general the natural status of the environment. Plants respond physiologically to water shortage in many physiological ways, including leaf rolling, stomata closure, decreased photosynthesis and growth as well as increased respiration (Blödner et al. 2007; Shinozaki et al. 2007). Furthermore drought may affect numerous aspects of plant metabolism and gene expression. Upon drought stress, different plant species trigger the biosynthesis of the signal molecule abscisic acid (ABA) which downstream induces stomatal closure and activates stress tolerance effector genes (Bahrun et al. 2002; Zhu 2002). Moreover the expression of genes involved in signaling pathways (Shinozaki et al. 2007; Batista et al. 2008), antioxidant stress molecules (Smirnoff 1998), protein degradation (Aranjuelo et al. 2011) and

protein folding (Porcel et al. 2005) were induced in plant species following water shortage. In general, plant responses during drought are involved in maintenance of homeostasis, detoxification of harmful elements and recovery of growth (Hajheidari et al. 2005).

It is expected that drought-affected areas as well as the frequency and duration of summer droughts will increase during the coming years (Leuschner 2009; Allen et al. 2010). Although adaptive responses of sessile organisms have evolved for millions of years in response to different stressors, rapid climate change may constrain them (Davis et al. 2001). Thus, knowledge of responses that confer stress-defense and resistance are pivotal because they represent potential mechanisms to improve stress tolerance. Infection with mycorrhizal fungi can increase the ability of plants to tolerate drought by enhancing water uptake, maintenance of a higher stomatal conductance, improved osmotic adjustment and improved nutritional status (Dosskey et al. 1990; Morte et al. 2001). Especially *C. geophilum* has been reported to be more resilient to drought stress than other ECM (Mexal et al. 1973; Theodorou 1978; Coleman et al. 1989). Pigott et al (1982) showed that *C. geophilum* remained alive throughout long periods of drought, thus being the dominant fungal ECM species following long-periods of drought stress. *C. geophilum* was able to increase drought tolerance in hybrid larch plantlets by regulating the ABA response even when mycorrhizae formation was prevented by a cellophane membrane (Rincón et al. 2005). This fact points out that *C. geophilum* synthesizes diffusible compounds of low molecular weight that affect plant growth and plant tolerance to drought.

About one decade ago, molecular approaches began to dissect some of the mechanisms governing plant tolerance and response to drought stress. Although a variety of studies have been carried out in this field, also in relation to the role of ECM taxa, a complete understanding of how fungal ECM play a role in resilience of plants to drought stress is far from being reached.

1.5 Proteomics as a tool to monitor molecular changes

Proteins are essential parts of organisms and participate in virtually every process within cells. For this reason, they are the subject of intense research in life science. Proteomics, the large-scale study of proteins, involves structural and functional aspects of proteins, analysis of posttranslational modifications (PTMs), subcellular localization as well as protein-protein or protein-DNA interactions. Furthermore, one of the most important areas in this field comprises the study of all proteins expressed in a cell, tissue or organism at a specific time under specific conditions, termed “Differential Proteomics”.

At present, numerous and diverse proteomic techniques have been reported in different papers (Monteoliva et al. 2004; Bantscheff et al. 2007; Mallick et al. 2010). However, the most common used techniques are bottom-up workflows, in which proteins are first broken up into peptides prior to identification of the proteins by mass spectrometry (MS) (Aebersold et al. 2003; Mallick et al. 2010). Those approaches encompass a prefractionation procedure of the complex sample-mixture. In general, gel-based and non-gel-based methods are used to diminish the sample complexity prior MS (Fig. 3).

Shot gun proteomics, **non-gel based methods** that are gaining popularity, involves mono- or bi-dimensional chromatographic runs to fractionate previously digested proteins. Further quantitative MS analyses can be achieved using label and label-free approaches. Labeled isotopes such as stable isotope labeling in cell culture (SILAC), isotope coded affinity tag (ICAT), tandem mass tag (TMT) or isobaric tags of relative and absolute quantification (iTRAQ) are used as internal standards and provide the basis to normalize quantitative variations among different MS (Yan et al. 2005). As an alternative, label free methods of protein quantitation compare peptide signal intensities measured in sequential MS analyses (Yan et al. 2005).

Although the use of gel-free technologies is rapidly growing, **gel-based methods** coupled with MS still remains the most popular and versatile procedure of proteome analysis. At present, gel-based methods are dominated by sodium dodecyl sulfate polyacrylamide gel electrophoresis (SDS-PAGE) and two-dimensional gel electrophoresis (2-DE), both coupled with MS techniques.

2-DE is characterized by its ability to resolve hundreds to thousands proteins simultaneously on a single gel (Beranova-Giorgianni 2003). It separates polypeptides according to two physico-chemical parameters: isoelectric point (first dimension) and molecular mass (second dimension). The resulting pattern of protein spots provide information on the composition of samples, but it also provides a picture of microheterogeneity of polypeptides caused by PTMs (Löster et al. 2002). Since its first implementation (Klose 1975; O'Farrell 1975) advances have been constantly refined, making this technique more friendly to use (Görg et al. 1985; Damerval et al. 1986; Rabilloud et al. 1994; Rabilloud et al. 1997; Görg et al. 1999). A significant step forward was the concept of implementing CyDyes (2-D DIGE, two-dimensional fluorescence difference gel electrophoresis), which offered substantial benefits over classical 2-DE (Ünlü et al. 1997). This system allows for multiplex separation of up to three samples on one gel. In general, groups of an experiment are labeled with Cy3 and Cy5, while Cy2 is used as an internal standard composed by the sum of all samples in an experiment. Consequently, using the same internal standard on every gel reduces the intrinsic experimental variation as well as the need of technical replicates. Although the main advantage of 2-DE relies in its capacity to provide a global view of a sample “proteome”, shortcomings have to be considered prior to selection of this technique. A key limitation of 2-DE lies in the exclusion of all proteins in a sample because of: (i) extreme differences in their solubility, (ii) a wide range in their expression levels, (iii) the presence of extremely basic and acidic proteins as well as extremely high and low molecular weight proteins that exceed the gel range capacity (Penque 2009). Furthermore sample preparation is a critical step for high-resolution of proteins in a 2-DE based proteomic approach. For these reasons, the optimal sample extraction protocol may be determined empirically, thus making this method rather complex and time consuming. However, combinations other than 2-DE coupled to MS are used by many researches to circumvent the limitations mentioned above. For instance, SDS-PAGE followed by tryptic digestion of proteins and further LC-MS have delivered satisfying results (Sickmann et al. 2003; de Groot et al. 2007).

Since tryptic digestion of proteins has a very well defined specificity, it is by far the most commonly used technique to cleave proteins prior to identification of peptides (Matthiesen 2006). After cleavage, the mass-to-charge (m/z) ratio of ions can be measured by MS, based upon their motion in an electric or magnetic field (Westermeier et al. 2008). All mass spectrometers typically consist of three main parts: (i) an ion source in which peptides are converted into ions.

The most common techniques enable peptides to be analyzed either in flowing liquid solution (electro spray ionization (ESI)) or in a dry crystalline state (matrix assisted laser desorption (MALDI)). (ii) In the analyzer, ions are first accelerated by an electrical potential. After acceleration, ions pass a field free region in which they are separated according to their mass-to-charge ratio. (iii) Finally a detector provides data for calculating the abundances of each ion present.

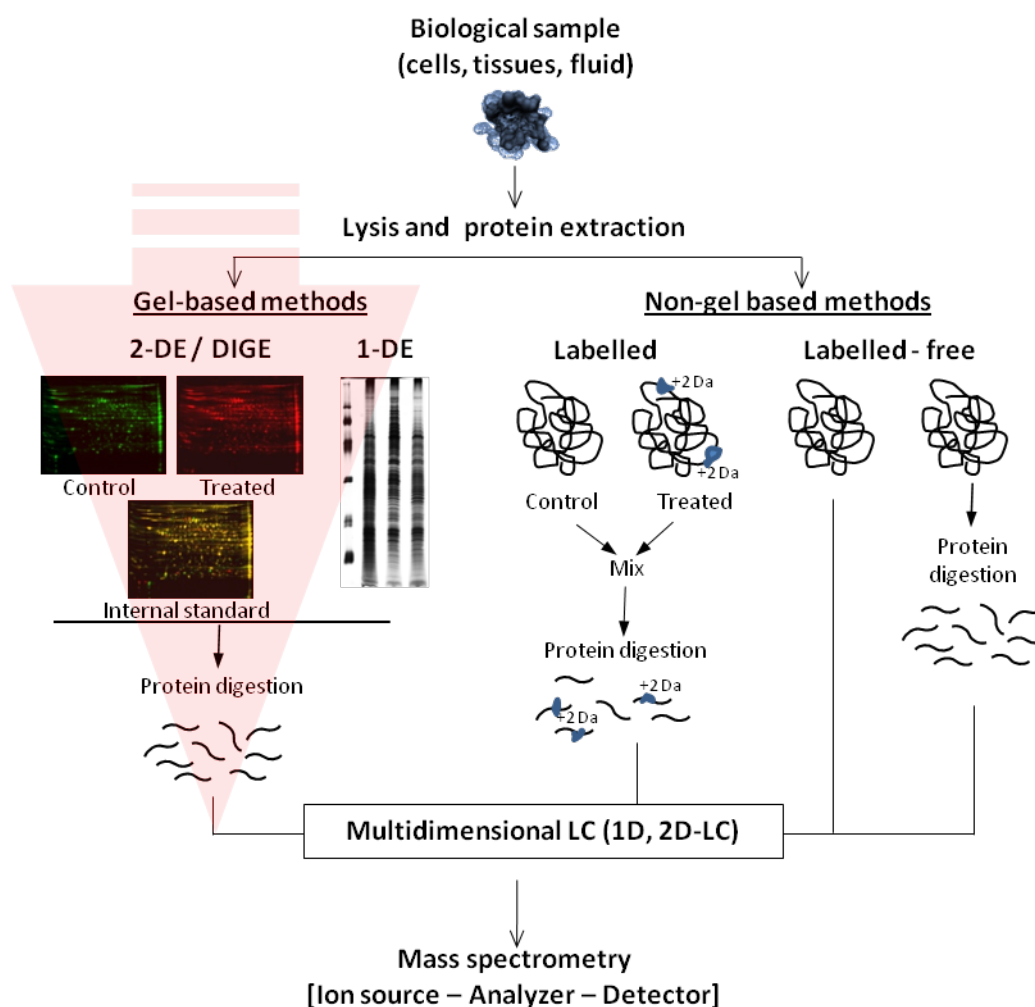


Fig. 3 - A scheme visualizing different used methods in proteomics (modified according to Barceló-Batllori (2009)). Following protein extraction, gel-based methods and non gel based methods are used to diminish sample complexity. MS is used to identify peptides. In the following work gel-based methods (using 2-DE and SDS-PAGE) coupled with LC-MS/MS were used for quantitative analysis.

Generally, the identification of proteins by MS is based on the comparison of identified peptides with a database of in-silico digested proteins. The identification of proteins by peptide mass fingerprinting (PMF) is a rapid and simple approach suitable for organisms that have a fully sequenced genome annotation. However, proteomic studies for organisms that lack an extensive and comprehensive genome catalogue require further information. This can be achieved by tandem MS, where precursor peptides are partially or completely sequenced. In those cases identification of proteins is based on homology driven proteomics (Shevchenko et al. 2009).

1.6 Specific objectives of the present work

The overall goal of the present study is to identify proteomic signatures and unravel mechanisms of molecular responses in European beech and *C. geophilum* in response to biotic and abiotic stresses. Differential proteomics will be implemented as the method of choice, since changes in protein abundance are directly involved in processes of cell controlling.

Specifically, the objectives of this study are the following:

- Optimization of the 2-D DIGE protocol as a tool to separate scarce and recalcitrant plant tissue.
- Elucidation of protein responses in European beech leaves exposed to twice ambient ozone exposure in natural field conditions. Using previous results at the transcript, metabolite and morphological level, the proteomic approach is expected to develop a better, integrated and global picture of beech leaves in response to elevated ozone. In addition, the interactive effect of ozone and the root pathogen *P. plurivora* on beech saplings will be studied. Within the frame of this work, two main questions will be assessed: i) What are the overall responses of beech saplings to elevated ozone? ii) If changes in the proteome occur, what is the degree of correlation with previous transcript analysis and with previous proteomic changes occurring in plants exposed to short-term periods of elevated ozone?
- Identification of changes in the protein expression pattern of European beech leaves following long-term exposure to elevated CO₂ and the root pathogen *P. plurivora*.

-
- Identification of quantitative changes in the proteom of *C. geophilum* isolates following gradual increases in drought-stress.

2 Material and Methods

- 2.1 European beech under the influence of abiotic and biotic stress
 - 2.1.1 Exposure to free air ozone fumigation and inoculation with *P. plurivora*
 - 2.1.2 Exposure to elevated CO₂ and further infestation with *P. plurivora*

- 2.2 *C. geophilum* exposed to water deprivation

- 2.3 Proteomic analyses
 - 2.3.1 Improvement of the 2-DE protocol
 - 2.3.2 2-D DIGE experimental design
 - 2.3.3 Relative mass spectrometry

2.1 European beech under the influence of abiotic and biotic stress

2.1.1 Exposure to free air ozone fumigation and inoculation with *P. plurivora*

The experiment was conducted during a period of 7 years at the outdoor lysimeter facilities of the Helmholtz Zentrum Research Center for Environmental Health in Munich, Germany (48°13' N 11°36' E, 490 m altitude). The trial consisted of eight lysimeters and a surrounding area, with four lysimeters exposed to ambient ozone concentrations (controls) and the other half subjected to twice ambient ozone (treatments) fumigation (Fig. 4). Details about the experimental design, including the free-air ozone exposure devices, were described by Schloter et al. (2005), Pritsch et al. (2008) and Winkler et al. (2009). In brief, forest soil from the forest site "Höglwald" was filled in and around lysimeters in 1999. For the subsequent 3 years, soil was left untreated to ensure the development of a representative soil structure. In November 2002, four nursery grown juvenile European beech trees (three-year-old and approx. 60 cm high) were planted in each lysimeter. Furthermore, 20 beech trees from the same age were planted in the area surrounding the lysimeters to provide a homogeneous stand. Twice ambient free air ozone fumigation started in July 2003 and ended after four vegetation periods in August 2006. Ozone was fumigated during the day and stopped for the first vegetation period in December 2003. For the year 2004 and 2005 ozone was fumigated from May (before bud break) until end of October (after leaf senescence). During the last experimental year, trees were fumigated from May until end of August. Levels of ozone concentration were restricted to 150 $\mu\text{l l}^{-1}$ in order to avoid acute injury to leaves. For the harvesting year 2006, the AOT 40 value of the twice ambient ozone fumigation was 52.6 $\mu\text{l l}^{-1} \text{ h}$.

In addition to the ozone fumigation, two control and two ozone treatment lysimeters (lysimeter 1, 2, 7 and 8; Fig. 4) were inoculated with the root pathogen *P. plurivora* on 30th of May, 2006 (Fig. 5). The fungal pathogen was introduced into three 40 cm holes around each tree and covered with 1 cm soil. Following inoculation, each lysimeter was irrigated with 12.5 l of distilled water to facilitate the infection of roots by the pathogen. One day after inoculation the irrigation was repeated with the same volume. Details about the infection procedure are given by Fleischman et al. (2009).

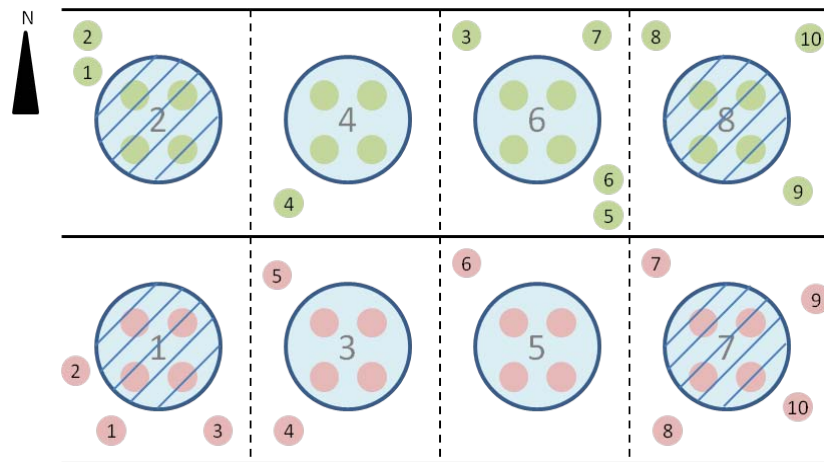


Fig. 4 - Schematic sketch of the lysimeter experiment. Each lysimeter consisted of four juvenile beech trees. Additionally, 20 juvenile beech trees were planted in the lysimeter around area. Green colored beech saplings were fumigated with ambient ozone while red colored saplings were fumigated with twice ambient ozone. Lysimeter 1, 2, 7 and 8 were additionally infected with *P. plurivora*.

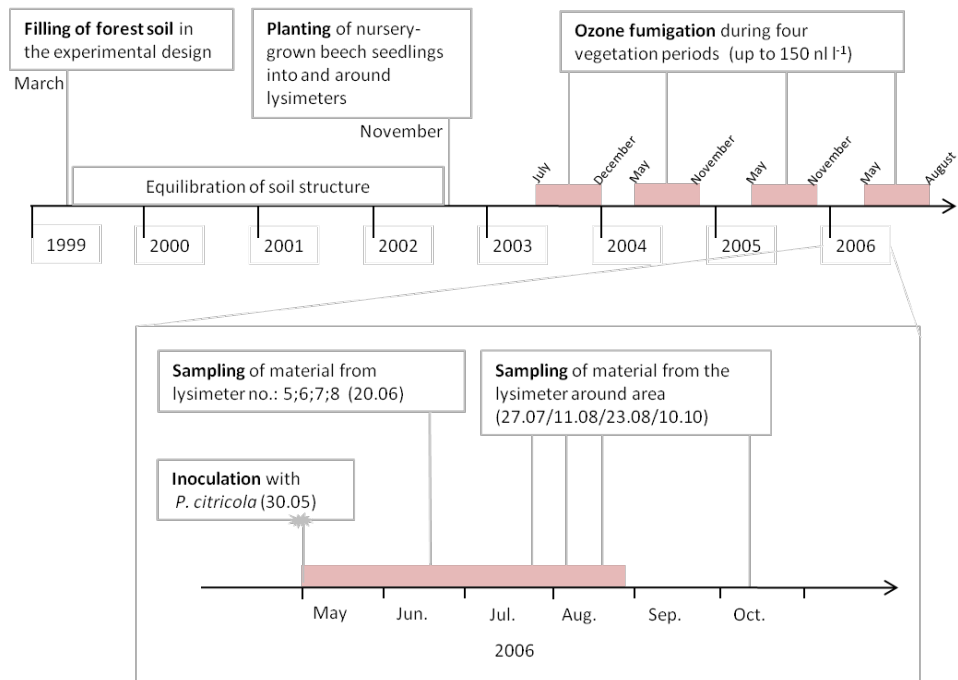


Fig. 5 - Schematic representation of the lysimeter experiment in the time line. Samples from the lysimeter around area were taken on four different time points (27th of July, 11th and 23rd of August and 10th of October). Beech trees grown in lysimeters were harvested on the 20th of July).

Sampling time points

In the present study, three leaves per tree grown in lysimeters 5, 6, 7, 8 were sampled on 20th of June, 2006. This way four different groups, each composed of four biological samples, were compared (ambient and twice ambient ozone treatment and further ambient and twice ambient ozone treatment following inoculation with *P. plurivora*).

Harvesting beech leaves from the surrounding area provided a higher number of biological replicates for both categories ambient and double ambient ozone fumigation (n= 10 saplings per treatment; Fig. 4). Three sun leaves from each plant were taken on 27th of July, 11th and 23rd of August and 43 days after ending the ozone fumigation on 10th of October 2006. All leaves were harvested at 9:00 o'clock in the morning and immediately frozen in liquid nitrogen. Fig. 5 gives an overview of the experimental setup.

2.1.2 Exposure to elevated CO₂ and further infestation with *P. plurivora*

The focus of the following experiment was on three year old nursery grown European beech saplings that were experimentally exposed to ambient and elevated (ambient + 300 $\mu\text{l l}^{-1} \text{ h}$) CO₂ regimes. In addition, half of the plants used were post-infected with the root pathogen *P. plurivora*. A total of six beech saplings were planted in each container (30x40x35 cm) using "Eurasburger" forest soil (Fig. 6). Since April 2003, 16 containers were exposed to ambient CO₂ and further 16 to elevated CO₂ fumigation in the greenhouse facilities of the Helmholtz Zentrum München by simulating the outside climatic conditions. During the winter period of the subsequent two years, saplings were placed outside under a pergola. Following hibernation, saplings were transferred again into the greenhouse. On March 4th 2005, saplings were transported to the chair of Grasland Research of the Technische Universität München for measurement of stem diameter, length and number of buds. Following measurement, saplings were split up in four chambers, each composed of eight containers, one container for each sampling time point (Fig. 7). In this way a total of four plant groups were used for the subsequent treatments (ambient CO₂, elevated CO₂ as well as both fumigation groups infected with *P. plurivora*). Light/dark periods were set at 14 h/10 h, respectively. Artificial light was situated

directly over trees with an intensity of $250 \mu\text{mol m}^{-2} \text{s}^{-2}$. The temperature was constant at $20 \text{ }^\circ\text{C}$. After development of leaves ambient CO_2 and elevated CO_2 levels were fumigated in two chambers respectively until the end of the experiment.

Pathogen inoculation

P. plurivora isolates “BoGa” was cultured in a sterile substrate consisting of vermiculite, wheat grain, calcium carbonate and V8-juice. Fungal infection of beech saplings was performed in two containers (ambient CO_2 and elevated CO_2) at the end of the light period. The inoculum (20 ml) was added at six positions in each container. After inoculation, development and release of zoospores was induced by overflowing containers for 38 h with water. The remaining saplings were mock inoculated with sterile culture media in the same way as infected saplings. Validation of *P. plurivora* infection in roots was performed by reisolation and amplification of pathogen DNA using polymerase chain reaction (PCR).



Fig. 6 - Frontal view of a phytotron with their eight containers. In two container six European beech saplings were subjected for a period of two years to $380 \mu\text{l l}^{-1} \text{h}$ and $680 \mu\text{l l}^{-1} \text{h}$ CO_2 fumigation respectively. Source: Fleischman et al. unpublished

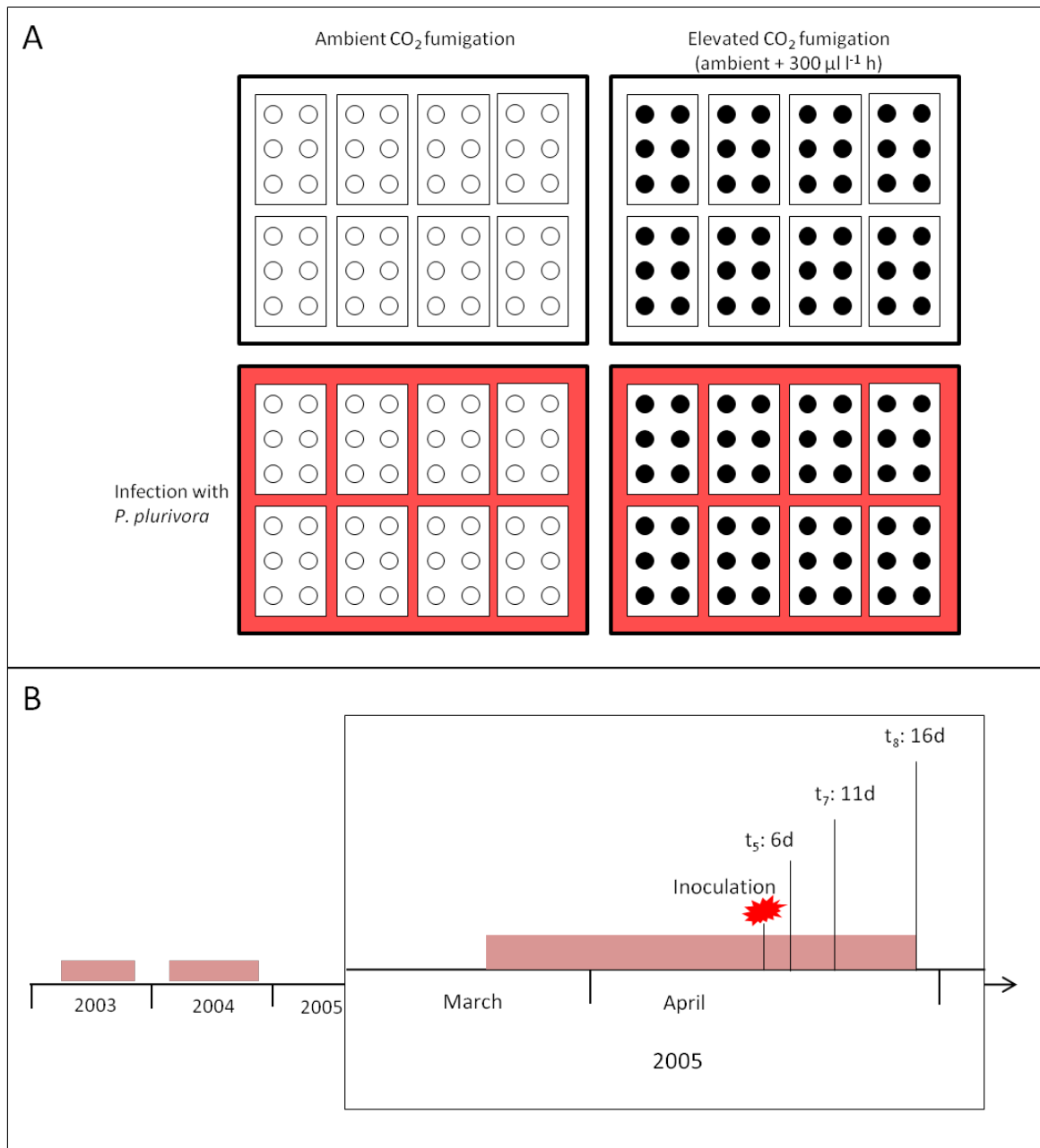


Fig. 7 - Schematic drawing of the experimental design. A, The experiment consisted of fumigation with ambient and elevated CO₂. Each container consisted of six beech saplings represented by circles. Containers with white circles were fumigated with ambient CO₂ in two climatic chambers. Containers with black circles were fumigated with elevated CO₂. Furthermore, chambers colored in red were inoculated with *P. plurivora*. B, Time line representation of the experiment. Red bars represent the period of CO₂ fumigation. Leaf material was sampled for proteome analysis on t₅, t₇, t₈ at respectively 6, 11 and 16 days after overflowing containers with water.

Sampling of beech leaves

At the end of the experiment, five years old beech saplings were fumigated for a period of two years with ambient and elevated CO₂. Following infection of roots, a total of eight sampling time points (t₁...t₈) were used for different analysis. In the present study the sampling times t₅, t₇, t₈ at respectively 6, 11 and 16 days after overflowing containers with water were used for proteomic analysis. For each time point, one container per group was used to harvest the leaf material from independent trees.

2.2 *C. geophilum* exposed to water deprivation

The influence of drought stress on *C. geophilum* strain “Cg 1.58” grown in agar medium was examined by incremental decreases in water, representing three drought stages. Species identification was previously confirmed by sequencing of the internal transcribed spacer (ITS) region using the primers ITS1 and ITS4 for PCR and sequencing (White 1990). The basal medium for the agar plates was a modified version of the MMN medium according to Marx and Bryan (1975) containing (l⁻¹): d-glucose, 20 mg; monopotassium phosphate (KH₂PO₄), 1 g; magnesium sulfate (MgSO₄ 7H₂O), 0.5 g; ammonium ferric citrate (C₆H_{5+4y}Fe_xN_yO₇), 0.5 ml; zinc sulfate (ZnSO₄), 0.5 ml; manganese(II) sulfate (MnSO₄), 0.5 ml; calcium chloride (CaCl₂), 5 ml; diammoniumtartrat ((NH₄)₂ C₄H₄O₆), 0.3 g; casein hydrolysate (13% N), 2 g; thiamin, 0.05 mg; biotin, 1 mg; MilliQ water up to 1 l and agar, 15 g.

The medium was heat-pressure sterilized (121 °C, 20 min) and exactly 25 ml was poured into each Petri dish. Four sterile polycarbonate (PC) filters (0.22 µm pore size, 25 mm diameter) (GE Water & Process Technologies, Deutschland GmbH, Willich, Germany) were placed equidistantly on the agar surface of each plate. Fungal inoculum discs were prepared from the growing margin of precultured fungal colonies grown on MMN agar medium using a 5 mm sterile cork borer. Individual disks were then placed in the center of every PC filter on the agar plates resulting in agar plates with four mycelial discs, each growing on a separate filter. Finally, plates were sealed with parafilm in order to prevent water loss from the agar. Cultures were incubated for six weeks at room temperature to allow mycelia to colonize the surface of filters. For a direct comparison

during the experiment, both controls ($n_{\text{control}}=36$ mycelia disks) and treatments ($n_{\text{treatment}}=36$ mycelia disks) were kept in the same sterile hood under controlled conditions (mean temperature 23 ± 0.6 °C; mean humidity $40 \pm 2.4\%$, light/dark periods were at 13.5 h/10.5 h respectively). Control plates were positioned under treated plates in order to keep all samples in the sterile hood. Additionally, treated groups of each time point were spatially randomized in order to minimize previously observed variations in the water loss among plates. Drought stress was applied at night by removing the parafilm from the treated plates. During the day, the lids were elevated with 1.8 mm thick silicon tubes in order to simulate higher evapotranspiration rates (Fig. 8B). Sampling of fungal mycelia was performed on three time points after beginning the treatment (t_1 : 30%, t_2 : 60%, t_3 : 85% mean water loss). Control and treated mycelia were harvested in parallel and shock frozen in liquid nitrogen. Each sample consisted of a mycelia pool harvested from three or four spatially randomized plates as it is shown in Fig. 9. As such, each time point was composed of three control and three treated samples. A general photographic documentation and the time line schematic sketch of the experiment is given in Fig. 8 and Fig. 10 respectively. Finally, samples were ground to a fine powder using a dismembrator (Resch MM300) without breaking the cooling chain. This material was further used for protein analysis.



Fig. 8 - Documentation of the experiment. A, Experiment before the third harvesting time point. B, Agar plate after water loss. C, control agar plate.

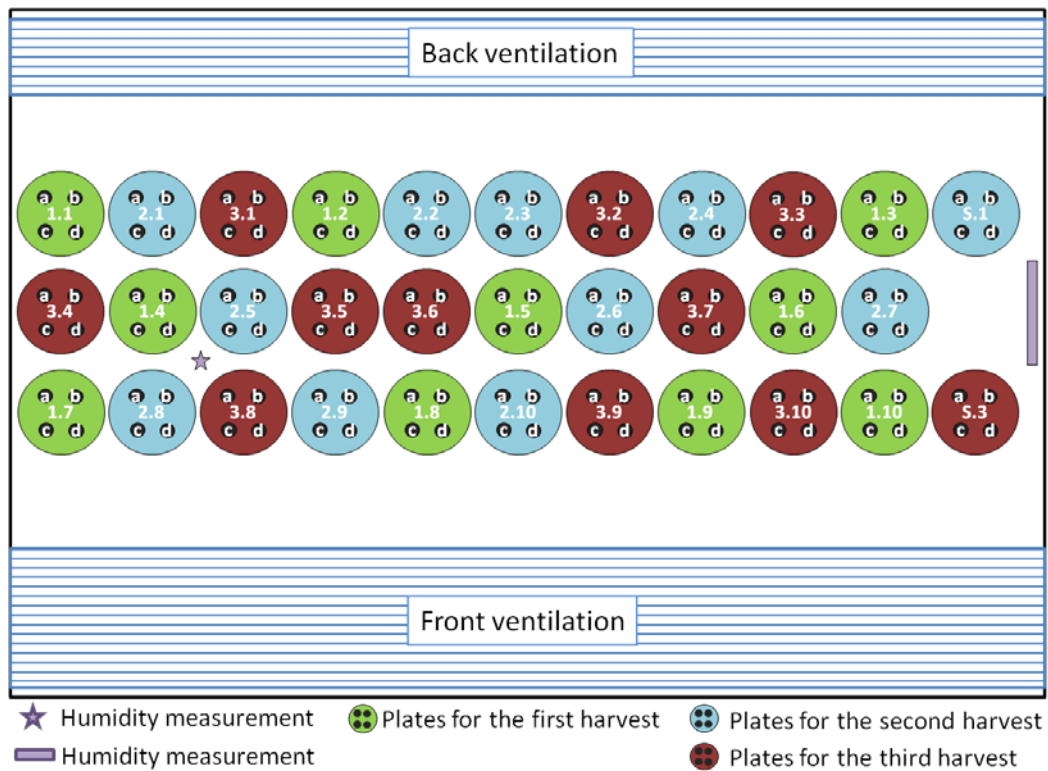


Fig. 9 - Overview of the experimental design. Treated samples were randomized among the sterile hood. All controls were positioned under the treated samples. Mycelia discs are represented by the symbols a, b, c, and d. Ten treated/control plates were used for each time point. Plates S.1 and S.3 were used as security plates for the time points 1 and 3 respectively.

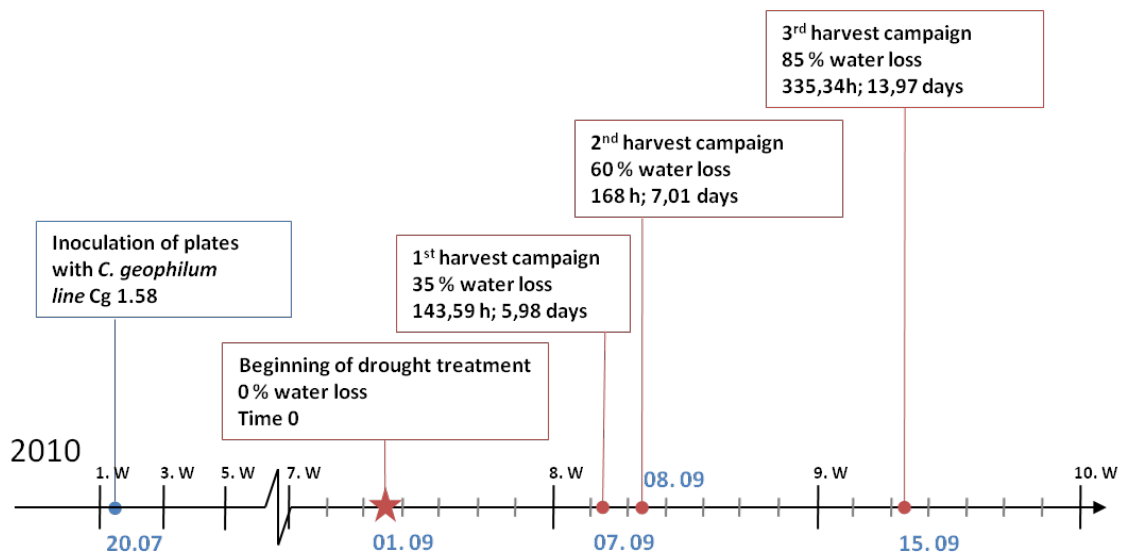


Fig. 10 - Schematic sketch of the drought experiment on *C. geophilum* strain Cg 1.58. Drought was applied after time 0 and continuously incremented during the time line analysis. W: week.

2.3 Proteomic analyses

All chemicals used for protein separation and extraction were of analytical grade, and MilliQ water was used for all buffers and solutions. Tab. 7 on the appendix summarizes frequently used chemicals and equipments in the present work.

2.3.1 Improvement of the 2-DE protocol

The extraction and separation of beech leaf proteins followed the protocol of Vâlcu and Schlink (2006a, b) with several modifications. These modifications are described in the present chapter, whereas details of the final protein extraction and separation protocol are given in chapter 2.3.2. Optimization of the 2-DE protocol was performed with the same material used for further experiments. Here, sun-leaves from nursery grown juvenile European beech trees were harvested from the lysimeter experiment, shock frozen in liquid nitrogen and stored at -80 °C. Portions of

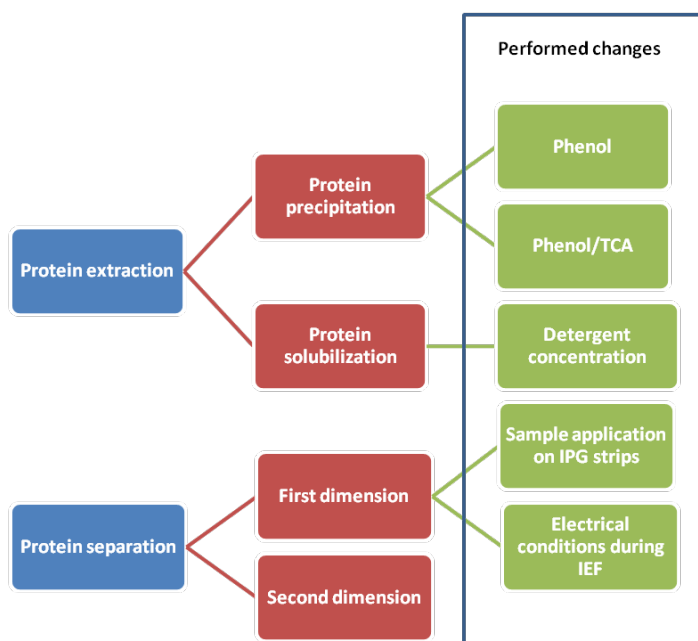


Fig. 11 - Flow-chart showing the modifications performed on the basis of the protocol of Vâlcu and Schlink (2006a, b).

100 mg leaf material were used to extract proteins from samples. Based on the protocols of Vâlcu and Schlink (2006a, b) single modifications in the protein extraction and separation protocol were performed for each run (Fig. 11). Three technical replicates were used for each modification in order to confirm changes in the quality of gels. Sample separation was performed under standard conditions according to the protein type and quantity, temperature and the chemicals used. The 2-DE protein separation was carried out on 24 cm long IPG strips (GE Helalthcare) and focused in an IPGphor (GE Helalthcare). Samples were equilibrated twice for 15 min then

separated in the second dimension (SDS-PAGE) as is described in the next chapter. All gels were silver stained according to Heukeshoven and Dernick (1988). Finally, for each modification, 2-DE gels were quantified according to the following patterns: (i) quality of proteins, (ii) spot number and (iii) reliability.

Following changes in the protocol of Vâlcu and Schlink (2006a, b) were performed:

Precipitation of proteins during the extraction procedure

- Phenol extraction methanol/ammonium acetate precipitation according to Carpentier et al. (2005): leaf material was resuspended in 500 µL of ice-cold extraction buffer (50 mM Tris-HCl pH 8.5, 5 mM EDTA, 100 mM KCl, 1% w/v DTT, 30% w/v sucrose) and 500 µL of ice-cold Tris buffered phenol (pH 8.0). Samples were vortexed for 15 min at 4 °C. Proteins were centrifuged (3 min, 6000 g, 4 °C) and the phenolic phase was collected, re-extracted with 500 µL of extraction buffer, and vortexed for 30 s. Proteins were centrifuged (3 min, 16000 g, 4 °C) and the phenolic phase was collected and precipitated over night with five volumes of 100 mM ammonium acetate in ice cold methanol.
- Phenol/TCA protein precipitation according to Wang et al. (2006): 100 mg of powder tissue was resuspended in 1000 µL 10% TCA, ice-cold acetone, vortexed thoroughly for 1 min and centrifuged at 16.000 g for 3 min (4 °C). The remaining pellet was washed with 0,1 M ammonium acetate in 80% methanol, vortexed and centrifuged (16.000 g; 3 min; 4 °C). The pellet was dried for 10 min on a centrifugal evaporator at room temperature and resuspended in 1000 µL of a 1:1 solution containing phenol buffer (pH 8.0) and SDS buffer (Wang et al. 2003). The pellet was vortexed thoroughly for 5 min and centrifuged at 16.000 g for 5 min (4 °C). The pellet was washed twice (first time in 100% methanol, second time in 80%). Following each washing step, the pellet was vortexed and centrifuged as previously mentioned.

Electrical conditions of the isoelectric focusing (IEF) separation

Based on the electrical standard protocol suitable for the first-dimension IEF (GE-Healthcare 2004), electrical conditions were changed as it is shown in Tab. 1.

Tab. 1 - Electrical conditions for running 4-7-cm Immobiline DryStrip gels on Ettan IPGphor II isoelectric focusing unit according to the manufacturer protocol. Changes in the protocol are listed below. Running conditions were set at: temperature 20 °C; current 50 µA per strip.

	Electrical conditions				
	Program 1	Program 2	Program 3	Program 4	Program 5
Conditions according to the manufacturer (GE Helathcare)		500 V 1 h	500-1000 V 7 h	1000-8000 V 3 h	8000 V 5 h
Performed changes	150 V 6 h	300 V 4 h	300-1000 V 11.25 h	No changes	No changes

Applied detergent concentrations during protein extraction

The UTO lysis buffer containing 2% OG as detergent was elevated to a concentration of 4%.

Loading of proteins prior IEF

Proteins were cuploaded onto the stripes prior IEF. Changes occurred when adding the sample solution to the rehydration solution, which is required for reswelling the drystrips.

2.3.2 2-D DIGE experimental design

Extraction of beech leaves proteins

Samples were ground to a fine powder using a micro dismembrator (Braun, D) without interrupting the cooling chain. Soluble proteins were extracted using 100 mg of fresh weight material according to the protocol of Vâlcu & Schlink (2006a) with several modifications. In brief, proteins were precipitated over night at -20°C in 10% TCA, 1% PVPP, 0.07% 2ME in ice cold acetone (Damerval et al. 1986). Pellet was centrifuged at 26.000 x g for 30 min (4°C). The supernatant was removed and the remaining pellet was washed in ice cold acetone with 0.07% 2ME for one hour at -20°C. The washing procedure was repeated once. Finally the pellet was centrifuged (26.000 x g, 30 min, 4°C), dried for 1 h on ice, resuspended in 1 ml extraction buffer (7 M urea, 2 M thiourea, 2% OG, 40 mM Tris) and sonicated for 30 min in a water-bath sonicator

at 4-7°C. The extract was centrifuged at 4°C and the pH was adjusted to 8.5 using 100 mM NaOH. Total protein amount from each sample was measured based on a modified Lowry test using the RC-DC™ Protein Assay kit (BioRad, D) and bovine serum albumin (BSA) as standard in order to generate a regression line.

Separation of proteins

Prior to separation, 50 µg of each sample and internal standard were labeled with 200 pmol of CyDyes diluted in DMF. A randomized sample labeling with Cy3 and Cy5 dyes was used in order to avoid systemic errors coming from the different label quality of Dye colors to proteins. Cy2 was used to label the internal standard that consisted of equal amounts of all the samples to be analyzed within the overall experiment. Labeling reaction was quenched with 10 mM lysine for 10 min. Finally 1/6 volume of extraction buffer II (7 M urea, 2 M thiourea, 2% OG, 600 mM DTT, 3% Pharmalyte 3-10) was added to each lysate respectively. Cy2, Cy3 and Cy5 labeled proteins were pooled and brought up to a final volume of 450 µl with rehydration buffer (7 M urea, 2 M thiourea, 2 mM 2-hydroxyethyl disulfide, 2% OG, 0.5% Pharmalyte 3-10 and 0.002% bromophenol blue). Proteins were passively rehydrated over night into 24 cm pH 4-7 strips (GE healthcare), followed by isoelectric focusing using a manifold equipped IPGphor (GE healthcare). The system was programmed for strips pH 4-7 as follows: 150 V for 6 h, 150-300 V for 4 h, 300-1000 V for 11.25 h, 1000-8000 V for 3 h and 8000 V for 5 h. Prior SDS-PAGE, strips were equilibrated twice for 15 min in 10 ml of equilibration solution (6 M urea, 75 mM Tris-HCl pH 8.8, 30% glycerol, 2% SDS, 0.002% bromophenol blue). The first equilibration was performed using 1% w/v DTT. During the second equilibration, proteins were alkylated with 2.5% w/v iodoacetamide. Second-dimensional SDS-PAGE was performed using an Ettan Dalt six chamber (GE Healthcare) in 12.5%, 1 mm thick polyacrilamide gels. Electrophoresis was carried out at 30 mA for one hour followed by 48 mA for the subsequent hour. Finally 98 mA were applied until the bromophenole blue reached the bottom of the plates.

Image acquisition and analysis

Gels were scanned with a Typhoon 9410 Variable Mode Imager (GE Healthcare) at 100 μm resolution. Cy2, Cy3 and Cy5 images were acquired by excitation of gels at 488, 532, 633 nm respectively, coupled with an emission filter of 520 nm, 580 nm and 670 nm respectively. Matching, detection, and background subtraction of single spots was carried out using the software Progenesis SameSpots (Nonlinear Dynamics). The spot alignment was automatically performed by the software and manually confirmed after spot by spot comparison. Mismatched spots were corrected manually. To guarantee high levels of quality, spots contours were edited manually on the master image and tags were assigned only for well resolved protein spots.

Statistical analysis

The abundance of each protein spot was estimated by the volumes (sum of pixel intensity within the spot boundary). Exported spot volumes were evaluated with the R environment (<http://www.r-project.org>) using the following packages: base, stats and multtest. In order to use high quality protein spots, three technical gel replicates were used to assess the degree of intra and interspecific spot variation. Only spots that showed low variations compared to the internal standard of a gel and low gel-to-gel variations were used for follow-up analysis. We refer to these spots as “well behaved” spots. These spots were compared for statistically significant differences among treated groups. Spots belonging to one gel were first normalized using the Cy5/Cy2 and Cy3/Cy2-ratios of the respective gels. In a second step gel-to-gel variations were corrected for each of the implemented normalization method, namely Z score and robust Z score normalization, volume linear scaling normalization using the geometrical and the arithmetic mean, loess normalization, and finally quantile normalization. In terms of the underlying principle used for normalizing, following four different types of normalization methods were used: Z score and robust Z score normalization constitute the first type, volume linear scaling normalization using the geometrical and the arithmetic mean constitute the second type, while loess normalization and quantile normalization are the third and the fourth type, respectively. Only spots showing significant differences in at least two (out of four) different normalization types were considered differentially expressed. As such, artifacts created by the outcomes of single normalization techniques were successfully disregarded. Statistical differences among groups

were tested taking the requirements of each analysis into account. For each group, the normality of the distribution was tested spot by spot with the Shapiro-Wilk test. In experiments having one independent factor, differentially expressed proteins were identified by computing a Welch t-statistic in case of normally distributed groups or by a Mann-Whitney-U-Test in case of non-normally distributed data. Experiments in which more than two conditions were involved (i.e. four treatment groups or two sample groups compared over the time) a two-way analysis of variance (ANOVA) was implemented. The calculated values were post-hock corrected for multiple comparisons using both the stringent Bonferroni correction and a false discovery rate (FDR) correction according to Benjamini and Hochberg (2000). Last correction is a less conservative procedure which expects the proportion of false positives among all significant tests. The levels of significance were defined as: *, $p \leq 0.05$; **, $p \leq 0.01$; ***, $p \leq 0.001$. Finally, graphical representation of results was performed using boxplots, Q-Q plots and heatmap diagrams.

Protein digestion and identification by liquid chromatographic-tandem mass spectrometry (LC MS/MS)

Preparative gels loading 700-800 μg total protein amount were run and stained with colloidal Coomassie G-250 (CBB) according to Candiano et al. (2004). Low abundant protein spots were visualized using 150-250 μg total protein amount, and silver stained with a MS compatible method according to Heukeshoven & Dernick (1988) without using formaldehyde and glutaraldehyde in the sensitizing and silver solution. Selected spots were manually excised using a scalpel. CBB extracted spots were then destained in 40% ethanol/50 mM ammonium bicarbonate ultra pure. Silver stained spots were destained in a 2% potassium hexacyanoferrate/3.2% sodium thiosulphate 1:1 mixture and washed five times with water. Spots were dehydrated with acetonitrile (ACN) and dried in a vacuum centrifuge. Gel pieces were rehydrated in 10 ng/ μL trypsin solution (Sigma-Aldrich) in 50 mM ammonium bicarbonate, and incubated over night at 37 °C. Hydrophilic peptides were extracted with 40 mM ammonium bicarbonate 10% ACN at room temperature for 10 min. Hydrophobic peptides were extracted with 47% v/v ACN, 5% v/v formic acid (FA) and the extraction step was repeated twice. All three supernatants were pooled together, concentrated in a vacuum centrifuge, acidified with formic acid and stored at -20 °C.

Peptide mixtures were analyzed by online capillary liquid chromatography coupled to a tandem mass spectrometer. Depending on the mass spectrometer used, the peptide digest (10 μ l) was separated on PepMapTM 75- μ m ID x 15-cm C18 or ReproSil-Pur 75 μ m x 20 mm C18 columns via 0.1% FA in water within 30-60 min. Data acquisition was performed in a data-dependent or in positive ion mode. After MS analyses, raw tandem mass spectra were searched using SEQUEST or Mascot algorithms with carbamidomethyl cysteine, oxidized methionine, phosphorylation of serine, threonine tyrosine and/or pyro-Glu/Gln N-termini as variable modifications. Trypsin was specified as the proteolytic enzyme and up to two missed cleavages were allowed. All data were searched against a database generated from 247416 expressed sequence tags (ESTs) from *F. sylvatica*. ESTs annotations were identified by searching with a protein Viridiplantae index from Swiss-Prot (BLASTX) and TrEMBL (BLASTX) database using UniProtKB (<http://www.uniprot.org>). Details showing variable parameters for the used mass spectrometer are given in Tab. 2.

Tab. 2 - Table showing variable parameters for the identification of proteins/peptides with different mass spectrometers. LC: liquid chromatography; ESI: electrospray ionization.

Variable parameters	Parameters used to identify proteins in ozone treated samples	Parameters used to identify proteins in
Liquid chromatograph	Online capillary HPLC (LC-Packing)	Online Easy-nLC (Proxeon, Bruker)
Mass spectrometer	Nanospray LCQ Deca XP ion trap mass spectrometer (Thermo-Finnigan)	Electrospray ionization (ESI) iontrap mass spectrometer (AmaZon ETD, Bruker)
LC-trap column	PepMapTM 75- μ m ID x 15-cm C18	ReproSil-Pur 75 μ m x 20 mm C18, 5 μ m
LC-flow rate	200 nl/min	20000 nl/min
Solvent used for elution of peptides	5–40% linear gradient in 0.1% formic acid	0 to 40% acetonitrile in 0.1% formic acid
Peptide separation time	30 min	60 min
ESI-capillary voltage	5 V	2000 V
Data acquisition	Data-dependent mode m/z 300–2000	Positive ion mode from m/z 50 to 3000, followed by data-dependent MS/MS acquisitions from m/z 100 to 2800
Data analysis program used for protein identification	SEQUEST	Mascot
Variable modifications during the search	Oxidation of methionines (116 Da) and carbamidomethylation of cysteines (157 Da)	Oxidation of methionines, carbamidomethyl cysteine, phosphorylation of serine, threonine and tyrosine and pyro-Glu/Gln N-termini

2.3.3 Relative mass spectrometry

Protein extraction for *C. geophilum*

A total of 100 mg nitrogen-grounded powder of each pooled control and drought stressed *C. geophilum* sample was collected separately in 1.5 ml tubes. Samples were directly resuspended in the extraction buffer containing 7 M urea, 2 M thiourea, 100 mM DTT, 2% OG, 0.5% Pharmalyte 3-10, 2% sodium dodecyl sulfate. Extracted proteins were precipitated for five hours in 1000 ml precooled (-20°C) precipitation solution (10% TCA, 1% PVPP, 0.07% 2ME in acetone). After centrifugation for 30 min at 26.000 x g (4°C) proteins were washed with 0.07% 2ME at -20 °C for one hour. The washing procedure was repeated once and dried in a speedvac at room temperature for 7 min. Samples were then sonicated at 7 °C for 30 min and from time to time vortexed for a few seconds. Finally the dried pellet was resuspended in 2x SDS sample loading buffer containing 50 mM DTT and reduced at 95°C for 10 min, followed by alkylation with 55 mM IAA for 30 min in the dark. The protein concentration of each sample was determined with at least four technical measurements using the Coomassie (Bradford) Assay Kit (Thermo Scientific) in micro titer plates according to the manufacturer's instructions.

Protein separation and mass spectrometric analysis

A total of 100 µg of each protein sample was loaded into a 4–12% NuPAGE gel (Invitrogen, Darmstadt, Germany) in a XCell SureLock™ electrophoresis Cell (both Invitrogen™) with NuPAGE® MOPS SDS Running Buffer (1x). Together with two BSA standards applied into the borders of the gel, samples were separated at 200 V for 45 min according to Laemmli (1970) until the bromophenol blue reached the bottom of the gel. Proteins were stained with colloidal Coomassie G-250 according to Candiano et al. (2004) prior to in-gel trypsin digestion. In-gel trypsin digestion was performed according to standard procedures. Eight bands were manually excised using a scalpel and destained in 40% ethanol/50 mM ammonium bicarbonate ultra pure. Protein bands were dehydrated with ACN and dried in a vacuum centrifuge. Gel bands were rehydrated in 10 ng/µL trypsin solution in 50 mM ammonium bicarbonate and incubated at 37 °C over night. Tryptic peptides were extracted with 40 mM ammonium bicarbonate 10% ACN at

room temperature for 10 min. Peptides were extracted with 47% v/v ACN, 5% v/v formic acid and the extraction step was repeated twice. All three supernatants were pooled together, concentrated in a vacuum centrifuge, acidified with formic acid and stored at -20 °C. Further protein separation and analysis by online capillary liquid chromatography coupled to a tandem mass spectrometer was performed, which is described in section 2.3.2, for CO₂ treated samples (page 46-47. Tab. 2). Following mass spectrometric analysis, MS/MS spectra were searched against a database generated from 175.829 clean reads and 19168 contigs from mycelium of *C. geophilum* tissue. Protein functions were identified by searching Swiss-Prot/TrEMBL database using UniProtKB (<http://www.uniprot.org>).

Statistical analysis

Peptide counting was used as the method of choice to quantify protein abundance between groups. This semi comparative method measures the total number of tandem mass spectra (MS/MS spectra) that matched a protein in a complex mixture. Only proteins with at least two confident identified peptides were considered for protein identification. To account for experimental variability, normalization of spectral counts was performed using the log₂ transformation of NASF (normalized spectral abundance factor) values. In order to avoid dividing by zero during the log transformation, pseudo counts were generated according to Laplace's rule by adding one to each spectral count. The Shapiro-Wilk test was used to test for normality of distribution. A two group comparison analysis was performed for each time point implementing a Welch's t-test, in case of normally distributed data, or in case of non-normal data, a Mann-Whitney-U-test. Statistical differences between the control and the drought stressed group ($p \leq 0.05$) were determined using a Bonferroni and a FDR correction according to Benjamini et al. (2000). Only significant different proteins with at least differences of more than two spectral counts in at least one control versus treatment sample were considered as differentially abundant protein.

3 Results and discussion

- 3.1 Improvement of the 2-D electrophoresis protocol

- 3.2 Leaf injury and proteomic changes in juvenile European beech trees following three year exposure to free-air elevated ozone and inoculation with the root pathogen *P. plurivora*
 - 3.2.1 Visual ozone damage in leaves
 - 3.2.2 Ozone responsive proteins detected by 2-D DIGE in juvenile beech trees around the lysimeters
 - 3.2.3 Juvenile beech trees fumigated with free-air elevated ozone and post infected with the root pathogen *P. plurivora*

- 3.3 Changes in the proteome of beech saplings upon pathogen inoculation and elevated CO₂ concentrations

- 3.4 *C. geophilum* facing drought stress

3.1 Improvement of the 2-D electrophoresis protocol

Sample preparation is one of the most critical steps for high-quality resolution of proteins in a 2-DE based proteomic approach. Plant tissue is especially demanding when using 2-DE due to the abundance of interfering compounds such as polysaccharides, pigments and secondary metabolites. Thus, removal of such compounds becomes a crucial matter for sample preparation. Although several authors addressed new methods to better resolve proteins from recalcitrant plant tissue (Mechin et al. 2003; Wang et al. 2003; Carpentier et al. 2005; Gómez-Vidal 2008) the optimal sample extraction and separation protocol of a specific sample material must be determined empirically to perform an optimal protein separation (GE-Healthcare 2004). Extraction and separation of soluble proteins by means of 2-DE was previously optimized for leaves as well as roots of European beech seedlings (Vâlcu et al. 2006a, b). In the following experiments, the general suitability of the extraction protocol proposed by Vâlcu and Schlink (2006a, b) needed to be modified due to the use of ontological different leaf samples (Fig. 12).



Fig. 12 - Extraction of leaf proteins from European beech sapling according to the protocol of Vâlcu and Schlink (2006a, b). Low protein separation is observed as black smearing on the gel.

Protein spots from the 2-D gels lack a well defined resolution and quality. Reasons for such massive streaking phenomenon are diverse and may be related to the presence of carbohydrates, time of focusing and application point of protein samples during IEF (Carpentier et al. 2005; Vâlcu et al. 2006b). Based on the work of Vâlcu and Schlink (2006a, b) different settings were tested in order to enhance the quality and reliability of separated spots. Optimization consisted of changes in one step of the protocol, while other steps were kept constant. For each modification in the protocol, proteins were separated as technical triplicates.

Evaluation of a suitable protein precipitation protocol

Three types of protein precipitation methods were tested which are currently used in plant proteomics to selectively separate proteins from salt, nucleic acid and recalcitrant plant compounds such as secondary metabolites. The precipitation protocol of Damerval et al. (1986), which was used by Vâlcu and Schlink (2006a), is a commonly used method, allowing the extraction of total proteins based on simultaneous precipitation and denaturation with TCA and 2ME in cold acetone (TCA-A). An alternative precipitation method described by Carpentier et al. (2005) uses ammonium acetate in combination with phenol. For this method, the authors suggests a high clean up capacity and power to purify samples from carbohydrates, which is known to block gel pores and cause precipitation of proteins. The third separation method, which is a combination of TCA/acetone, and phenol extraction (phenol/TCA) has been successfully applied in different recalcitrant plant tissues (Wang et al. 2006). Fig. 13 shows the extracted leaf proteins with the three previous mentioned precipitation protocols.

The differences in the number of spots detected for each method was assessed. The highest numbers of spots were achieved by the TCA-A method, which showed on average 820 ± 18 spots. Unexpected was the precipitation with phenol and phenol/TCA, which showed a lower spot number of 656 ± 23 and 493 ± 22 respectively. However, in all three implemented procedures, vertical streaking lines and a low spot resolution of 2-DE gels were observed. As the method of Damerval et al. (1986) contained the highest amount of spots, this method was selected for the further separation of proteins.

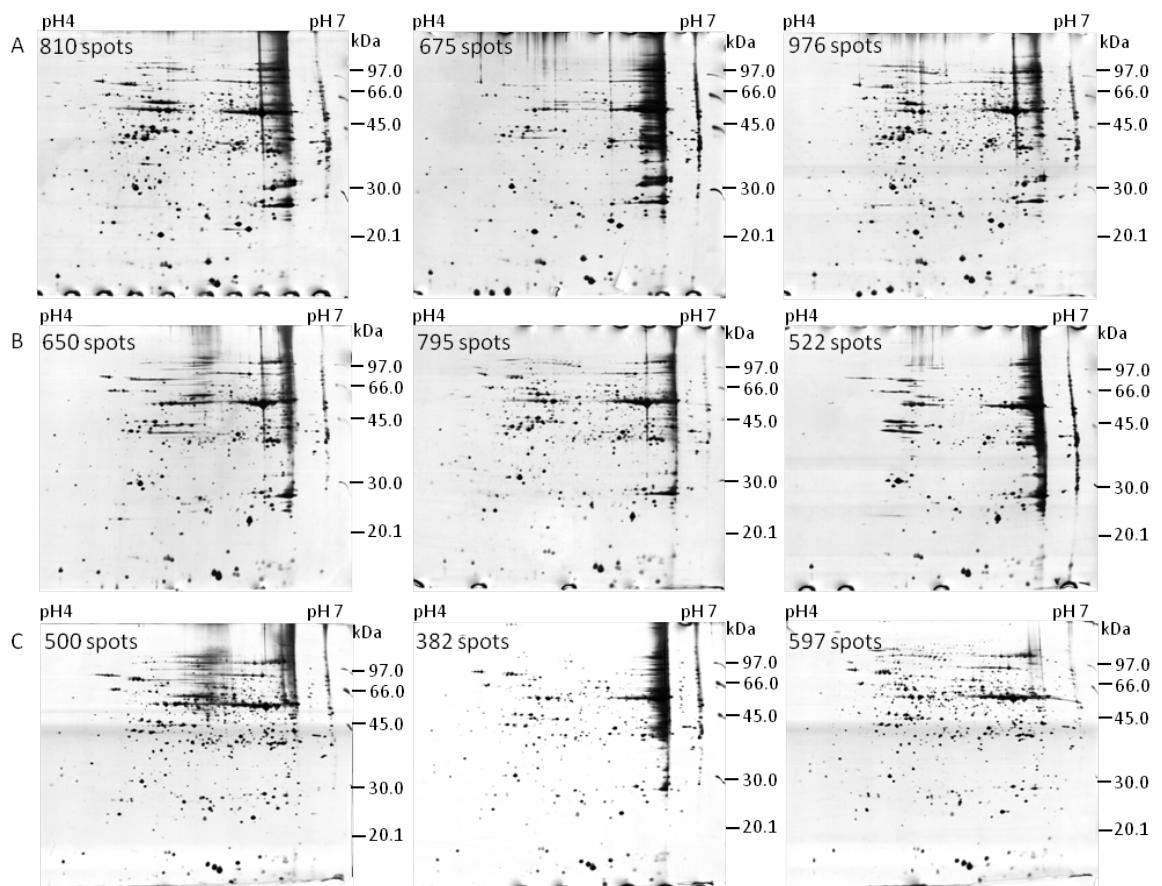


Fig. 13 - 2-DE separation of proteins from European beech trees using three different protein precipitation procedures. A, TCA-A precipitation; B, phenol precipitation; C, TCA/acetone combined with a phenol precipitation (phenol/TCA). Spot numbers indicate the amount of spots manually counted for each 2-DE gel.

Improvement of running conditions during IEF

Protein aggregation and precipitation are effects that could be observed when samples enter the gel in the presence of high voltages (Westermeier et al. 2008). In order to minimize this effect the initial voltage was reduced from 500 V to 150 V and prolonged from 1 h to 6 h. Furthermore the voltage gradient was prolonged as it was shown in Tab. 1. Separated proteins clearly showed melioration with regard to the resolution of protein spots (Fig. 14). Nevertheless the number of spots showed no increase over the technical triplicates (703 ± 18).

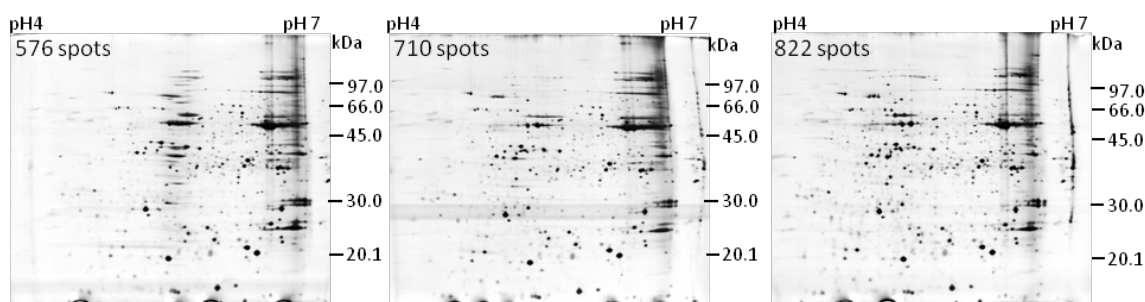


Fig. 14 - 2-DE spot profile for European beech leaves separated with lower IEF voltages at the starting point.

Changes in the detergent concentration of the lysis buffer

Detergents are used to disrupt hydrophobic interactions and solubilize a large subset of protein populations. In general, they are typically used at concentrations of 1–4%, however; how much of each needs to be determined empirically. In order to meliorate the low gel resolution, which was ultimately caused by low solubility of proteins, the concentration amount of the detergent (OG) was doubled from 2% to 4%. Proteins extracted with 4% OG exhibit melioration with regard to the gel quality, but fewer spots were resolved in the overall gel image (Fig. 15; 583 ± 2 spots). For this reason, the concentrations of OG used in the protocol were kept at 2%.

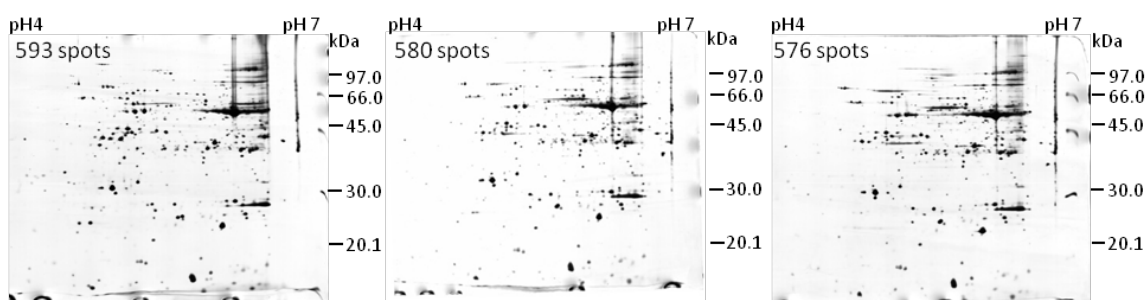


Fig. 15 - 2-DE gels showing separated proteins with 4% OG in the extraction buffer.

Optimization of the protein loading methods for the IEF

Two methods of protein loading were tested in the present work. Depending on the application point, proteins will have different titration curves and therefore different mobility characteristics (Westermeier et al. 2008). Several methods are described to load proteins onto the IEF gels. Cup

loading, by which proteins approach the gel from a specific point, work usually much better for very acidic gradients. The samples are transported faster into the gel, thus reducing the chances of protein interactions. However, proteins with isoelectric points close to the pH of application point have low mobility and solubility. As a consequence, cuploaded proteins may precipitate at the application point and build a vertical streak in the second dimension. Rehydration loading circumvents the above mentioned problems by loading proteins evenly over the entire gel. In the following step we changed cuploading application to rehydration loading.

Fig. 16 shows the separation of proteins using rehydration loading instead of the previous used cup loading. Changing the application method clearly improved the quality of 2-DE gels. Moreover this method circumvents the precipitation of proteins by cup loading and revealed a high proportion of acidic spots (1306 ± 9) while maintaining reproducibility.

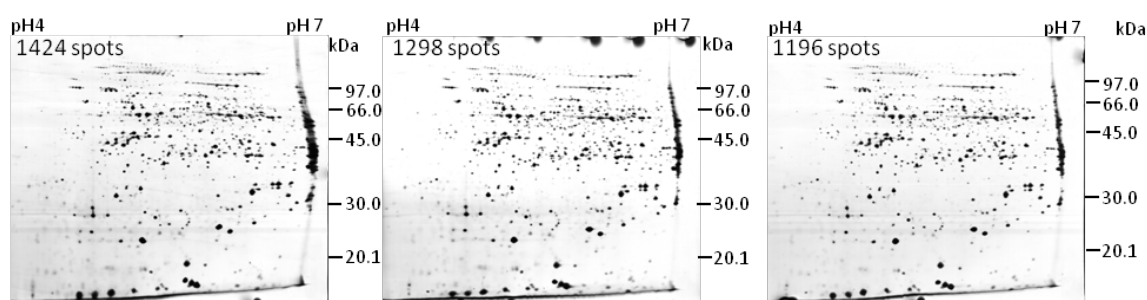


Fig. 16 - Improvement of 2-D gel pattern resolution by sample rehydration loading.

Changes performed during optimization of the method are listed in Tab. 3.

Tab. 3 - Gel quality, reproducibility and spot yield for each performed modification on the protocol. Gel quality as well as reproducibility was defined in a scale of 1 (showing the best values) to 5 (showing the worst values). The spot yield was counted for each replicate and expressed as mean value with the corresponding standard deviation (SD).

Performed changes	Gel quality					Reproducibility					Spot number			Mean	Relative SD [%]
	1	2	3	4	5	1	2	3	4	5	Gel #1	Gel #2	Gel #3		
Evaluation of TCA-acetone as precipitant of proteins				x						x	810	675	976	820	18
Evaluation of Ammoniumacetat/Phenol as precipitant of proteins				x						x	650	795	522	656	21
Evaluation of TCA/Phenol as precipitant of proteins			x							x	500	382	597	493	22
Changes in the electrical conditions of the IEF			x							x	576	710	822	703	18
Doubling the detergent concentration in the lysisbuffer		x				x					593	580	576	583	2
Rehydration loading	x					x					1424	1298	1196	1306	9

Assessing the role of technical variation on 2-D gels

Technical reproducibility is particularly important in 2-D gel electrophoresis, as this technique is often used for the quantitative analysis of protein abundances. Although the use of spectrally resolvable fluorescent dyes (Cy2, Cy3, and Cy5) has been reported to lower gel-to-gel variation, there are different sources of technical variation that must be considered when designing an experiment. Overlooking these sources of variation may easily obscure the biological changes under investigation. To estimate the degree of spot variability a two-step analysis was implemented using a set of three gels representing technical triplicates. First, the intra specific spot variation was assessed using both channels, the Cy3/Cy2 and Cy5/Cy2 ratio, for each implemented normalization (Fig. 17). By implementing this method it was possible to identify and discard spots with variances over and below the 95% and 5% percentile respectively. In a second step, gel-to-gel variances were estimated for each spot and only stable spots in between the 10-90 percentile were selected for follow-up analysis. Throughout the selection of “well behaved spots”, significant differences in the following comparative analyses are assigned as real change, occurring upon treatment conditions rather than resulting from the inherent technical variation of the system. From the total number of 1012 spots recognized on average in the 2-D DIGE gels, following number of spots were used for each normalization method: Z score normalization: 544 spots; robust Z score normalization: 544 spots; volume scale normalization: 544 spots; volume

geometrical mean normalization: 544; loess normalization: 540 spots; quantile normalization: 540 spots. Spots discarded from the follow-up analysis are observed on the 2-D gel in Fig. 18.

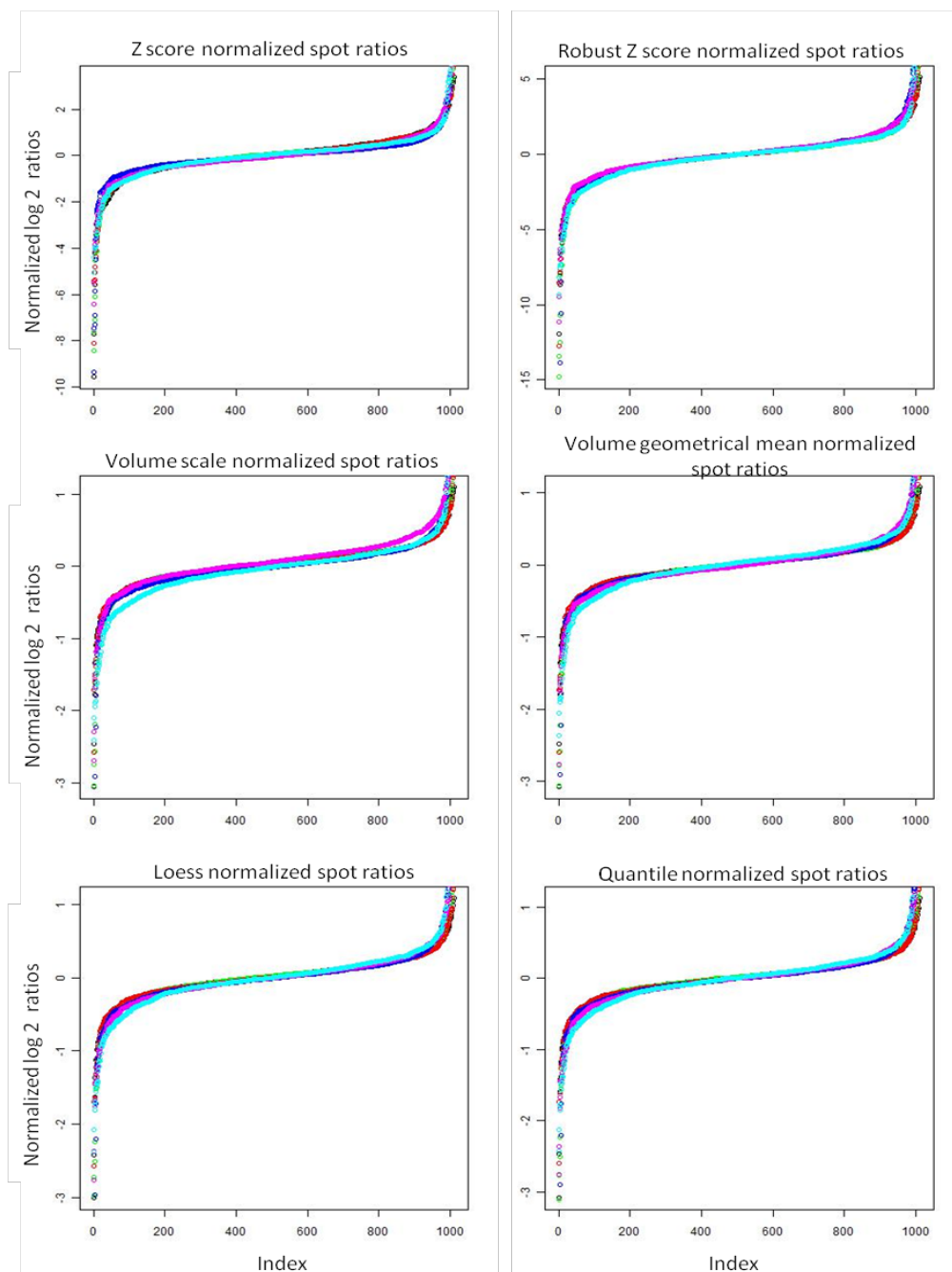


Fig. 17 - Log₂ transformed spot ratios (Cy3/Cy2 and Cy5/Cy2). In each graph every channel (two per gel) is represented by a single color. The index classifies spot ratios in ascending order.

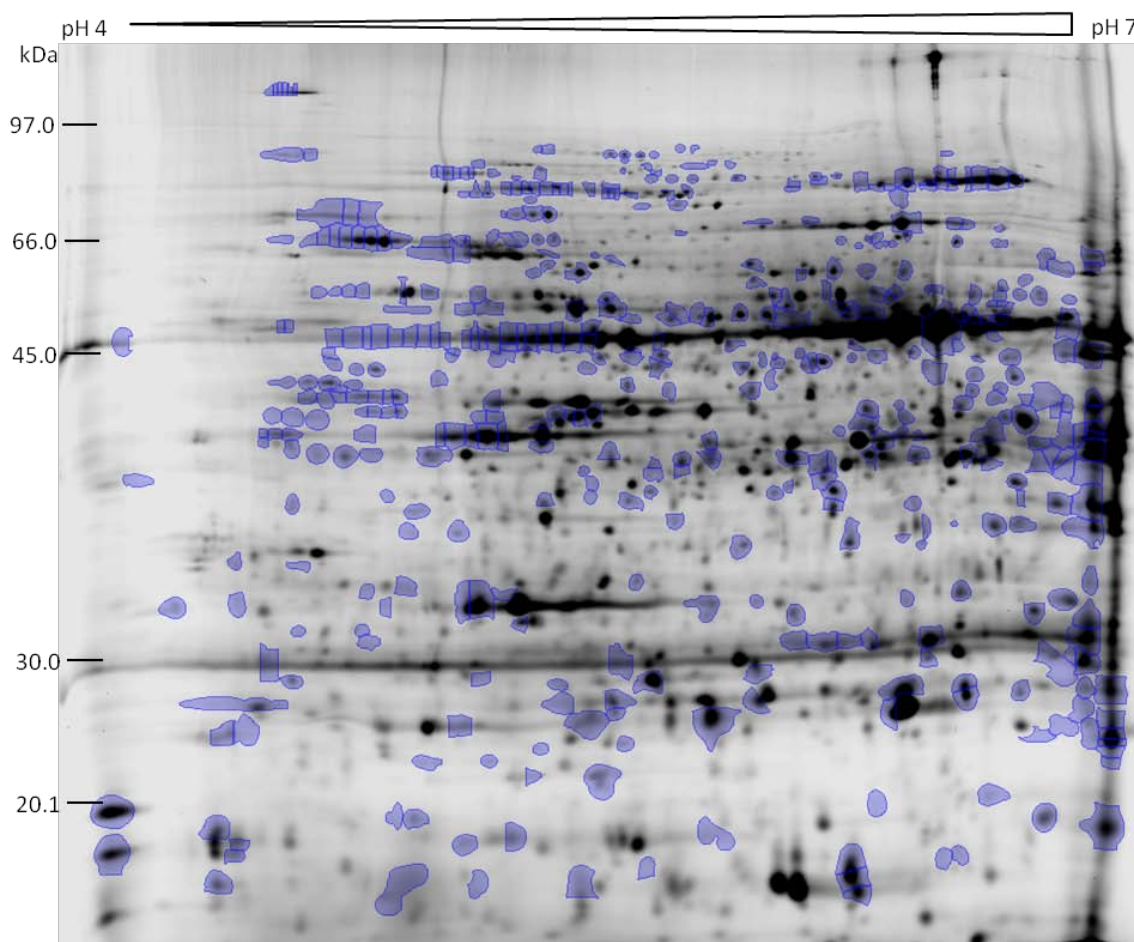


Fig. 18 – 2-D DIGE gel showing one of the used technical replicates. Blue labeled protein spots were discarded from the follow-up analysis due to high technical variances in between and among gels.

3.2 Leaf injury and proteomic changes in juvenile European beech following three year exposure to free-air elevated ozone and inoculation with the root pathogen *P. plurivora*

3.2.1 Visual ozone damage in leaves

In the present study, typical ozone-induced brownish patches were examined on beech leaves grown inside lysimeters during the vegetation period 2006 (Fig. 19). These measurements take into account 32 leaves per group, which were monitored during the time period of 14th of June, 4th of July and 08th, 14th and 22nd of August. On the 14th of July, more than 15 days after starting

the ozone fumigation in the year 2006, leaves did not show foliar injury either in the ambient or in the twice ambient ozone exposed groups. This trend was also stable for the second measurement on the 4th of July. The first significant difference between both groups tended to be visible on the 8th of August. Leaves exposed to twice ambient ozone showed on average 3% foliar injury, which translates to twice as much brownish patches as the controls. Although the internal variation among groups was high, significant differences between both groups ($p \leq 0.05$) became visible for the last two examined time points on the 14th and 22nd of August, reaching values between 0-30% leaf injuries. Foliar injury was, on average for each time point, more than two to three times higher in elevated ozone exposed leaves compared to the controls.

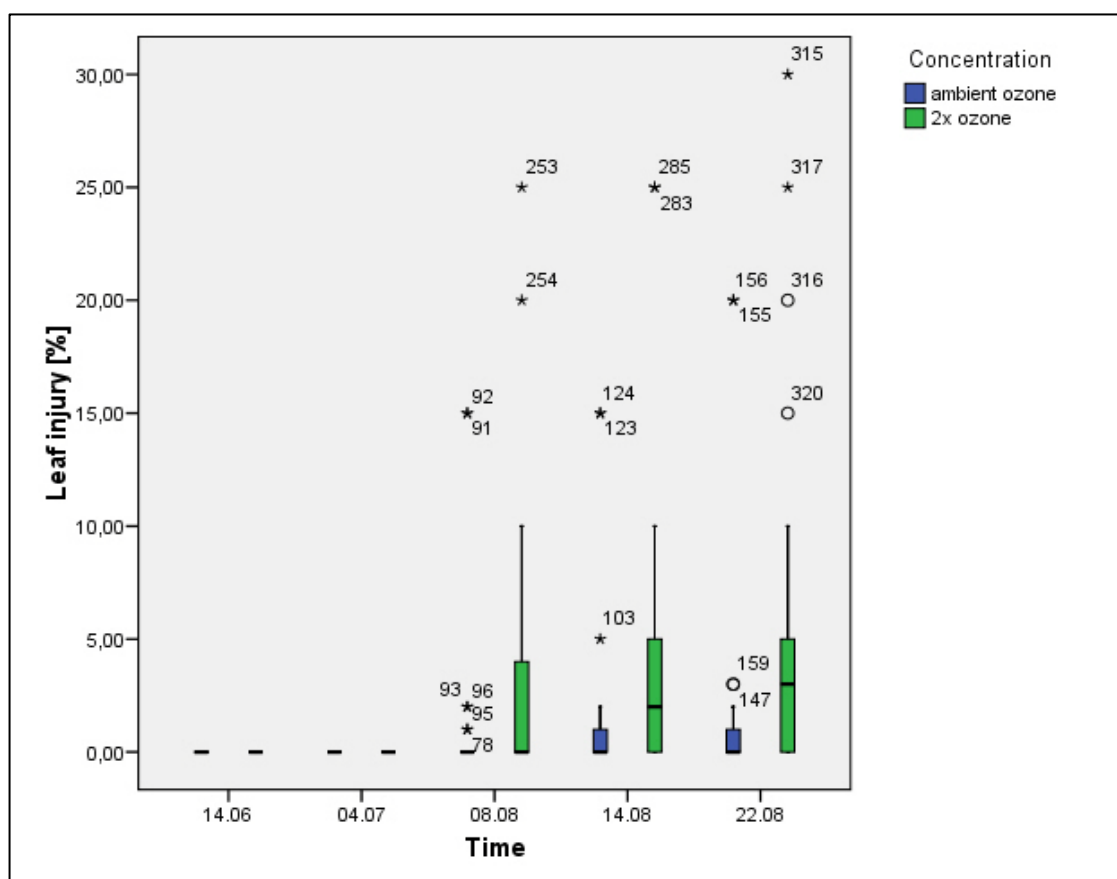


Fig. 19 - Total discolored leaf area after ambient and twice ambient ozone fumigation. Box plots show the median, 25th and 75th percentiles, extremes and range of values. Statistical differences between ambient and twice ambient ozone exposed leaves were observed for the time point of 14th and 22nd of August ($p \leq 0.05$). Data source: Grams et al. unpublished.

These results provide basic information on the induced response of juvenile beech trees to ozone exposure throughout the experimental year 2006. Similar visual symptoms have been observed on different plant species due to elevated ozone exposure (Agrawal et al. 2002; Cho et al. 2008) and are a common indicator of a hypersensitive response, probably induced by the higher concentrations of accumulated ROS. Since elevated ozone was damaging leaf tissue, it is presumed that photosynthesis and the CO₂ uptake of beech trees was affected at least in the second half of August.

3.2.2 Ozone responsive proteins detected by 2-D DIGE in juvenile beech trees around the lysimeters

The low spot separation and labeling quality of two gel images resulted in the exclusion of samples from tree number 7 of both groups at 27th of July. Furthermore plantlets 8, 9 and 10 from the sampling time point of the 10th of October were totally excluded from the experiment due to the lack of starting material. As such, a total of 108 gel images (36 controls, treated and internal standard respectively) were used for statistical analysis. Differences in the protein abundance between control and treated samples were assessed for each time point using a Mann-Whitney-U-test or a Welsh test depending on the requirements described in chapter 2.3.3. The results presented here showed that at least in two different types of normalization methods; 87, 70, and 100 protein spots were regulated in elevated ozone-exposed leaves for the sampling time point of 27th of July, 11th and 23rd of August respectively. In contrast, following 43 days of recovery after elevated ozone exposure, beech leaves showed on 10th of October only one spot to be significantly different. Regarding the number of modulated proteins, a similar trend was observed during the analysis of gene expression of the same experimental setup. These results showed the highest number of regulated transcripts at the end of July and at the beginning of August, while the lowest number were observed on the subsequent sampling time points, including the 10th of October (Olbrich et al. 2009). Also, the ozone-induced visible injuries in leaves became significant and more abundant on the monitored time points in August, but in contrast to the modulated transcripts/proteins, no visible symptoms were manifested in July. These results clearly reflect the

fact that juvenile beech trees activate molecular defense mechanisms at an early stage of the ozone-plant interaction, much earlier than when visible damage was induced.

The heatmap diagram highlighted in Fig. 20 indicates common spots that were statistically significant during the harvesting time points of July and August. With the exception of four treatment samples labeled in red, the right cluster clearly revealed differences between control and treated groups. However, samples from different harvested time points tended to cluster together, showing no general difference in the modulation of proteins over the three time points. This result is also reflected in the applied 2-way-ANOVA, which showed no statistical differences in treated spots over the three sampling time points in July and August (data not shown).

Of the total differentially displayed spots in at least two normalization methods, the focus laid on those showing absolute expression levels over 30%. Furthermore, for the follow-up analysis, few spots showing significant changes after just one normalization method were taken into account. These spots were selected because previous analyses performed with the same data and the software DeCyder (thus, using a different normalization method) showed significant changes between control and treated samples (data not shown).

Out of these spots, a total of 75 resembled the preparative gel spot pattern. These spots were subjected to LC-MS/MS followed by a homology driven search. The mass spectra of 2 spots failed to show any peak while 28 spots resulted in multiple protein mixtures. As for the remaining 45 spots, proteins were identified as a single protein. On the basis of biological function, proteins were classified according to eleven groups: [1] Calvin cycle, [2] photosynthesis, [3] mitochondrial electron transport chain, [4] carbon metabolism/catabolism, [5] photorespiration, [6] nitrogen metabolism, [7] stress response, [8] defense response, [9] detoxification, [10] degradation and [11] protein folding. As it is shown in Fig. 21, the most affected group upon elevated ozone fumigation was the Calvin cycle followed by detoxifying related proteins and proteins regarding the defense mechanism.

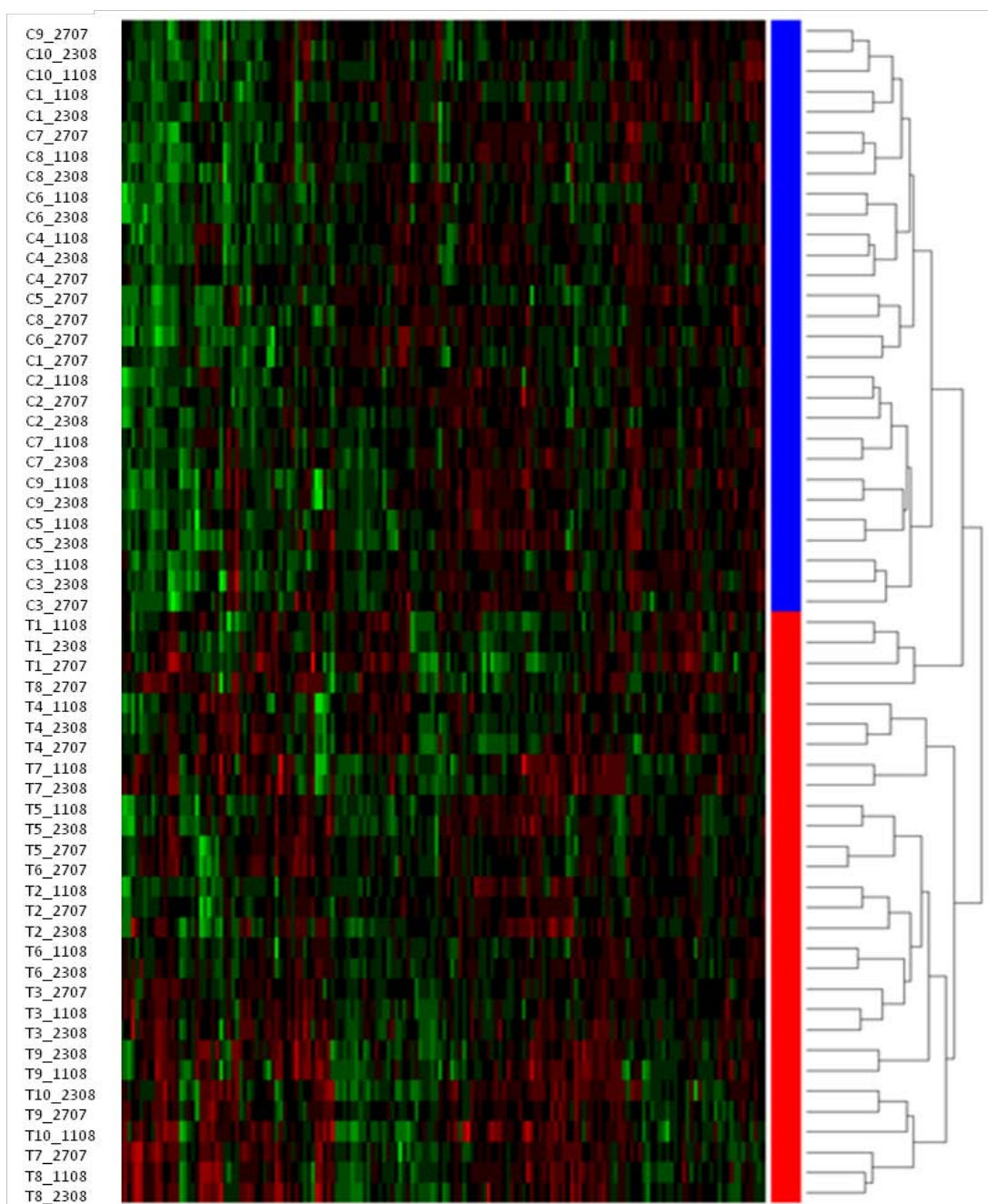


Fig. 20 - Heat map diagram displaying identical protein spots modulated on the 27th of July, 11th and 23th of August 2006. Values are log₂ ratios. Green=down-regulation; Red=up-regulation. Right dendrogram: clustered display of data of ambient and twice ambient fumigated samples. The color bar at the right indicate samples treated with ambient (blue) and twice ambient (red) ozone fumigation. Samples labeled on the left with "C" and "T" indicate controls and treatments respectively.

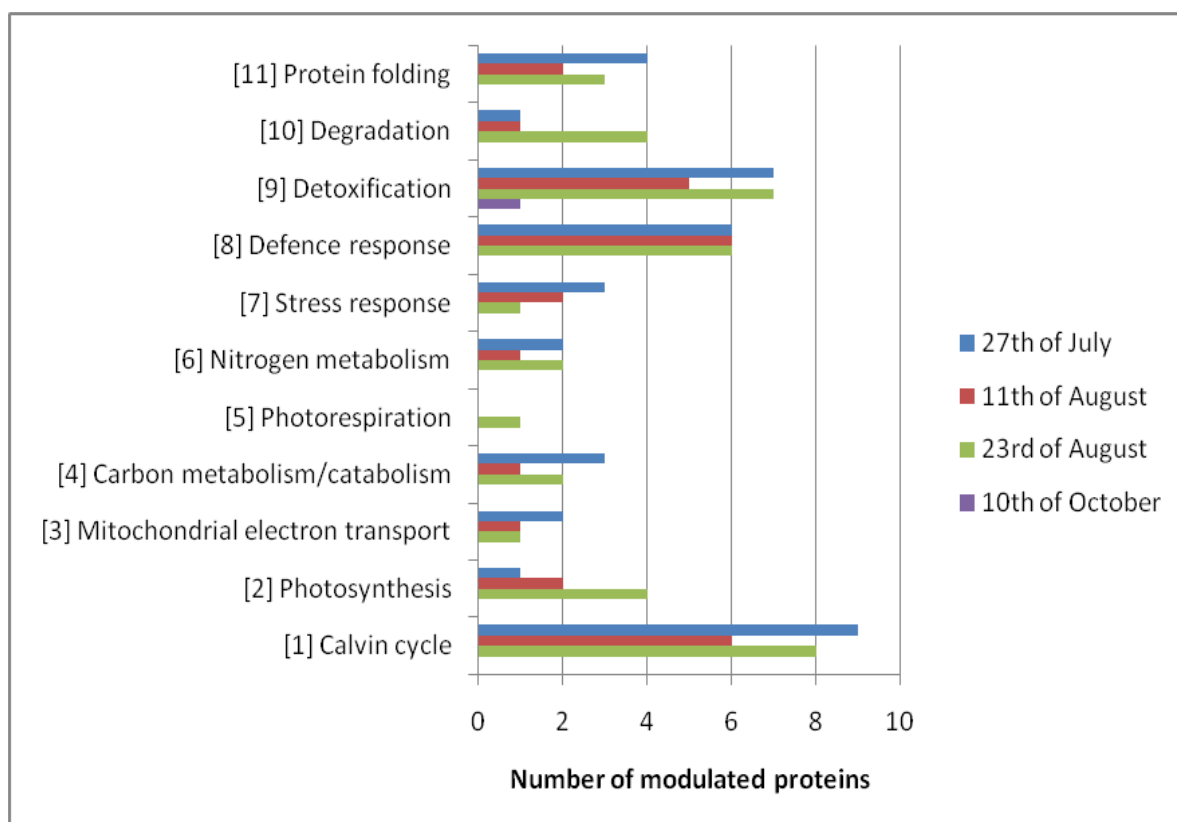


Fig. 21 – Bar diagram showing the amount of identified proteins classified according to biological functions for each single time point.

Statistical information about spots representing single proteins is summarized in Tab. 4, whereas the appearance of modulated spots on the gel is illustrated in Fig. 22 and Fig. 23. Differences between total amount of regulated protein spots and number of identified proteins rely in (i) the presence of multiple proteins for a specific spot, (ii) the occurrence of a protein in multiple locations on the 2-D gel and (iii) the lack of information for several spots, since they were not visualized on the preparative gels. In the following section it will be attempt to characterize differentially expressed proteins showing a single annotation in a spot.

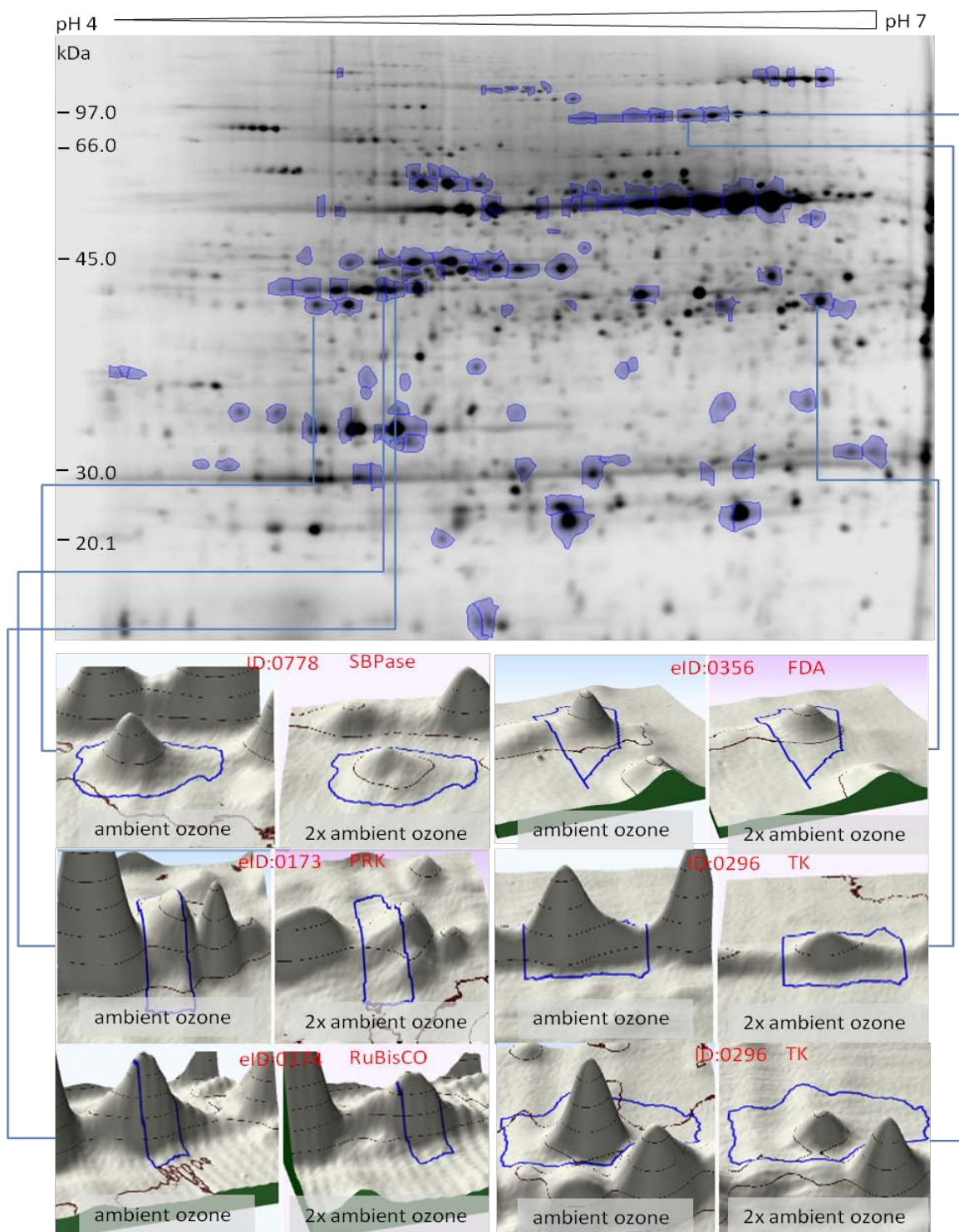


Fig. 22 – Cy2 labeled 2-D gel of separated proteins from European beech leaves. Blue labeled spots on the 2-D gel were down-regulated following elevated ozone exposure. Zoomed squares at the bottom exemplify patterns of protein regulation between control and treated samples. SBPase: sedoheptulose 1,7 bisphosphatase; PRK: phosphoribulokinase; RuBisCO: ribulose-1,5-bisphosphat-carboxylase/-oxygenase; FDA: fructose bisphosphate aldolase; TK: transketolase.

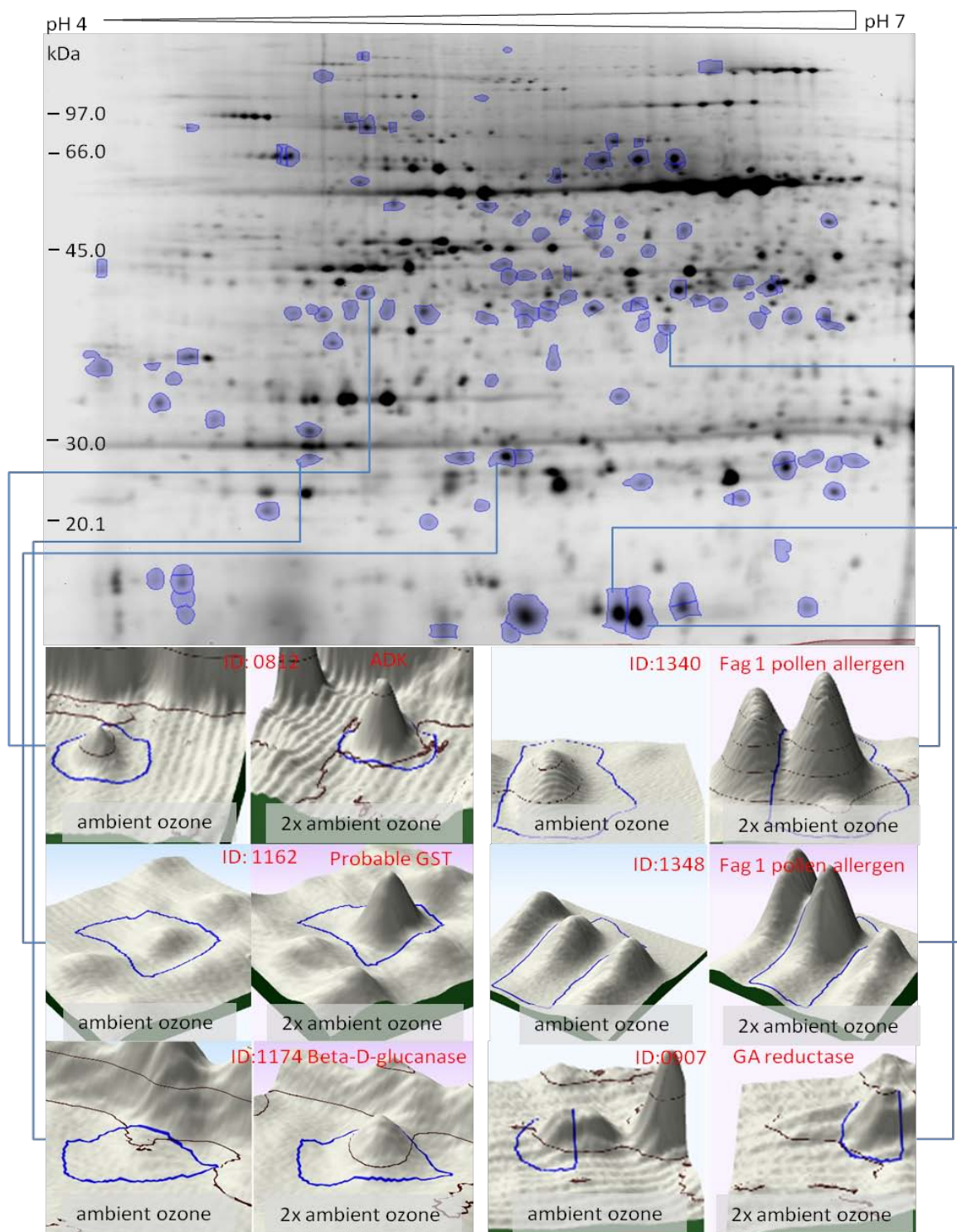


Fig. 23 - Cy2 labeled 2-D gel of separated proteins from European beech leaves. Blue labeled spots on the 2-D gel were up-regulated following elevated ozone exposure. Zoomed squares at the bottom exemplify patterns of protein regulation between control and treated samples. ADK: adenosine kinase 2; Probable GST: probable glutathion S-transferase; GA reductase: galacturonic acid reductase.

Tab. 4 continued. List of single proteins identified in a spot for the sampling time point of 11th of August.

Spot ID	Accession number	Identified protein	p-values Bonferroni corrected						q-value				Z-ratio		Protein fold change					
			ZS-N	RZ-N	VS-N	VG-N	L-N	Q-N	ZS-N	RZ-N	VS-N	VG-N	L-N	Q-N	ZS-N	RZ-N	VS-N	VG-N	L-N	Q-N
Calvin cycle																				
eID:0173	P27774	Phosphoribulokinase, chloroplastic						*							-1,51					
eID:0174	Q40281	RuBisCO activase, chloroplastic						*	*	*	*	*		-1,79	-1,72	-0,39	-0,42		-0,33	
ID:0651	Q40281	RuBisCO activase, chloroplastic						*	*	*	*			-1,42	-1,37	-0,35	-0,36			
ID:0778	P46283	Sedoheptulose-1,7-bisphosphatase, chloroplastic						*							-1,24					
ID:0779	O20252	Sedoheptulose-1,7-bisphosphatase, chloroplastic	*	*				**	*	**	**				-1,64	-1,74	-0,35	-0,38		
ID:0295	Q43848	Transketolase, chloroplastic						*			*				-1,29			-0,33		
Photosynthesis																				
ID:1307	P26291	Cytochrome b6-f complex iron-sulfur subunit, chloroplastic						*	*		*				-1,19	-1,11		-0,31		
eID:0101	Q9ZUC1	Quinone oxidoreductase-like protein At1g23740, chloroplastic						*	*	*	*	*	*		1,82	2,03	0,94	0,82	0,81	0,90
Mitochondrial electron transport																				
ID:1372	P80499	Cytochrome c oxidase subunit 5B, mitochondrial	*		*	*	*	*	**	*	**	**	**	**	2,93	3,04	1,77	1,64	1,43	1,35
Carbon metabolism/catabolism																				
ID:0845	Q9SN86	Malate dehydrogenase, chloroplastic						*	*	*	*	*	*		3,11	3,39	1,81	1,57	1,46	1,54
Nitrogen metabolism																				
ID:0673	P15102	Glutamine synthetase leaf isozyme, chloroplastic						*	*		**				-1,13	-1,14		-0,32		
Stress response																				
ID:0812	Q9LZG0	Adenosine kinase 2						*								0,86				
eID:0031	P43309	Polyphenol oxidase, chloroplastic											*	*					1,07	1,10
Defense response																				
eID:0353	Q9ZT66	Endo-1,3;1,4-beta-D-glucase						*	*	*	*	*	*	*	1,25		0,54	0,54	0,51	0,49
ID:1174	Q9ZT66	Endo-1,3;1,4-beta-D-glucase						*	*	*	*	*	*	*	2,21	2,47	1,82	1,35	1,60	1,53
eID:0053	B7TWE7	Fag s 1 pollen allergen ⁺					*	*	*	*	*	*	*	*	2,13	2,60	1,17	1,01	1,43	1,41
eID:0290	B7TWE7	Fag s 1 pollen allergen ⁺					*	*	*	*	*	*	*	*	3,06	3,34	2,21	1,73		2,19
ID:1340	B7TWE7	Fag s 1 pollen allergen ⁺	**				**	**	**				**	**	2,27				1,63	1,33
ID:1348	B7TWE7	Fag s 1 pollen allergen ⁺					*	*	*	*	*	*	*	*	2,59	2,73	1,37	1,19	1,81	1,46
Detoxification																				
ID:0907	A1Y2Z0	Galacturonic acid reductase ⁺						*	*		**	*	*		1,77	1,85		0,84	0,64	0,67
ID:1162	Q03662	Probable glutathione S-transferase											*							1,22
ID:1166	Q03662	Probable glutathione S-transferase						*	*	*	*	*	*	*	1,47	1,57	0,74	0,66	0,57	0,56
eID:0526	Q23264	Putative selenium-binding protein	*	*				**	*	*	*				-1,56	-1,55	-0,35	-0,39		
ID:0993	Q8LAS8	S-formylglutathione hydrolase						*	*		*	*	*		-1,76	-1,81		-0,43	-0,43	-0,43
Degradation																				
ID:0450	Q9FMP3	Dihydropyrimidase +									*						0,43			
Protein folding																				
ID:0863	Q68BK5	Peptidyl-prolyl cis-trans isomerase ^o									**	*	*				0,85	0,48	0,37	
ID:1014	Q68BK5	Peptidyl-prolyl cis-trans isomerase ^o									*						0,75			

Tab. 4 continued. List of single proteins identified in a spot for the sampling time point of 23rd of August.

Spot ID	Accession number	Identified protein	p-values Bonferroni corrected					q-value					Z-ratio		Protein fold change				
			ZS-N	RZ-N	VS-N	VG-N	L-N	Q-N	ZS-N	RZ-N	VS-N	VG-N	L-N	Q-N	ZS-N	RZ-N	VS-N	VG-N	L-N
Calvin cycle																			
eID:0173	P27774	Phosphoribulokinase, chloroplastic																	
eID:0174	Q40281	RuBisCO activase, chloroplastic	**	**	**	**	**	*				**							
ID:0651	Q40281	RuBisCO activase, chloroplastic	***	***	*	**	**				***	***	***	***	***	***	***	***	***
ID:0778	P46283	Sedoheptulose-1,7-bisphosphatase, chloroplastic									*	*	*						
ID:0779	O20252	Sedoheptulose-1,7-bisphosphatase, chloroplastic	**	***	**	***	***	*			***	***	***	***	***	***	***	***	***
ID:0295	Q43848	Transketolase, chloroplastic									**	**	**	**	**	**	**	**	**
ID:0296	Q43848	Transketolase, chloroplastic									***	*	**	**	*				
ID:0626	Q43848	Transketolase, chloroplastic									*								
Photosynthesis																			
eID:0350	P26291	Cytochrome b6-f complex iron-sulfur subunit, chloroplastic									**	**		**	**				
ID:1307	P26291	Cytochrome b6-f complex iron-sulfur subunit, chloroplastic									**	**							
eID:0165	Q40459	Oxygen-evolving enhancer protein 1, chloroplastic									*	*	*	*					
eID:0101	Q9ZUC1	Quinone oxidoreductase-like protein At1g23740, chloroplastic				*					**	**	**	**	**	**			
Mitochondrial electron transport																			
ID:1372	P80499	Cytochrome c oxidase subunit 5B, mitochondrial	*		*	*	*	*			**	**	**	**	**	**	**	**	**
Carbon metabolism/catabolism																			
ID:0845	Q9SN86	Malate dehydrogenase, chloroplastic									*	*	*	*	*	*	*	*	*
ID:0860	Q9SID0	Probable fructokinase-1/2									**	*							
Photorespiration																			
ID:0170	O49954	Glycine dehydrogenase [decarboxylating], mitochondrial																	*
Nitrogen metabolism																			
ID:0673	P15102	Glutamine synthetase leaf isozyme, chloroplastic	*	*							**	***							
ID:0999	P15102	Glutamine synthetase leaf isozyme, chloroplastic									**	*							
Stress response																			
ID:0812	Q9LZG0	Adenosine kinase 2		*	**						**	**	***						
eID:0031	P43309	Polyphenol oxidase, chloroplastic						**	*										***
Defense response																			
eID:0353	Q9ZT66	Endo-1,3;1,4-beta-D-glucanase									**	**	**	**	**	**	**	**	**
ID:1174	Q9ZT66	Endo-1,3;1,4-beta-D-glucanase									**	**	**	**	**	**	**	**	**
eID:0053	B7TWE7	Fag s 1 pollen allergen ⁺	**	**	**	**	**	***			***	***	***	***	***	***	***	***	***
eID:0290	B7TWE7	Fag s 1 pollen allergen ⁺									**	**	**	**	**	**	**	**	**
ID:1340	B7TWE7	Fag s 1 pollen allergen ⁺	**				**	***			***	***	***	***	***	***	***	***	***
ID:1348	B7TWE7	Fag s 1 pollen allergen ⁺	*	*	**	**	**	**			**	**	**	**	**	**	**	**	**
Detoxification																			
ID:0462	O04130	D-3-phosphoglycerate dehydrogenase									*	*							
ID:0907	A1Y2Z0	Galacturonic acid reductase ⁺	*			*	*	*			**	**	**	**	**	**	**	**	**
ID:1162	Q03662	Probable glutathione S-transferase																	*
ID:1166	Q03662	Probable glutathione S-transferase									**	**	**	**	**	**	**	**	**
eID:0526	O23264	Putative selenium-binding protein	**	***		*	*	*			***	***	***	***	***	***	***	***	***
ID:0993	Q8LAS8	S-formylglutathione hydrolase			*	*	*	*			**	**	**	**	**	**	**	**	**
Degradation																			
ID:0262	P35100	ATP-dependent Clp protease ATP-binding subunit clpC homolog, chloroplastic									*	*	*	*	*	*	*	*	*
eID:0124	A7LAB9	Cysteine protease Cp ⁺																	**
ID:0445	Q9LD90	Dihydropyrimidinase ⁺																	*
ID:0450	Q9FMP3	Dihydropyrimidinase ⁺						*			**	**	**	**	**	**	**	**	**
Protein folding																			
ID:0562	P34106	Alanine aminotransferase 2									*	*	*	*	*	*	*	*	*
ID:1014	Q68BK5	Peptidyl-prolyl cis-trans isomerase ^o			*						**	**	**	**	**	**	**	**	**
ID:0434	Q9XF61	Protein disulfide-isomerase																	*

present in the leaves was affected after treatment, ozone may indirectly reduce CO₂ fixation by reducing amounts of RuBisCO activase. As a consequence of decreased CO₂ fixation, less enzyme intermediates are needed in the Calvin cycle to process the substrate. These results indicate a general reduction of the Calvin cycle, which may also be explained by decreased levels of the mitochondrial glycine dehydrogenase (spot ID:0170^{23.08}) a protein involved in photorespiration and therefore coupled to the Calvin cycle.

Calvin cycle activity has been put forward as a major sink of adenosine triphosphate (ATP) and nicotinamide adenine dinucleotide phosphate (NADP) produced during photosynthesis (Lawson et al. 2002). Thus, an overall decrease in the activity of the Calvin cycle upon ozone exposure would release an accumulation of both photosynthetic products. In order to prevent photooxidative damage, plants may down-regulate the electron transport chain of photosynthesis and the photosystem II (Ranieri et al. 2001; Bohler et al. 2007). The results presented in this study support previous hypothesis since in the photosynthetic electron transport chain elevated ozone exposure decreased abundance levels of two isoforms of cytochrome b6-f complex iron-sulfur subunit (spot ID:1307^{11.08, 23.08}/eID:0350^{23.08}). Furthermore an oxygen evolving enhancer protein 1 (spot eID:0165^{23.08}) peripherally bound to photosystem II also decreased in abundance. In contrast, a quinone oxidoreductase-like protein (spot eID:0101^{27.07, 11.08, 23.08}), an enzyme not belonging to the photosystem element, was up-regulated during the three sampling time points of the ozone exposure. The up-ward trend is consistent with a previous work carried out on poplar trees exposed to short-term ozone exposure (Bohler et al. 2007). This behavior was explained as a possible reaction to avoid electron leakage during photosynthesis. The present findings overlap rather well with previously reported transcript analysis from this study, which revealed a down-regulation of ESTs related to photosynthesis (chloroplast thioredoxin M-type, chlorophyll a/b-binding protein type Ia and Ib, and oxygen evolving enhancer protein precursor and chloroplast envelope quinone-oxidoreductase of electron transport and photosystem I reaction center subunit XI and subunit X psaK) on the 27th of July and partially on the 11th of August 2006 (Olbrich et al. 2009). For both sampling time points the transcript analysis also demonstrates increased levels of the NADP: quinone oxidoreductase (Fig.24).

Elevated ozone also decreased gene expression levels of quinone oxidoreductase-like protein in two silver birch genotypes subjected to ozone exposure over a period of two growing seasons

(Kontunen-Soppela et al. 2010). Furthermore similar results as in this experiment were found in soybean leaves following short-time periods of ozone exposure (Ahsan et al. 2010).

An ozone related down-regulation of enzymes associated with the Calvin cycle suggests that less triose-phosphates are produced during the CO₂ fixation process, thus leading to a decreased availability of substrates for energy production (Bohler et al. 2007). Initially most triose-phosphates are used in the synthesis of starch and sucrose, the primary products of photosynthesis and the most important energy source in plants. The results presented here indicate a general down-regulation of the Calvin cycle, and consequently its product triose-phosphate. This suggestion might further explain the reduced levels of starch and sucrose concentrations in leaves exposed to elevated ozone fumigation (Fleischman 2009). Similar results were reported in juvenile as well as mature beech leaves exposed to elevated ozone (Liu et al. 2004; Blumenröther et al. 2007).

Carbon metabolism/catabolism

In contrast to the Calvin cycle and the photosynthetic apparatus, five proteins involved in carbon metabolism/catabolism increased in concentration in elevated ozone exposed beech leaves. There is strong evidence that catabolic pathways (e.g. glycolysis, hexose monophosphate pathway, Krebs cycle and the mitochondrial electron transport system) are up-regulated upon ozone exposure in order to maintain the energy and the reducing power needed to detoxify and repair cellular damage caused by ROS (Dizengremel 2001; Bohler et al. 2007; Dizengremel et al. 2009; Ahsan et al. 2010). In fact, the present results showed that in July and at the end of August, higher protein amounts of a probable fructokinase isoform (spot ID:0860^{27.07, 23.08}/ID: 0848^{27.07}) were present. This phosphotransferase is involved in carbon metabolism/catabolism used for respiration and biosynthesis of starch and other complex carbohydrates (Odanaka et al. 2002). Moreover, twice ambient ozonated beech leaves showed increased levels of the Krebs cycle related malate dehydrogenase in July and August (spot ID:0845^{27.07, 11.08, 23.08}). Similarly, proteins needed for generating an electrochemical potential and for production of ATP in the mitochondrial electron transport chain, namely cytochrome c oxidase subunit 5B (spot ID:1372^{27.07, 11.08, 23.08}) and ATP synthase subunit d (spot ID:1250^{27.07}), were up-regulated in treated leaves (Fig.24).

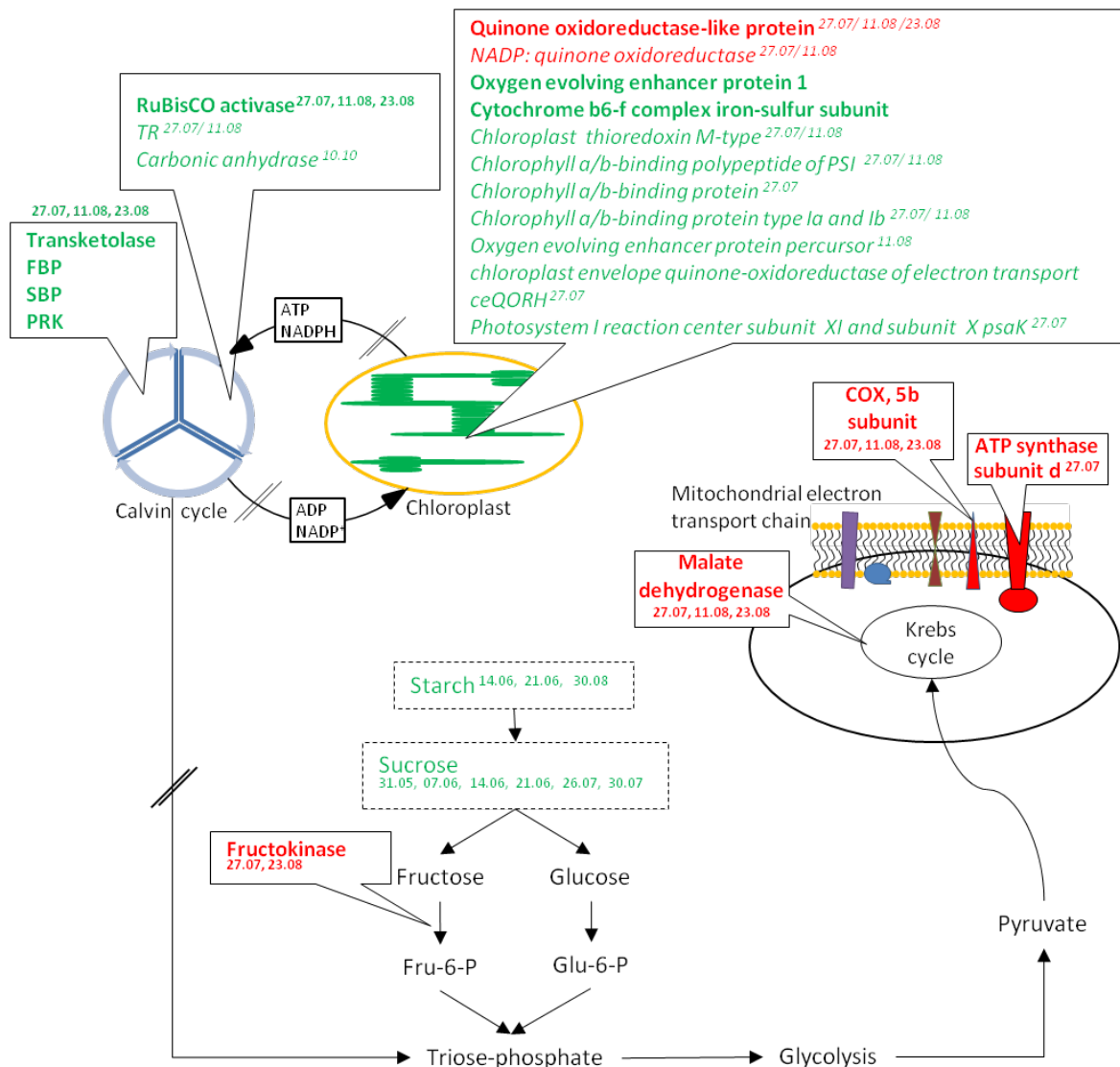


Fig.24 - Molecular responses in the carbon metabolism of beech leaves to elevated ozone exposure. Transcripts/proteins/metabolites labeled in green and red are respectively down and up-regulated. Transcripts are indicated in italics. Proteins are represented by the bolted text in the legend symbols. Date after the transcripts/proteins/metabolites indicate the date of specific regulation. RuBisCO activase: ribulose-1,5-bisphosphate carboxylase oxygenase activase; TR: thioredoxin; ceQOR: chloroplast envelope quinone-oxidoreductase of electron transport; FBP: Fructose-bisphosphate aldolase; PRK: phosphoribulokinase; TKTL: transketolase; SBP: sedoheptulose-1,7-bisphosphatase; COX: 5b subunit, cytochrome c oxidase subunit 5B.

In Scots pine needles, ozone led to increased enzymatic activities of cytochrome oxidase (Luethy-Krause et al. 1990). Furthermore, ozone increased mitochondrial respiration rates of aspen clones (Coleman et al. 1995), hybrid polar (Reich 1983) and ginkgo biloba (He et al. 2007). Higher amounts of both molecules points to an increase in respiration, which is a putative defense response and repair mechanism in ozone damaged tissues (Bahl et al. 1993). Moreover, an

increase in respiration was observed to be linked with a simultaneous reduction in photosynthesis (Roshchina et al. 2003), which already have been shown in this experiment. These observed changes in photosynthesis and the fact that the leaf starch and sucrose concentrations were significantly reduced in this experiment (Fleischman 2009), indicates that beech leaves activate the catabolic pathways to degrade starch and sucrose in order to feed the Krebs cycle with pyruvate, thus providing energy needed to counteract ROS-related stress.

Defense and stress related responses

Stress/defense related responses were among the main effects after beech leaves were exposed to long-term elevated ozone fumigation. Two isoforms of the PR class 2 protein 1,3;1,4- β -D-glucanase (spot eID:0353^{27.07, 11.08, 23.08}/ID:1174^{27.07, 11.08, 23.08}), were significantly increased in abundance in July and August. Among other roles it mediates specific degradation of cell wall 1,3;1,4- β -D-glucans, thus weakening and decomposing fungal cell walls containing glucans (Edreva 2005). Other studies proposed that the mechanism of its generation is mediated by ethylene, a plant stress hormone that has also been induced in plants by the effect of ozone (Ernst et al. 1996; Thalmair et al. 1996). One of the highest expression levels was observed in July and August in four isoforms of the enzyme fag s 1 pollen allergen (spot eID:0290^{27.07, 11.08, 23.08}/ID:1348^{27.07, 11.08, 23.08}/eID:0053^{27.07, 11.08, 23.08}/ID:1340^{27.07, 11.08, 23.08}), a PR class 10 protein. Proteins belonging to the group PR-10 were identified as major tree pollen allergens in birch and related species. Fag s 1 pollen allergen showed allergens cross-reactive with the major birch pollen allergen Bet v 1, which is the main cause of type I allergies observed in early spring (Egger et al. 2008). It has been reported that beech-pollen-allergic individuals tested positive to the recombinant Fag s 1.0101 produced in *E. coli* following a basophil mediator release assay and analysis of immunoglobulin E (Du et al. 2011). The response of this enzyme reported here can be used as a basis for further studies to assess the potential of allergen sources in beech under polluted conditions.

The group of PR proteins, which are induced by different stress stimuli are assigned an important role in plant defense against pathogenic constraints (Edreva 2005) and abiotic stresses such as heavy metal salts, u.v.-B light and ozone (Ernst et al. 1992; Agrawal et al. 2002; Fühns et al. 2008; Du et al. 2010). The results presented here and previously described transcript analysis (Olbrich et

al. 2005; Olbrich et al. 2009) demonstrate that PR-proteins play a role in the molecular response of European beech to elevated ozone exposure. Although the synthesis of PR-proteins have been described under both biotic and abiotic stressors, the mechanisms of its regulation is not very well understood. One likely cause of a common modulation against different stressors could be evolutionary pressure towards the protection of the plant against different pathogens and abiotic stresses (Kim et al. 2009).

Regarding stress-related responses, elevated ozone influenced to a high degree the synthesis of polyphenol oxidase (PPO, spot eID:0031^{27.07, 11.08, 23.08}) on July and August. This result is supported by previous studies that indicate induced activity of PPO in plants under stress, wounding and pathogen attack (Thipyapong et al. 1997; Tran et al. 2011), thus substantiating the role of PPO in resistance to abiotic stress and pathogens. With respect to this protein category, an overall accumulation of adenosine kinase (ADK, spot ID:0812^{27.07}) and an ankyrin repeat domain-containing protein (spot eID:0677^{27.07}) was found on 27th of July. ADK participates in the regeneration of S-adenosyl-methionine (SAM). Since SAM serves as a precursor of the plant hormone ethylene, a signaling-molecule which regulates plant defense responses, including cell death, the present result indicates ADK as an important enzyme involved in the defense, adaptation and/or cell death mechanism to long-term ozone exposure in beech leaves. Parallel to this, ankyrin repeat domain-containing protein has been proposed as regulator of JA and SA (Zhou et al. 2006), molecules involved in the response to different stressors by containing and spreading leaf lesions and cell death (Overmyer et al. 2000; Yuan et al. 2008; Castagna et al. 2009). The increased amounts of PPO and the possible increase in levels of JA, SA and ethylene support the idea that different defense mechanisms act in concert as synergistic/antagonistic partners to control the spread or containment of leaf lesions in ozone-exposed juvenile beech trees.

Detoxification mechanism

Ozone spontaneously generates ROS in the leaf apoplast, which in last instance, may destroy lipids, proteins, terpenoids, carbohydrates, and nucleic acids (Horling et al. 2001; Langebartels et al. 2002). This damage is kept under control by antioxidant molecules and enzymes in different cell compartments (Hajheidari et al. 2005). In accordance with previous research, beech trees

showed a total of seven differentially expressed proteins under elevated ozone exposure, all of which show directly or indirectly an association to the detoxification system.

Two of these spots (spot ID:1162^{27.07, 11.08, 23.08} and ID:1166^{27.07, 11.08, 23.08}) showing higher levels in treated leaves in July and August were identified as a glutathione S-transferase. This enzyme plays an important role in the detoxification process of cells by catalyzing the conjugation of electrophilic xenobiotic substrates with the tripeptide glutathione (GSH), thus limiting damage in oxidative stress conditions (Sharma et al. 1994; Dixon et al. 2010). Another two up-regulated proteins involved in the detoxification process were D-galacturonic acid reductase (GalUR, spot ID:0907^{27.07, 11.08, 23.08}) and D-3-phosphoglycerate dehydrogenase (PHGDH, spot ID:0462^{23.08,10.10}). Previously, it was reported that *A. thaliana* and potato plants overexpressing GalUR gene showed increased levels of ascorbic acid, an essential antioxidant in cell metabolism (Agius et al. 2003; Hemavathi et al. 2009). In addition, serine, mediated among others by PHGDH, is a likely precursor of the strong antioxidant compound cysteine (Larsson et al. 1979). Since antioxidants are important free radical scavengers, the present results indicate that higher amounts of both proteins are synthesized in beech leaves to counteract enhanced levels of oxygen radicals encountered in an elevated ozone environment.

Up-regulated spot eID:0807^{27.07} encodes for an epoxide hydrolase 3. In view of the fact that epoxide hydrolase convert reactive epoxides to trans-dihydrodiols, which are conjugated and excreted from cells, its modulation indicates the role of epoxide hydrolase 3 in the process of detoxification. Moreover, increased levels of this enzyme may indicate increased synthesis of cutin, a polymer that has been reported to accumulate in the cell wall of wounded tissues (Benedetti et al. 1998).

In contrast, three proteins of this category were down-regulated upon elevated ozone exposure. Cytoplasmic aconitate hydratase (spot ID:0160^{27.07}), a protein which participates in the glyoxylate cycle, was observed on the 27th of July. The active enzyme contains an iron-sulfur cluster that is lost among others under oxidative stress conditions, thus leading to an increase in free Fe²⁺ in the cytosol. In turn, the released Fe²⁺ may react with H₂O₂ to form a powerful reactive hydroxyl radical, thereby enhancing cell death (Moeder et al. 2007). The decreased ratios of aconitate hydratase observed in the present study suggest that less Fe²⁺ is released under elevated ozone conditions, thus preventing synthesis of Fe²⁺-mediated radicals. The last two proteins were

identified as putative selenium-binding protein 1 (SBP1, spot eID:0526^{27.07, 11.08, 23.08}) and the GSH providing enzyme S-formyl glutathione hydrolase (spot ID:0993^{27.07, 11.08, 23.08}). Since the synthesis of SBP1 is likely involved in detoxification mechanisms (Shinozaki et al. 1997; Hugouvieux et al. 2009) and GSH is pivotal for reducing poisonous H₂O₂ accumulated during ozone stress, no satisfactory explanations was found for their observed down-regulation in elevated ozone treated plants. The downward expression of both proteins most likely suggests increased vulnerability of plants to toxic injury.

Protein folding and degradation

Plants exposed to increased concentrations of oxidative stress may induce synthesis, degradation and rebuilding of proteins as they adapt to new, adverse environmental conditions. Misfolded and damaged proteins are eliminated by housekeeping degradation proteins and replaced by newly formed ones i.e., pathogenesis-related proteins or detoxification proteins (Grudkowska et al. 2004). In contrast to the control group, elevated ozone fumigated trees showed six modulated proteins associated with degradation and protein folding functions. Two isoforms of alanine aminotransferase 2 (spot ID:0562^{27.07, 23.08}/ID:0565^{27.07}), a transporter protein involved in amino acid biosynthesis, appeared to undergo decreased amounts at both the transcript (Olbrich et al. 2009) and the protein level. Also spot ID:0262^{23.08} identifying a subunit clpC homolog of the Clp protease showed decreased amounts upon elevated ozone exposure. In contrast, cysteine protease (spot eID:0124^{27.07, 23.08}), a multi-faceted protein induced under stress and senescing conditions, revealed higher amounts under elevated ozone exposure. Additionally, two putative molecular chaperones known to play a key role in stabilizing and refolding proteins during cellular exposure to stress appeared to be oppositely regulated. Protein disulfide-isomerase (spot ID:0434^{27.07, 23.08}) appeared to increase, which was previously reported in poplar leaves exposed to short-time periods of ozone stress (Bohler et al. 2007; Bohler et al. 2010). In contrast, two isoforms of peptidyl-prolyl cis-trans isomerase (spot ID:1014^{11.08, 23.08}/ID:0863^{11.08}) showed a downward trend in July and August.

Accelerated senescence

There is strong evidence that elevated ozone exposure induces early leaf senescence in plants (Miller et al. 1999; Saleem et al. 2001; Olbrich et al. 2005; Bohler et al. 2007). These detrimental effects can be attributed to the ozone-induced oxidative stress as a result of increases in ROS production. In the present study, premature leaf senescence could be indicated by the modulation of four proteins involved in nitrogen metabolism, protein degradation and the carbon fixation. One of the processes associated with senescence is the reallocation of nutrients that

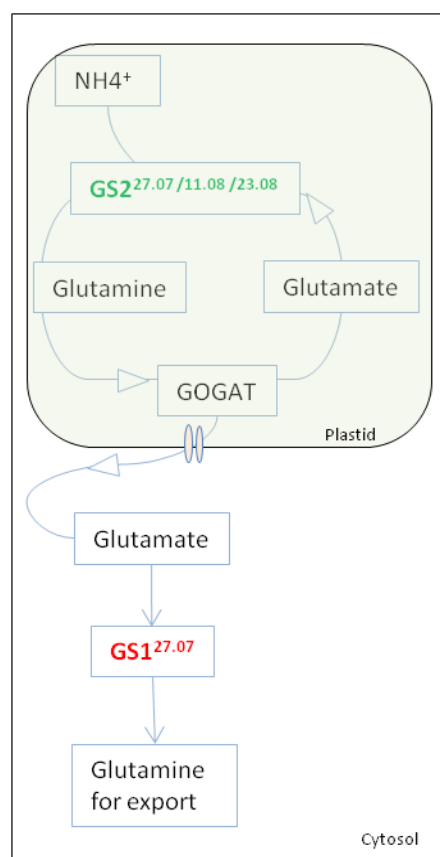


Fig. 25- Schematic representation of the altered GS1 and GS2 amounts during elevated ozone exposed leaves. GS1, cytosolic glutamine synthetase 1; GS2, chloroplastic glutamine synthetase. The red and green colored protein represents up- and down- regulated isoforms respectively.

were previous invested in leaves. Beech trees exposed to elevated ozone showed increased amounts of cytosolic glutamine synthetase (GS1, spot ID:1177^{27.07}) in July and decreased ratios of its chloroplastic isoform (GS2, spot ID:0999^{27.07, 23.08}/ID:0673^{11.08, 23.08}) for the three time points analyzed in July and August (Fig. 25). Among both isoforms, GS2 has been reported to be the prominent, active enzyme in healthy plants showing photosynthetically competent tissues, whereas GS1 was described as a minimally represented enzyme (Edwards et al. 1989). During senescence, ammonia assimilation is progressively shifted from the chloroplast to the cytosol (Brugière et al. 2000; Cantón et al. 1999) (Fig. 25). The present results confirm the early studies showing that under natural senescence and certain stress conditions, plants enhance GS1 synthesis in order to generate glutamine for nitrogen transport to sink tissues.

One of the obvious enzymatic events that occur in the senescence process is the activation of protein degrading enzymes. As previously described, cysteine protease (spot eID:0124^{27.07, 23.08}) is involved in a variety of proteolytic functions and has been previously detected during senescence processes (Buchanan-Wollaston et al. 1997; Solomon et al. 1999; Grudkowska et al. 2004). For instance, the expression of the senescence-associated gene SAG 12 coding for a cysteine proteinase, is specifically controlled by

developmental senescence in *A. thaliana*. Its expression appears to be controlled by developmental pathways that are induced during aging, for example when plants reduce photosynthetic output (Noh et al. 1999). In fact, the higher amounts of cysteine protease observed in this study correlate negatively with the decreased amounts of carbon fixation and photosynthesis related proteins, as well as transcripts related to photosynthesis.

The up-regulated protein dihydropyrimidinase (spot ID:0445^{23.08}/ID:0450^{27.07, 11.08, 23.08}) was observed in elevated ozone treated beech leaves. Although it has been associated with cellular response to nitrogen levels, further functional characterization is needed to better understand its role in elevated ozone exposed beech leaves.

Correlation between modulated transcripts and proteins

Another focus in the present study was the correlation between quantified mRNA levels and protein abundances as a tool to understand cellular processes. Joint analysis of the transcriptomic and proteomic profiles appears obvious following the general assumption that a change on the mRNA level leads to a change on the protein level (Perco et al. 2010). Furthermore, through this combined analysis it is possible to validate molecular mechanism systemically in juvenile beech trees exposed to elevated ozone concentrations.

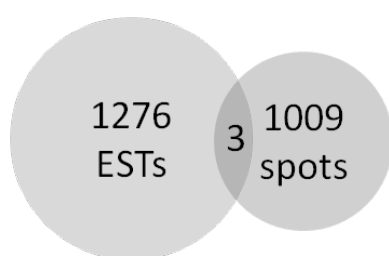


Fig. 26 - Venn-Diagram based on the number of used transcripts and protein spots. Only 3 transcripts/proteins were commonly modulated between both omics approaches. ESTs, expressed sequence tags used for the transcript analysis.

Although the comparative analysis used the same sample source and harvesting time points, only three proteins, namely chloroplastic fructose-bisphosphate aldolase, alanine aminotransferase and a chloroplastic quinone oxidoreductase-like protein showed a direct feature overlap with the transcript analysis (Fig. 26). The moderate correlation is not surprising and has been reported in other studies, although in different magnitudes (Greenbaum et al. 2003; Koji et al. 2003; Perco et al. 2010). This is explained by various reasons, and can be grouped based on sources. Technical reasons imply i) selection of high spot resolution IEF stripes on the 2-D gel which was at the expense of smaller used pH ranges, thus reducing the amount of analyzed spots. ii) In many cases multiple proteins were identified in

one spot, making a comparison of modulated transcript and proteins impossible. iii) Proteins with extreme low- and high molecular weights as well as proteins with extreme basic and acidic characteristics are difficult for 2D-PAGE to separate, thus limiting the number of identified proteins. Biological reasons for the low overlap may be explained by post-transcriptional regulators (i.e. miRNA interactions) resulting in translational repression and gene silencing, and post-translational modifications that may affect protein half-life. However, when the resulting data were compared at the functional classification level, in other words, transcripts/proteins that are commonly modulated in specific processes, higher correlations were achieved. This is observed in particular in photosynthetic pathways, as well as in pathways related to disease/defense response and detoxification mechanisms. The findings at the protein level might validate transcript analysis and confirm that the pathways mentioned above are altered by the effect of long-term ozone exposure on beech trees. Oppositely other processes such as nitrogen metabolism and pathways related to mitochondrial activity showed no correlation between both omics levels.

3.2.3 Juvenile beech trees fumigated with free-air elevated ozone and post infected with the root pathogen *P. plurivora*

The aim of this study was to assess the role of long-term elevated ozone impact on the protein expression patterns of beech trees influenced by the root pathogen *P. plurivora*. Each treatment was represented by four trees grown inside lysimeters. Previous transcript analysis from the same experiment clearly showed differences between twice ambient ozone exposed plants (n=8) and plants with an additional *P. plurivora* infection (n=8) (Ernst D, 2011. Personal communication), although the magnitude of the response was lower when comparing trees under the exposure of different ozone concentrations. Despite this fact, the results presented here show no significant difference in any of the group interactions, neither when ambient ozone treated saplings were compared with saplings exposed to twice ambient ozone, nor when inoculated with *P. plurivora* (Fig. 27). Already in the previous study, comparing ambient and twice ambient ozone fumigated trees, high standard deviations were observed between spots of different groups (data not shown). For this reason, and the fact that the present study consist of only four biological replicates, there is strong evidence to assume that the effect of the induced biotic and abiotic

stress might be overlaid by biological variation of the system. In fact, a major obstacle to reliably determining quantitative changes in the protein expression is to overcome differences imposed by technical and biological variation (Molloy et al. 2003). As for the present study, only spots showing low variances among gels were used it is possible that the variability presented here is of biological nature.

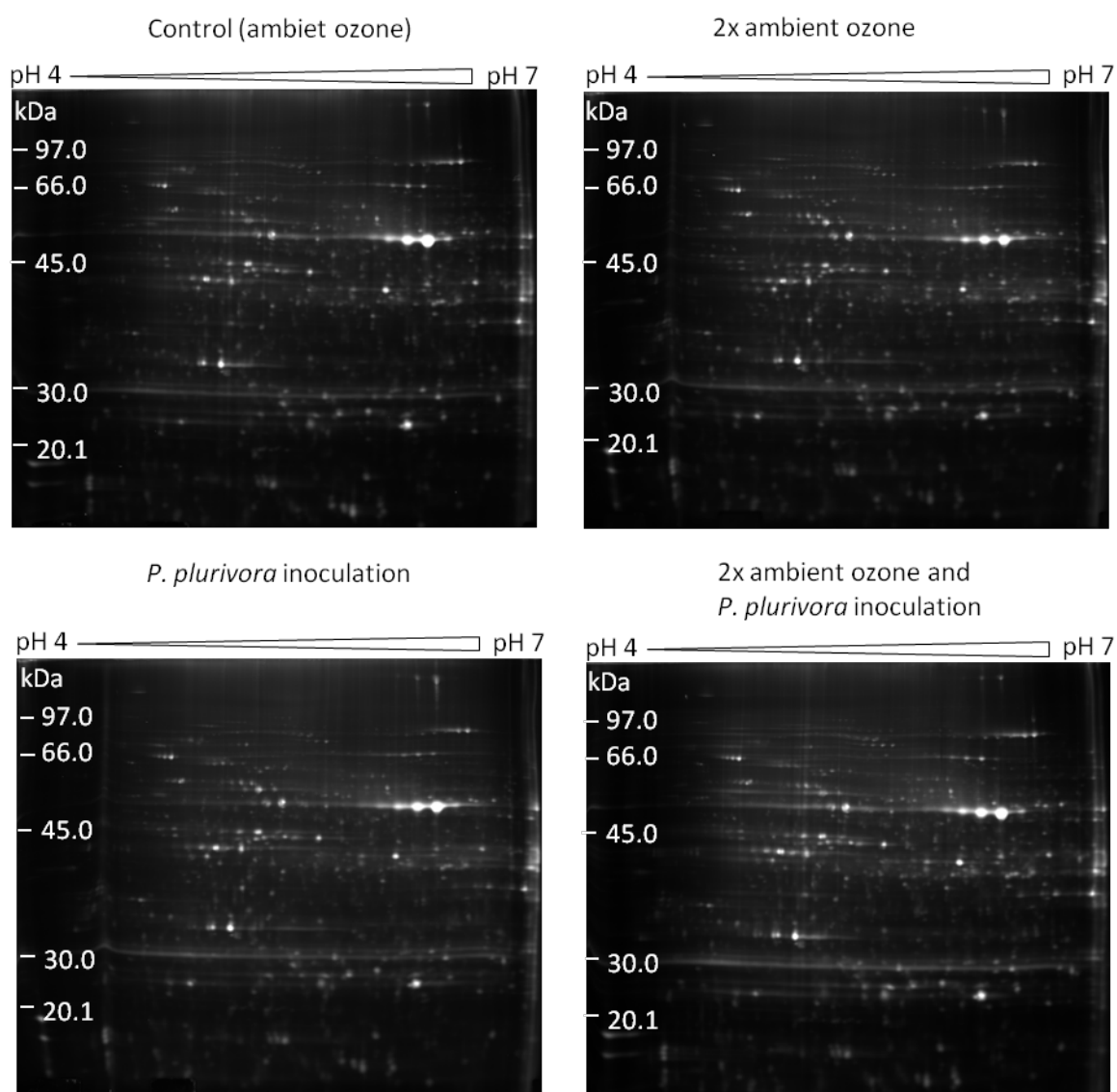


Fig. 27 - Raw 2-D DIGE gels showing separated leaf proteins from beech trees grown under ambient and 2x ambient ozone conditions as well as under *P. plurivora* inoculation and the combined effect of both treatments. No of the treatments showed statistical differences compared to the controls (ambient ozone treated beech trees).

The origin of biological variance arises, among other factors, from differences in microenvironments and genotypical variations within a heterozygous organism (Jorge et al. 2005). In European beech, the biological variability has already been encompassed in several genetic, enzymatic and morphological traits such as the spatial and temporal variation in gene frequency (Jump et al. 2006), allelic variations (Sander et al. 2000), enzyme gene markers (Müller-Starck et al. 1992), and the morphological plasticity (Kramer 1995). Notwithstanding these extensive descriptions, no data has been reported to explain the proteome variability. Thus, more information is needed to assess the bio-variability in the proteome of European beech at both the individual and the population level.

3.3 Changes in the proteome of beech saplings upon pathogen inoculation and elevated CO₂ concentrations

To characterize the effect of elevated CO₂ and *P. plurivora*, and their putative interaction on beech saplings, a two-way ANOVA was applied for each independent time point. For the protein extraction and follow-up analysis, one sample from the elevated CO₂ treatment at t₈, as well as one control, and one sample of the double treatment at t₇ were excluded due to the low amount of starting material. Out of the “well behaved” protein spots, 10 and 1 spot/s showed for the time point t₅ and t₈ respectively significant changes between ambient and elevated CO₂ treated plantlets (Fig. 28, Tab. 5). These results showed that elevated CO₂ had a major effect on two isoforms of the RuBisCO protein (spot eID:0181 and ID:0436), which showed decreased contents of nearly 50% compared to ambient fumigated CO₂ saplings (Tab. 5). These results matched with previous works, where elevated CO₂ exposure caused a decline in photosynthesis or RuBisCO content (Moore et al. 1999). Plant species that showed decreased RuBisCO levels following elevated CO₂ exposure, generally decreased their photosynthetic capacity (Bowes 1993b; Webber et al. 1994; Moore et al. 1998). This behavior most likely indicates an acclimation of beech saplings to elevated CO₂ concentrations.

The effect of elevated CO₂ may further induce an accumulation of a putative lactoylglutathione lyase (spot ID:0699), a putative minor allergen Alt a (spot eID:0180, eID:0181), a chloroplastic protein ycf2 (spot eID:0403) and a cysteine synthase (spot ID:0678) (Tab. 5). Cysteine synthase is

required for a variety of key metabolic pathways. Limitations in plant nutrients, such as sulfur and nitrogen deficiencies, may curb plant's ability to synthesize cysteine (Hesse et al. 2004). In fact, there is evidence that elevated CO₂ concentrations reduce plant N content, which is probably caused by dilution in plant tissues and decreases in root specific uptake (Taub et al. 2008). It is possible that plants enhance biosynthesis of cysteine as a consequence of plant nutrient deficiency. However, these results should be carefully interpreted, since the identified proteins were only the most probable among multiple identified proteins.

Furthermore, when ambient CO₂ treated saplings were compared with plantlets inoculated with *P. plurivora* or with the double treatment, three protein spots were differentially displayed at t₈ (Tab. 5). Despite this fact, no proteins could be identified since the expressed spots were not visible in the preparative gels or the mass spectra displayed no peak during the analysis. As so far, these results demonstrate that beech leaves showed a response to the effect of elevated CO₂ and *P. plurivora* as well as the combined effect of both treatments. However, most of these effects need to be elucidated or validated with other molecular techniques in order to understand plant response to the studied biotic and abiotic stressors.

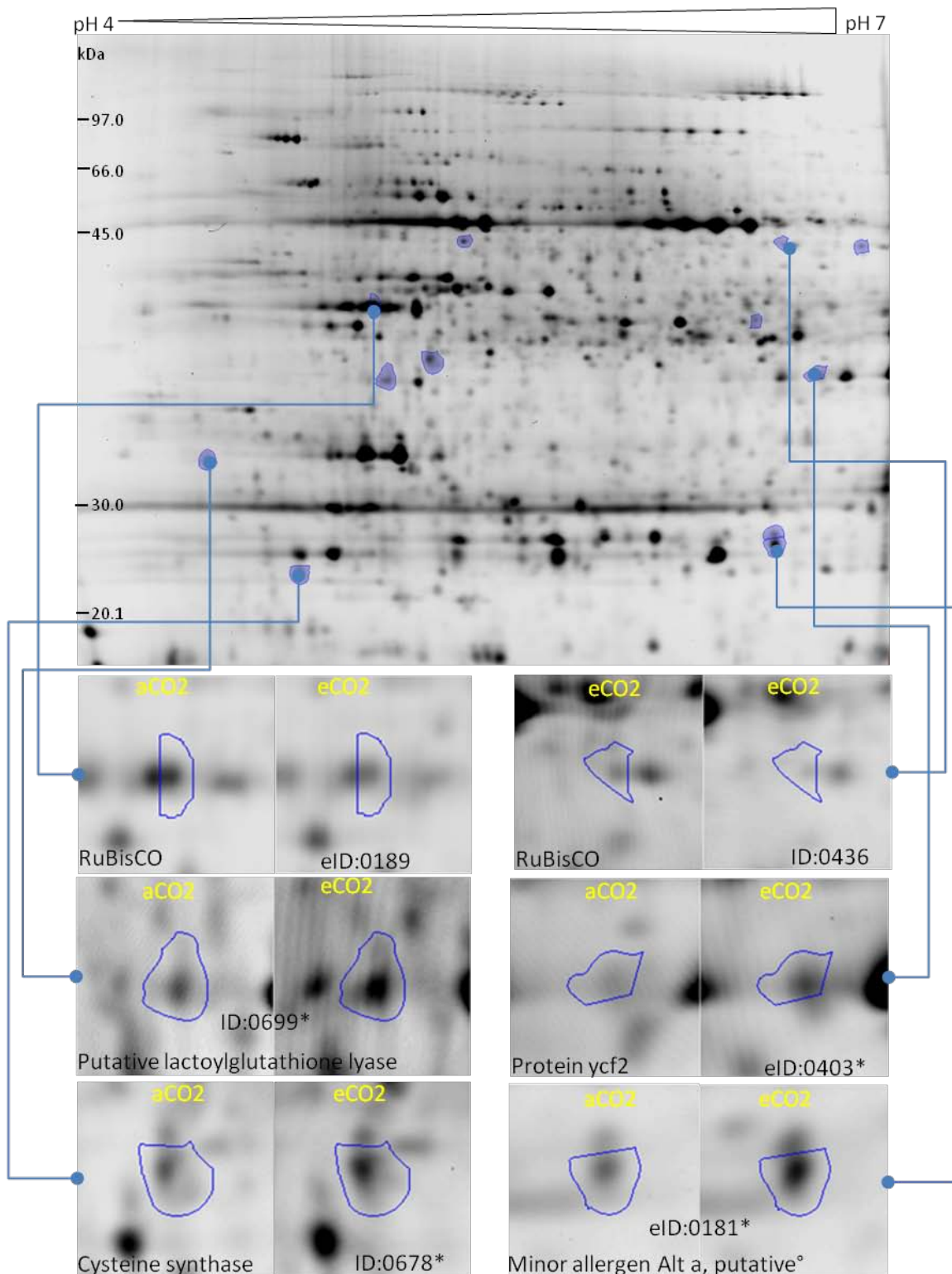


Fig. 28 – 2D-DIGE map of beech leaves. Labeled spots on the 2-D gel show statistical different spots between ambient (aCO₂) and elevated (eCO₂) CO₂ treated groups. Zoomed spots below the 2-D map indicate the abundance of a sample from the aCO₂ and the eCO₂ treatment. *: spots with multiple identified proteins.

Tab. 5 - List of significant regulated protein spots for the single sampling time point of the experiment.

Spot ID	Time point	Accession number	Identified protein	Two-way ANOVA aCO ₂ vs. eCO ₂										Z-ratio		Fold change expression						
				Bonferroni corrected					FDR corrected					ZS-N	RZ-N	VS-N	VG-N	L-N	Q-N			
				ZS-N	RZ-N	VS-N	VG-N	L-N	Q-N	ZS-N	RZ-N	VS-N	VG-N							L-N	Q-N	
eID:0180 ⁺	t ₅	B9T876	Minor allergen Alt a, putative [°]	***							*	*			0,48	0,64						
eID:0181 ⁺	t ₅	B9T876	Minor allergen Alt a, putative [°]	*****							**	*			0,52	0,75						
eID:0189	t ₅	Q40281	RuBisCO									*										
ID:0432 ⁺	t ₅		No visualization on preparative gels								*	*			0,66	0,93						
ID:0436	t ₅	Q40281	RuBisCO								*	*			-0,45	-0,55						
ID:0450	t ₅		No MS information was provided								*	*			-0,48	-0,60						
ID:0678 ⁺	t ₅	Q43317	Cysteine synthase								*	*			0,51	0,74						
ID:0699 ⁺	t ₅	Q39366	Putative lactoylglutathione lyase								*	*			0,46	0,66						
ID:0855	t ₅		No visualization on preparative gels								*	*			0,74	1,10						
ID:1010 ⁺	t ₅	B9N5B8	Predicted protein [°]								*					0,51						

Spot ID	Time point	Accession number	Identified protein	Two-way ANOVA aCO ₂ vs. eCO ₂										Z-ratio		Fold change expression							
				Bonferroni corrected					FDR corrected					ZS-N	RZ-N	VS-N	VG-N	L-N	Q-N				
				ZS-N	RZ-N	VS-N	VG-N	L-N	Q-N	ZS-N	RZ-N	VS-N	VG-N							L-N	Q-N		
eID:0403 ⁺	t ₈	P09975	Protein ycf2	*****	*****	*****	*****	*****	*****	*****	*****	*****	*****	*****	0,53	2,03	1,33	0,56	0,51	0,50			

Spot ID	Time point	Accession number	Identified protein	Two-way ANOVA aCO ₂ vs. P. plurivora inoculation										Z-ratio		Fold change expression						
				Bonferroni corrected					FDR corrected					ZS-N	RZ-N	VS-N	VG-N	L-N	Q-N			
				ZS-N	RZ-N	VS-N	VG-N	L-N	Q-N	ZS-N	RZ-N	VS-N	VG-N							L-N	Q-N	
ID:0368	t ₈		No MS information was provided	*****							***	*			0,51	0,74						0,24

Spot ID	Time point	Accession number	Identified protein	Two-way ANOVA aCO ₂ vs. eCO ₂ + P. plurivora inoculation										Z-ratio		Fold change expression							
				Bonferroni corrected					FDR corrected					ZS-N	RZ-N	VS-N	VG-N	L-N	Q-N				
				ZS-N	RZ-N	VS-N	VG-N	L-N	Q-N	ZS-N	RZ-N	VS-N	VG-N							L-N	Q-N		
ID:0600	t ₈		No visualization on preparative gels			*****	*****					*	*	*	*			0,67	0,61	0,60	0,64		

Spot ID	Time point	Accession number	Identified protein	Two-way ANOVA P. citricola inoculation vs. eCO ₂ + P. plurivora inoculation										Z-ratio		Fold change expression							
				Bonferroni corrected					FDR corrected					ZS-N	RZ-N	VS-N	VG-N	L-N	Q-N				
				ZS-N	RZ-N	VS-N	VG-N	L-N	Q-N	ZS-N	RZ-N	VS-N	VG-N							L-N	Q-N		
ID:0600	t ₈		No visualization on preparative gels			*****	*****					*	*	*	*			0,66	0,58	0,57	0,60		

aCO₂: ambient CO₂; eCO₂: elevated CO₂.

Spot ID: number of the spot in the master gel.

Time point: sampling time points of the experiment (t₅=6 and t₈=16 days after overflowing containers with water).

Accession number: protein number from the UniProt database.

Identified protein: best homologous protein found in Swiss-Prot and/or TrEMBL database.

Values from the two-way ANOVA are given as asterisk (*: p≤0.05; **: p≤0.01; ***: p≤0.001).

FDR: false discovery rate corrected values according to Benjamini and Hochberg (2000).

ZS-N: Z score normalization; RZ-N: robust Z score normalization; VS-N: volume scale normalization; VG-N: volume geometrical mean normalization; L-N: loess normalization; Q-N: quantile normalization. Normalization methods labeled with the same color explain the fact that both methods are similar in their mathematical approach.

Z-ratios are calculated by taking the difference between the averages of the observed spot Z scores and dividing by the standard deviation of all of the differences for that particular comparison.

Protein fold change: Average ratio calculated from the normalized protein volumes ((average volume of treatments - average volume of controls)/average volumes of controls). Red and green colored numbers below the protein ratio/fold change indicate up- and down-regulated proteins respectively.

[°] indicates that only a hit in TrEMBL was found.

⁺ Multiple identified proteins in a spot. Listed protein represent the protein with the highest score value, showing at least 50 score value differences to the next protein.

3.4 *C. geophilum* facing drought stress

Stress responses in fungal ECM are important research fields in forest ecosystems to understand fungal-plant interactions and stress tolerance in trees. *C. geophilum*, one of the fungal ECM symbiotically associated to forest trees may enhance nutrient availability and drought stress tolerance in its host partners (Dosskey et al. 1990; Rincón et al. 2005). By using a relative mass spectrometric approach, the aim of this study was to identify drought-related proteins in water deprived *C. geophilum* isolates grown under controlled conditions. To characterize the degree of drought stress on cultures of *C. geophilum*, the relative water loss was continuously measured in the treated plates during the entire experiment (Fig. 29). For the first harvesting time point, a mean of 35% relative water loss from the agar was chosen (t_1), which was reached after 6 days (143,6 h) of desiccation.

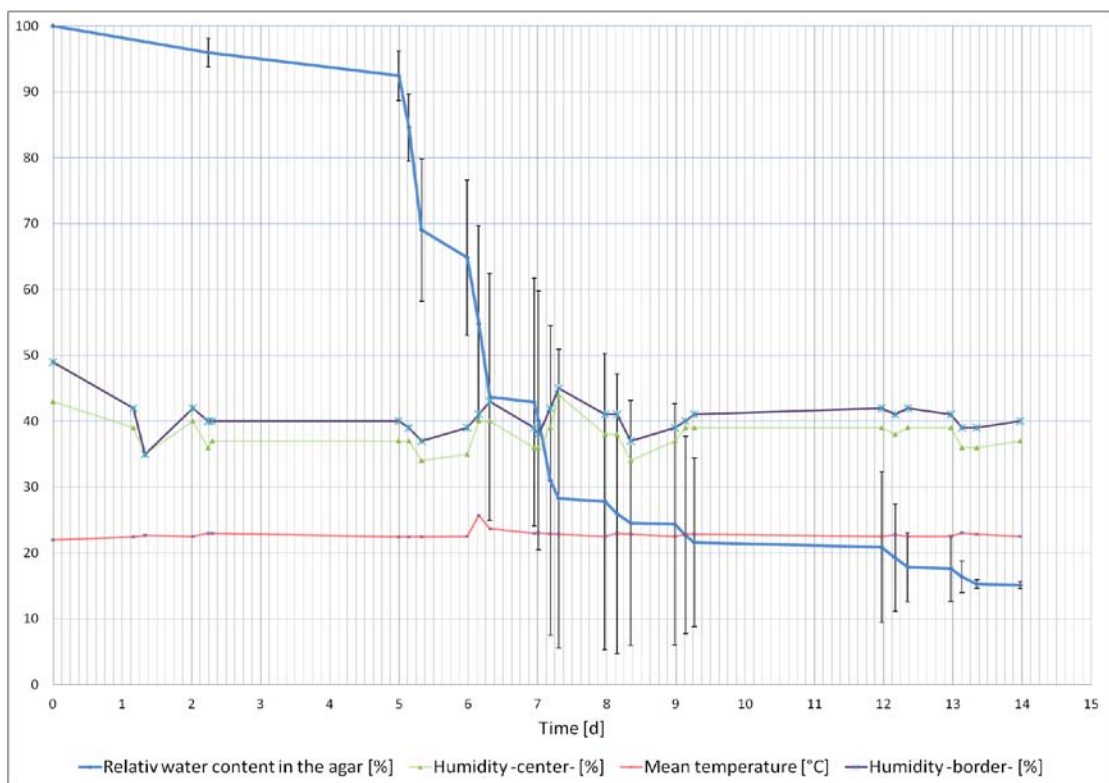


Fig. 29 - Recorded measures for i) relative water content (blue line; measurements are given in %), ii) temperature (red line; measured in °C) and iii) humidity (green and violet line measured in the center and the border of the sterile hood respectively; measurements are given in %). Vertical lines indicate the standard deviation.

The second sampling time point (t_2) was set after 7 days (168 h), when the agar plates reached on average a relative water loss of 60%. For the last sampling time point (t_3) almost 14 days (335.3 h) after beginning of water deprivation, the remaining plates exhibited on average 85% water loss from the agar. Interestingly, the water loss standard deviation increased drastically after beginning the treatment, showing the highest levels during t_2 on day 7. After day 8, the standard deviations started to decrease, reaching the lowest values during the last stage of the drought treatment. The high standard deviations among plates are explained by the heterogeneous air circulation in the sterile hood. This observation is mirrored, at least to some degree, in the different humidity values measured in the center and the border of the chamber (Fig. 29).

Influence of drought on the proteome of *C. geophilum* isolates

In the present study, 9 out of 525 identified proteins were differentially displayed compared to the controls (Fig. 30). Cultures experiencing an average of 35% water loss showed 2 proteins that changed their abundance, whereas cultures experiencing an average of 85% water loss increased to 8 differentially displayed proteins (Fig. 30). Contrary to these results, no significant effect was observed for the second time point. Although the average water loss increased from 35% in t_1 to 60% in t_2 , it is likely the high experimental and technical variations between groups (i.e. water loss, general protein amount, technical variability of the MS/MS) were high enough to mask the effect of the drought treatment.

The results from the water-stressed fungal strain showed a quantitative modulation of proteins involved in stress response and tolerance, carbon metabolism and the transport and signaling machinery (Tab. 6). Interestingly, the overlap of the proteome changes induced during low (t_1) and high drought stress (t_3) was observed only for one protein, namely a LEA (late embryogenesis abundant) domain containing protein which did not show expression in *C. geophilum* cultures under moist conditions (Tab. 6). Also an isoform of this enzyme was up-regulated for the time point t_1 . LEA proteins are wide spread proteins that have been identified in different plant organs, particularly in seeds during their maturation phase, when tolerance to desiccation is required. Although their precise molecular function is not completely understood, they are believed to play a role in enhancing tolerance to dehydrative stress environments such as desiccation (Close 1996; Goyal et al. 2005; Boucher et al. 2010).

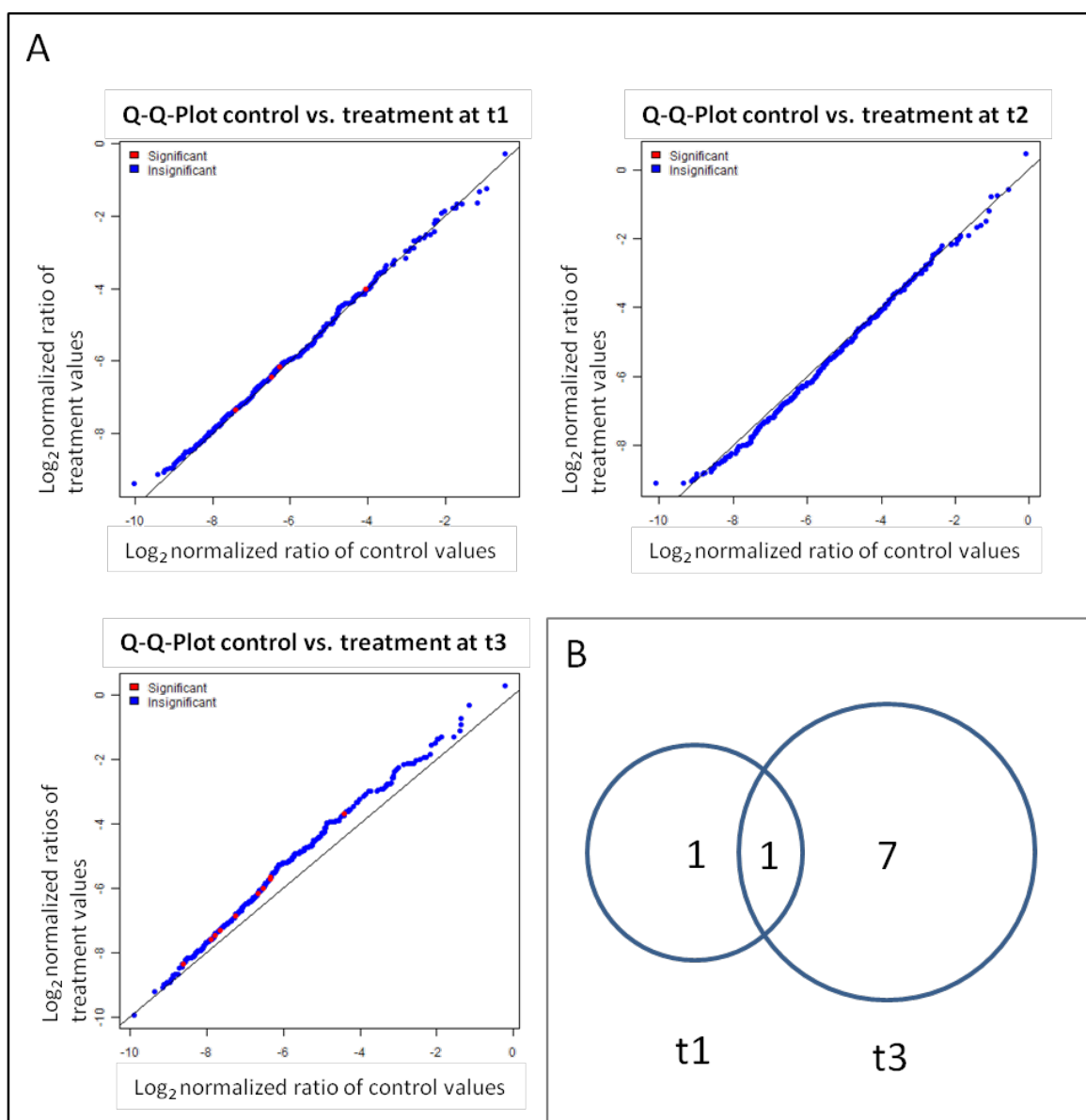


Fig. 30 - A) Distribution of quantitative protein values from control and drought stressed cultures of *C. geophilum* for each analyzed time point. Significantly different proteins ($q \leq 0.05$) before manually curation are colored in red. B) Venn diagram showing the overlap of manually curated significant different proteins in *C. geophilum* exposed to mild (t_1) and severe (t_3) drought stress.

Previous studies found that LEA proteins were capable of suppressing protein aggregation and inactivation under water-stress conditions (Goyal et al. 2005), and were accumulated in different drought stressed plant species, thus protecting against water stress (Porcel et al. 2005). The activation of this protein in the present study affirms that its role is related to water stress, and may act as chaperone by maintaining the structures of other proteins and vesicles, in the

sequestration of ions, or in binding or replacement of water as it was previously reported (Heyen et al. 2002; Kovacs et al. 2008; Boucher et al. 2010).

Another effect observed during severe drought stress was the increased synthesis of three enzymes associated with the carbon metabolism (Fig. 31). Pyruvate kinase (PK) is a key regulatory enzyme of the glycolytic pathway that catalyses the irreversible synthesis of ATP and pyruvate. The regulation of PK is directly linked to the allosteric effector acetyl-CoA.

When acetyl-CoA levels drop, the activities of PK increase and flux through the Krebs cycle is enhanced, thus providing energy for cells (Garrett et al. 2008). Cell stress response, which leads to the new formation of transcripts/proteins/metabolites, requires extra energy. Under such conditions, cells likely require greater ATP synthesis to increase energy for molecular responses. Thus, severe drought stress enhances synthesis of PK in *C. geophilum*, possibly to feed the Krebs cycle with carbon skeletons needed for energy and amino acid biosynthesis. As PK is also an ATP-producing enzyme, its up-regulation may also directly augment the energy levels required by cells exposed to drought stress. Higher activity rates of at least some elements of the Krebs cycle are being proposed in this present study, since the enzyme citrate synthase showed slightly increased abundances in cultures exposed to severe drought stress.

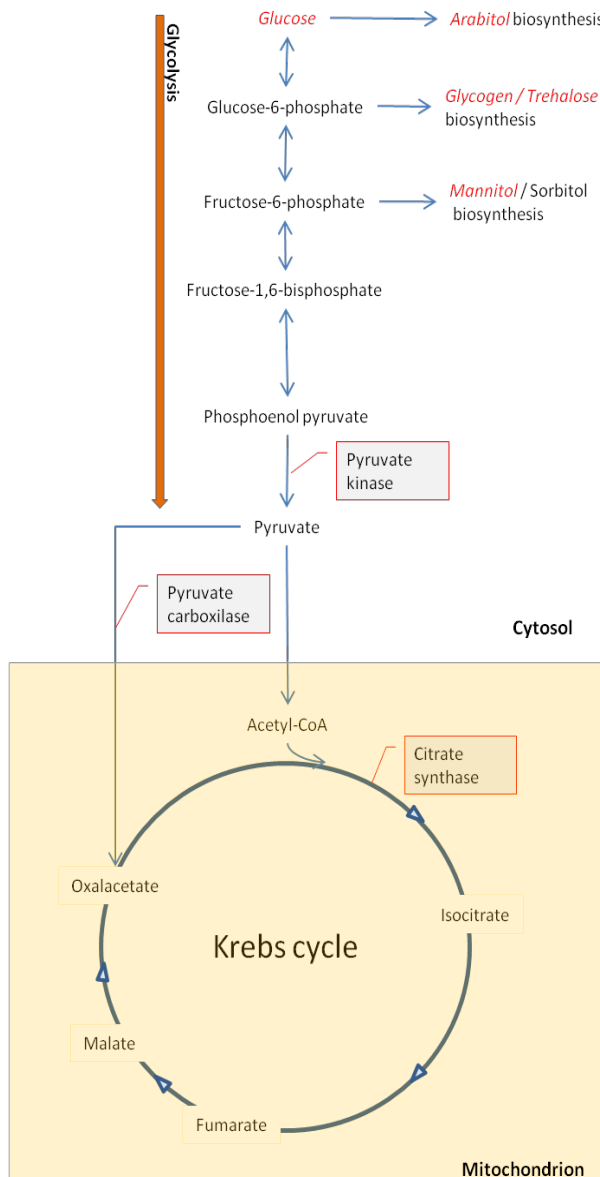


Fig. 31 - Reconstruction of the carbon metabolic pathway for C. geophilum cultures under drought treatment. Text in italics is drawn from literature, whereas the information presented in boxes is collected in the present study. Significantly up-regulated proteins/metabolites are labeled in red.

This conclusion is further supported by higher rates of the anaplerotic enzyme pyruvate carboxylase, which can replenish the Krebs cycle in fungal tissues (Scheromm et al. 1990; Wingler et al. 1996).

One of the focuses of the present study was to elucidate the modulation of protein abundances related to the synthesis of sugar or sugar alcohols. Previous studies on mycorrhizal fungal symbionts exposed to drought stress reported that sugar and/or sugar alcohols were synthesized as osmotic protectants and as a way to avoid irreversible cellular and subcellular damage (Fig. 31, metabolites in italics) (Hoekstra et al. 2001; Shi et al. 2002). In fact, after exposure to severe drought, *C. geophilum* induces the synthesis of a trehalose phosphorylase. This enzyme synthesizes trehalose, a disaccharide composed of two glucose molecules, which have been involved in resistance to drought, and in a variety of stress related responses in plants (Goddijn et al. 1999; Sang-Eun et al. 2005). Although trehalose showed a low p-value in this study ($p=0.0006$; data not shown), the results need to be validated since both the Bonferroni, as well as the FDR corrected p-value showed a non-significant, but noteworthy trend in increased abundances compared to the controls.

During the last stage of the time-course analysis, a non-specified signal transduction protein was massively induced by the effect of severe water loss (Tab. 6). Drought stress signal-transduction consists of ionic and osmotic homeostasis signaling pathways, detoxification (i.e., damage control and repair) response pathways, and pathways for growth regulation (Zhu 2002). Therefore, this protein may be involved in a variety of metabolic processes in which it activates a membrane receptor that in turn alters intracellular molecules, causing a response. In relation to this result, a protein similar to a metal resistance protein YCF1 (yeast cadmium factor protein 1), showed increased amounts in the treated group (Tab. 6). The yeast YCF1 is a member of the ABC transporter family of proteins that catalyzes the energy dependent export of glutathione S-conjugate. The major function of YCF1 is attributed to the excretion and/or sequestration of toxic compounds by transporting conjugated xenobiotics out of the cytosol to the extracellular space, or into intracellular compartments (Ishikawa et al. 1997). Although this protein was increased at relatively low levels, previous studies demonstrated that low expression levels induced notorious effects in *A. thaliana* YCF1 expressors. These findings might indicate that signal transduction and membrane trafficking proteins are important in *C. geophilum* stressed cultures. Furthermore, the present results are supported by multiple studies involving various organisms exposed to drought

stress, all of which observed the modulation of regulatory signal transduction pathways (Zhu 2002; Shinozaki et al. 2007; Batista et al. 2008) and transmembrane proteins (Shi et al. 2009; Xu et al. 2009).

In the present study, we observed increased levels of a mitochondrial nuclease and a RAD52 DNA repair protein in treated cultures (Tab. 6); both molecules are intimately involved in DNA repair. Specifically, the endo-exonucleases of fungi have been reported to play a role in repair, replication and recombination of mitochondrial DNA (Tomkinson et al. 1993). Moreover, the RAD52 DNA repair protein is highly conserved among eukaryotes and plays a role in double-strand break repair and homologous recombination. Mutations in the RAD52 expressing gene lead to defects in meiotic and/or mitotic recombination (Fraser et al. 1993; Symington 2002). This results point out that severe drought stress may induce DNA damage in *C. geophilum* cultures, forcing cells to restore the integrity of the genome by activating DNA repairing systems.

Tab. 6 – Identification of differentially displayed proteins by relative mass spectrometry (LC-MS/MS)

Protein identity	MW	p-value	q-value	Average ratio	Protein name (TrEMBL annotation)	Accession number	Score	Protein name (Swiss-prot annotation)	Accession number	Score
Regulated proteins in t₁ (on average 35% water loss)										
Stress tolerance										
Cg-lib123_c507	72	0,0003	0,0205	↑1,96	LEA domain containing protein [Pyrenophora tritici-repentis strain Pt-1C-BFP]	B2WCV1	627	Hansenula MRKII killer toxin-resistant protein 1 [Saccharomyces cerevisiae]	P41809	97
<u>F05GI4501C0IAH*</u>	38	0,0000	0,0008	↑1,85	LEA domain containing protein [Pyrenophora tritici-repentis strain Pt-1C-BFP]	B2WCV1	627	Hansenula MRKII killer toxin-resistant protein 1 [Saccharomyces cerevisiae]	P41809	97
Regulated proteins in t₃ (on average 85% water loss)										
Stress tolerance										
<u>F05GI4501C0IAH*</u>	38	0,0000	0,0008	↑1,85	LEA domain containing protein [Pyrenophora tritici-repentis strain Pt-1C-BFP]	B2WCV1	627	Hansenula MRKII killer toxin-resistant protein 1 [Saccharomyces cerevisiae]	P41809	97
Carbon metabolism										
Cg-lib123_c4899	47	0,0005	0,0231	↑1,48	Pyruvate carboxylase [Pyrenophora tritici-repentis strain Pt-1C-BFP]	B2WFT6	589	Pyruvate carboxylase [Aspergillus niger]	Q9HES8	558
Cg-lib123_c692	176	0,0014	0,0426	↑1,30	Pyruvate kinase [Pyrenophora teres f. teres strain 0-1]	E3RS31	2,489	Pyruvate kinase [Emericella nidulans]	P22360	2,186
Cg-lib123_c759	151	0,0006	0,0231	↑1,17	Citrate synthase [Phaeosphaeria nodorum]	Q0V2M2	2,188	Citrate synthase, mitochondrial [Emericella nidulans]	O00098	2,145
Transport and signaling										
<u>Cg-lib123_c1197</u>	103	0,0000	0,0025	↑1,14	Similar to vacuolar metal resistance ABC transporter [Leptosphaeria maculans]	E5ABP3	1,484	Metal resistance protein YCF1 [Saccharomyces cerevisiae]	P39109	1,041
Cg-lib123_lrc1293	71	0,0009	0,0319	↑9,65	Signal transduction protein [Pyrenophora tritici-repentis strain Pt-1C-BFP]	B2WM65	347	Uncharacterized threonine-rich GPI-anchored glycoprotein PJ4664.02 [Schizosaccharomyces pombe]	Q96WV6	81
Stress response										
Cg-lib123_c487	93	0,0006	0,0231	↑1,37	RAD52 DNA repair protein RAD52 [Paracoccidioides brasiliensis strain ATCC MYA-826 / Pb01]	C1HAB8	74	Uncharacterized protein YBR255C-A [Saccharomyces cerevisiae]	Q3E776	86
<u>Cg-lib123_c1639</u>	111	0,0000	0,0006	↑1,33	Mitochondrial nuclease [Metarhizium anisopliae ARSEF 23]	E9F484	533	Mitochondrial nuclease [Saccharomyces cerevisiae]	P08466	375

* indicate proteins regulated in *C. geophilum* under mild as well as severe drought stress

Underlined proteins indicate proteins that show statistical significances (p≤0.05) following a Bonferroni correction. Average ratio was calculated from the normalized protein volumes (Average ratio=average treatment/average controls). Negative values are given as: average ratio=-1/average ratio. Information for trehalose phosphorylase is not included since the q value was over the significance threshold of 0.05.

4 Conclusions and outlook

- 4.1 Optimization of the protein separation protocol
- 4.2 Exposure to free-air ozone fumigation and inoculation with *P. plurivora*
- 4.3 Exposure to elevated CO₂ concentrations and inoculation with *P. plurivora*
- 4.4 *C. geophilum* facing drought stress
- 4.5 Outlook

The proteomic studies presented here addressed local responses of European beech following long-term exposure to elevated ozone and carbon dioxide, air pollutants that have a pronounced impact on plants in times of climate change. In addition, these studies evaluated the combined effects of the root pathogen *P. plurivora* in juvenile beech trees and beech saplings exposed to the above mentioned pollutants. Finally, the responses of *C. geophilum* under drought stress was investigated, as this fungal organism is essential in forest ecosystems and has been reported to display characteristics that can contribute to drought tolerance in plants.

4.1 Optimization of the protein separation protocol

The first results obtained from the 2-D gel protein separation were not satisfactory, and could not be used for the subsequent analysis. Although previous work dealt with optimizing a protein extraction and separation protocol for ontogenetically similar beech leaf material (Vâlcu et al. 2006a, b), problems arose particularly in the quality and the number of separated protein spots. The low resolution of 2-D spots probably resulted from the presence of polyphenols, which can build irreversible complexes with proteins, and/or the presence of polysaccharides and lipids that can cause severe disturbances in the 2-D gel pattern (Westermeier 2006). Consequently, protein separation needed to be optimized and tailored to the specific plant material being used. By empirically testing for the best suited sample separation methods, interfering compounds were ultimately eliminated, thus increasing the resolution of beech leaf proteins. Because the technical gel-to-gel variability has clear and predictable implications for the outcome of significant changes in comparative proteomics, it was also of interest to assess the degree of technical variance present in the 2-D DIGE approach. As a result, the quantitative 2-D DIGE analyses were restricted only to “well-behaved” proteins spots. Although an internal standard enables an accurate gel-to-gel spot quantification, depending on the used normalization, 468-472 spots were filtered due to high technical variations. Reasons for filtering 46-47% of the total spot amount were probably based on differences in different label quality of CyDye colors to proteins. The results presented here clearly exemplify 2-D electrophoresis as a multi-step process in which technical difficulties must first be overcome, before measuring quantitative changes between various treatments.

4.2 Exposure to free-air ozone fumigation and inoculation with *P. plurivora*

Responses of beech saplings after four vegetation periods of ozone exposure are clearly indicated at the protein level. However, 43 days after re-shifting beech trees to control conditions, all proteins except a phosphoglycerate dehydrogenase recovered from the ozone effects. This result mirrored the molecular plasticity of plants and reflects the speed in which plants might adapt to different ozone levels.

The results presented here confirm previous studies reported for other plant species i.e. poplar, rice and soybean which were treated with short-term elevated ozone concentrations. The molecular pathway that leads to the development of oxidative stress response can be rather complex. However, different plants species seem to respond in a similar way by reducing CO₂ fixation and increasing dark respiration. This trend is also observed in juvenile European beech trees following long-term ozone exposure.

Furthermore, the initial proteomic approach was supported by earlier work which focused on transcriptome analyses, non-structural carbohydrates and visually observed injuries. In sum, molecular events took place in the harvested tissue well before visible symptoms manifested. Results indicated that molecular responses are first intended to counteract deleterious effects of sublethal ozone concentrations. Later, when plant cells were not capable of supporting cell integrity, a hypersensitive response was probably induced to prevent the spread of leaf lesions, which then manifested visually as brownish patches on the leaves.

Another focus of the present work was the linkage between transcriptomic and proteomic analysis as a tool to understand systems biology of cellular processes. Although there were only 3 direct feature overlaps, rather good correlations were observed at the functional level, particularly in pathways such as photosynthesis, disease/defense responses and detoxification mechanisms. Most of the identified transcripts/proteins related to photosynthesis and carbon fixation decreased. In parallel, different transcripts/proteins implicated in detoxification processes, defense and degrading reactions were differentially displayed. These observations suggest that energy, which was already decreased following elevated ozone exposure, was reallocated and directed towards repair, detoxification and maintenance of cell structures. Such molecular changes may have long-term effects on growth performance and alter vulnerability to

pathogens (Luedemann et al. 2005; Olbrich et al. 2010). In the last instance, these results could lead to an altered plant-plant competitive balance as well as changes in plant biodiversity. Ultimately, a combination of several approaches including transcriptomics, differential proteomics, analysis of non-structural carbohydrates and visual effects appear to yield higher comprehensive information on responses of juvenile beech trees following ozone exposure.

The results illustrate that juvenile beech trees exposed to both pathogen inoculation and elevated ozone showed no statistically significant differences, possibly because the low number of biological replicates masked the effect of the treatment. Thus, these findings underline the necessity of having previous information on the biological diversity and the need of *a priori* analysis, such as statistical power as a tool to calculate the minimum sample size required to detect an effect of a given size.

4.3 Exposure to elevated CO₂ concentrations and inoculation with *P. plurivora*

The 2-D DIGE approach, in tandem with LC-MS/MS, demonstrated changes in the proteome of beech saplings following elevated CO₂ exposure, inoculation with *P. plurivora* and the combined effect of both treatments. Despite this fact, the magnitude of the response, especially involving the pathogen, was low compared to other studies previously reported in the literature (Schlink 2009; Vâlcu et al. 2009). This fact may be explained by responses to changing environments, which are largely determined by the physiological/ontological status of the plants, the environmental/experimental conditions and the number of biological replicates used for the experiment (Vâlcu et al. 2009). The main finding of the elevated CO₂ treatment reflects a clear down regulation in the abundance of the CO₂ fixation enzyme RuBisCO. This observation is supported by multiple other studies. This result indicates the capacity of beech leaves to acclimate to higher concentrations of CO₂. Moreover, other proteins related to secondary metabolism, transcript regulation, ATP binding and amino acid metabolism might be implicated in the adaptation of saplings to an elevated CO₂ environment. For instance, increases in the abundance of cysteine synthase may further indicate a limitation of N availability. Nonetheless,

these results must be validated as the differentially displayed proteins were identified in spots containing multiple proteins.

It was also possible to identify one spot representing the systemic response of beech saplings to *P. plurivora* inoculation and another spot representing the interaction between treatments. Although there are advantages of the 2-D DIGE technique, this study also mirrored the limitations of the method. These caveats include the identification of multiple proteins in a spot and the difference in the resolution of 2-D patterns using DIGE colors and silver or CBB stained preparative gels. Furthermore, it is possible that undetected proteins on the 2-D gel, such as those of hydrophobic nature, were affected, and that the technique used to assess the response was inappropriate in this case.

4.4 *C. geophilum* facing drought stress

Even though the results of this laboratory experiment cannot be directly translated to a natural system, this is the first study that provides molecular insight into large-scale proteome quantification in *C. geophilum* following drought stress. As such, it supplements basic knowledge, and set the stage to better understand regulatory interactions with plants at a later date. Throughout the relative mass spectrometric approach, it was indicated that *C. geophilum* modulates proteins as an adaptive response to low and severe stress conditions. Under drought stress new metabolites are needed to maintain cell homeostasis, which is supported by an increase in the abundance of an enzyme from the glycolytic pathway, possibly to feed the Krebs cycle with carbon skeletons needed for energy and amino acid biosynthesis. Also, the increased levels of citrate synthase indicate that at least a specific part of the Krebs cycle was activated throughout the induced drought.

The quantitative analysis also uncovered evidence that differentially abundant proteins were involved in repair and defense reactions commonly induced by multiple stresses. For instance, DNA repair enzymes accumulated in *C. geophilum* exposed to drought, which was likely caused by multiple environmental stresses, namely oxidative cell damage. It is possible, that this oxidative damage also increased abundances of a signal transduction and an ABC transporter protein. These enzymes might be activated in order to reestablish cellular homeostasis and to prevent damage in

cells. The activated LEA domain containing protein plays a special role in this study, since it was the only enzyme activated during low and severe drought stress. As the abundance of LEA proteins showed also increased levels in drought stressed tolerant plants, it should be of interest to know whether or not *C. geophilum* expressing this protein could have an effect on the drought tolerance of its symbiotic partner. Overall, the predominance of regulated proteins related to stress response, as well as transport and signaling machinery reflect the importance of cells in dealing with both osmotic control and increased levels of damaging compounds such as reactive oxygen species for adaptation and survival to drought stress.

4.5 Outlook

Especially in times of rapid climate change, sessile organisms have to cope with a wide range of environmental variability and stress. Adaptation strategies are therefore essential for survival. They depend on a series of mechanisms that are initiated at the molecular level. As such, the large-scale identification of transcripts, proteins, and metabolites is pivotal to understand the complexity of molecular responses and their consequences to physiological and morphological changes in living organisms. Therefore, the fields of transcriptomics, proteomics, and metabolomics are forward-looking platforms needed to understand molecular processes in biological systems. On the top of these platforms the field of interactomics might be useful to understand complex holistic networks in-between and among proteins and other molecules.

The work presented here focusing on the research of forest elements profited from the advantages of proteomic applications that, although still in its infancy, offer great potential for better understanding the molecular mechanisms of stress response. Because gene expression is regulated at several stages after transcription, monitoring the abundance of mRNA transcripts is not necessarily representative for alterations occurring on the protein and metabolite outputs of cells and tissues. As such, proteomic technologies provide a crucial tool to bridge the gap between the genome sequence and its products, the metabolites. However, compared to model organisms such as yeast, research in forest systems has yet to exploit fully the potential of proteomics. This field would benefit from genomic-data entries of forest species, as they represent an important tool in a proteomic approach.

Throughout the implemented homology driven proteomic approach, it was possible to discover the effect of abiotic stresses on the differential expression of proteins in important non-model organisms, namely European beech and *C. geophilum*. It should be noted in this regard that changes in the protein abundance were recorded at the organ or whole organism level, therefore, sample material was represented by the sum of healthy and unhealthy (necrotic) cells. Nevertheless, as it is well known, biochemical processes are not only determined by their timing, but also by the localization of molecular events. Thus, other emerging techniques such as matrix-assisted laser desorption ionization may provide additional information regarding the spatial distribution of modulated proteins/peptides and elicited metabolites in specific tissues following biotic and abiotic stresses.

Since the work presented here focused on mainly soluble proteins, the studies of single protein fractions, especially the membrane proteome, which play vital roles in the communication between cell and its environment, may provide an in depth understanding of the observed stress reactions. Further studies on post-translational modifications are other promising sources of additional information, as they are key modifying mechanisms for controlling the behavior of a protein. Finally, the work presented here paves the way for further studies focusing on specified molecular pathways, and marker-assisted breeding in order to improve our understanding of molecular responses and tolerance to single and combined stresses in forest elements.

From a systemic point of view, molecular science will take a step forward when integrating different “omic” approaches together with physiological and morphological data. Ultimately, linking such large numbers of datasets to coherent models will improve our understanding of the kaleidoscope of responses that enable organisms to adapt and tolerate to new environmental conditions.

5 References

- Aebersold R and Mann M (2003). "Mass spectrometry-based proteomics." Nature **422**(6928): 198-207.
- Agius F, Gonzalez-Lamothe R, Caballero JL, Muñoz-Blanco J, Botella MA and Valpuesta V (2003). "Engineering increased vitamin C levels in plants by overexpression of a D-galacturonic acid reductase." Nature Biotechnology **21**(2): 177-181.
- Agrawal GK, Rakwal R, Yonekura M, Kubo A and Saji H (2002). "Proteome analysis of differentially displayed proteins as a tool for investigating ozone stress in rice (*Oryza sativa* L.) seedlings." Proteomics **2**(8): 947-959.
- Ahsan N, Nanjo Y, Sawada H, Kohno Y and Komatsu S (2010). "Ozone stress-induced proteomic changes in leaf total soluble and chloroplast proteins of soybean reveal that carbon allocation is involved in adaptation in the early developmental stage." Proteomics **10**(14): 2605-2619.
- Ainsworth EA and Rogers A (2007). "The response of photosynthesis and stomatal conductance to rising [CO₂]: mechanisms and environmental interactions." Plant, Cell & Environment **30**(3): 258-270.
- Allen CD, Macalady AK, Chenchouni H, Bachelet D, McDowell N, Vennetier M, Kitzberger T, Rigling A, Breshears DD, Hogg EH, Gonzalez P, Fensham R, Zhang Z, Castro J, Demidova N, Lim JH, Allard G, Running SW, Semerci A and Cobb N (2010). "A global overview of drought and heat-induced tree mortality reveals emerging climate change risks for forests." Forest Ecology and Management **259**(4): 660-684.
- Aranjuelo I, Molero G, Erice G, Avice JC and Nogues S (2011). "Plant physiology and proteomics reveals the leaf response to drought in alfalfa (*Medicago sativa* L.)." Journal of Experimental Botany **62**(1): 111-123.
- Bae H and Sicher R (2004). "Changes of soluble protein expression and leaf metabolite levels in *Arabidopsis thaliana* grown in elevated atmospheric carbon dioxide." Field Crops Research **90**(1): 61-73.
- Bahl A, Loitsch SM and Kahl G (1993). "Air pollution and plant gene expression". "In: Plant Responses to the Environment". Gresshoff PM. Knoxville, Tennessee.
- Bahrn A, Jensen CR, Asch F and Mogensen VO (2002). "Drought-induced changes in xylem pH, ionic composition, and ABA concentration act as early signals in field-grown maize (*Zea mays* L.)." Journal of Experimental Botany **53**(367): 251-263.
- Bantscheff M, Schirle M, Sweetman G, Rick J and Kuster B (2007). "Quantitative mass spectrometry in proteomics: a critical review." Analytical and Bioanalytical Chemistry **389**(4): 1017-1031.
- Barceló-Batlloiri S and Gomis R (2009). "Proteomics in obesity research." Proteomics - Clinical Applications **3**(2): 263-278.
- Batista R, Saibo N, Lourenço T and Oliveira MM (2008). "Microarray analyses reveal that plant mutagenesis may induce more transcriptomic changes than transgene insertion." Proceedings of the National Academy of Sciences **105**(9): 3640-3645.

-
- Benedetti CE, Costa CL, Turcinelli SR and Arruda P (1998). "Differential expression of a novel gene in response to coronatine, methyl jasmonate, and wounding in the coi1 mutant of *Arabidopsis*." Plant Physiology **116**(3): 1037-1042.
- Benjamini Y and Hochberg Y (2000). "On the adaptive control of the false discovery rate in multiple testing with independent statistics." Journal of Educational and Behavioral Statistics **25**(1): 60-83.
- Beranova-Giorgianni S (2003). "Proteome analysis by two-dimensional gel electrophoresis and mass spectrometry: strengths and limitations." TrAC Trends in Analytical Chemistry **22**(5): 273-281.
- Blödner C, Majcherczyk A, Kües U and Polle A (2007). "Early drought-induced changes to the needle proteome of Norway spruce." Tree Physiology **27**(10): 1423-1431.
- Blumenröther MC, Löw M, Matyssek R and Oswald W (2007). "Flux -based response of sucrose and starch in leaves of adult beech trees (*Fagus sylvatica* L.) under chronic free-air O₃ fumigation." Plant Biology **9**(2): 207-214.
- Bohler S, Bagard, Mouhssin Oufir M, Planchon S, Hoffmann L, Jean-François YJ, Dizengremel HP and Renaut J (2007). "A DIGE analysis of developing poplar leaves subjected to ozone reveals major changes in carbon metabolism." Proteomics **7**(10): 1584-1599.
- Bohler S, Sergeant K, Lefèvre I, Jolivet Y, Hoffmann L, Renaut J, Dizengremel P and Hausman J-F (2010). "Differential impact of chronic ozone exposure on expanding and fully expanded poplar leaves." Tree Physiology **30**(11): 1415-1432.
- Borghetti M, Leonardi S, Raschi A, Snyderman D and Tognetti R (1993). "Ecotypic variation of xylem embolism, phenological traits, growth parameters and allozyme characteristics in *Fagus sylvatica*." Functional Ecology **7**(6): 713-720.
- Boucher V, Buitink J, Lin X, Boudet J, Hoekstra FA, Hundertmark M, Renard D and Leprince O (2010). "MtPM25 is an atypical hydrophobic late embryogenesis-abundant protein that dissociates cold and desiccation-aggregated proteins." Plant, Cell & Environment **33**(3): 418-430.
- Bowes G (1993). "Facing the inevitable: Plants and increasing atmospheric CO₂." Annual Review of Plant Physiology and Plant Molecular Biology **44**(1): 309-332.
- Bray S and Reid DM (2002). "The effect of salinity and CO₂ enrichment on the growth and anatomy of the second trifoliate leaf of *Phaseolus vulgaris*." Canadian Journal of Botany **80**: 349-359
- Brugière N, Dubois F, Masclaux C, Sangwan RS and Hirel B (2000). "Immunolocalization of glutamine synthetase in senescing tobacco (*Nicotiana tabacum* L.) leaves suggests that ammonia assimilation is progressively shifted to the mesophyll cytosol." Planta **211**(4): 519-527.
- Buchanan-Wollaston V and Ainsworth C (1997). "Leaf senescence in *Brassica napus*: Cloning of senescence related genes by subtractive hybridisation." Plant Molecular Biology **33**(5): 821-834.
- Bunny F (1996). "The biology, ecology and taxonomy of *Phytophthora citricola* in native plant communities in Western Australia". Murdoch, Murdoch University.
- Candiano G, Bruschi M, Musante L, Santucci L, Ghiggeri GM, Carnemolla B, Orecchia P, Zardi L and Righetti PG (2004). "Blue silver: a very sensitive colloidal Coomassie G-250 staining for proteome analysis." Electrophoresis **25**(9): 1327-1333.

-
- Cantón F, Suárez M-F, Josè-Estanyol M and Cánovas F (1999). "Expression analysis of a cytosolic glutamine synthetase gene in cotyledons of Scots pine seedlings: developmental, light regulation and spatial distribution of specific transcripts." *Plant Molecular Biology* **40**(4): 623-634.
- Carpentier SC, Witters E, Laukens K, Deckers P, Swennen R and Panis B (2005). "Preparation of protein extracts from recalcitrant plant tissues: an evaluation of different methods for two-dimensional gel electrophoresis analysis." *Proteomics* **5**(10): 2497-2507.
- Castagna A and Ranieri A (2009). "Detoxification and repair process of ozone injury: From O₃ uptake to gene expression adjustment." *Environmental Pollution* **157**(5): 1461-1469.
- Chen L-H, Yan W and Xu Y (2007). "Identification and preliminary analysis of the genetic diversity of *Cenococcum geophilum* Fr." *Agricultural Sciences in China* **6**(8): 956-963.
- Cho K, Shibato J, Agrawal GK, Jung Y-H, Kubo A, Jwa N-S, Tamogami S, Satoh K, Kikuchi S, Higashi T, Kimura S, Saji H, Tanaka Y, Iwahashi H, Masuo Y and Rakwal R (2008). "Integrated transcriptomics, proteomics, and metabolomics analyses to survey ozone responses in the leaves of rice seedling." *Journal of Proteome Research* **7**(7): 2980-2998.
- Close TJ (1996). "Dehydrins: Emergence of a biochemical role of a family of plant dehydration proteins." *Physiologia Plantarum* **97**(4): 795-803.
- Coleman M, Bledsoe C and Lopushinsky W (1989). "Pure culture response of ectomycorrhizal fungi to imposed water stress." *Canadian Journal of Botany* **67**: 29-39.
- Coleman MD, Isebrands JG, Dickson RE and Karnosky DF (1995). "Photosynthetic productivity of aspen clones varying in sensitivity to tropospheric ozone." *Tree Physiology* **15**(9): 585-592.
- Conway T and Tans P. (2011). "Trends in Atmospheric Carbon Dioxide." from <http://www.esrl.noaa.gov/gmd/ccgg/trends/>.
- Curtis PS and Wang X (1998). "A meta-analysis of elevated CO₂ effects on woody plant mass, form, and physiology." *Oecologia* **113**(3): 299-313.
- Damerval C, De Vienne D, Zivy M and Thiellement H (1986). "Technical improvements in two-dimensional electrophoresis increase the level of genetic variation detected in wheat-seedling proteins." *Electrophoresis* **7**(1): 52-54.
- Davis MB and Shaw RG (2001). "Range shifts and adaptive responses to quaternary climate change." *Science* **292**(5517): 673-679.
- De Groot MJ, Daran-Lapujade P, van Breukelen B, Knijnenburg TA, de Hulster EA, Reinders MJ, Pronk JT, Heck AJ and Slijper M (2007). "Quantitative proteomics and transcriptomics of anaerobic and aerobic yeast cultures reveals post-transcriptional regulation of key cellular processes." *Microbiology* **153**(11): 3864-3878.
- Dertz W (1996). "Buchenwälder im Zielkatalog der Forstwirtschaft". "Buchenwälder-Ihr Schutz und Ihre Nutzung". Osnabrück, Stiftung Wald in Not: 2-8.
- Dittmar C, Zech W and Elling W (2003). "Growth variations of common beech (*Fagus sylvatica* L.) under different climatic and environmental conditions in Europe - a dendroecological study." *Forest Ecology and Management* **173**(1-3): 63-78.
- Dixon DP, Skipsey M and Edwards R (2010). "Roles for glutathione transferases in plant secondary metabolism." *Phytochemistry* **71**(4): 338-350.
- Dizengremel P (2001). "Effects of ozone on the carbon metabolism of forest trees." *Plant Physiology and Biochemistry* **39**(9): 729-742.
- Dizengremel P, Thiec DL, Hasenfratz-Sauder M-P, Vaultier M-N, Bagard M and Jolivet Y (2009). "Metabolic-dependent changes in plant cell redox power after ozone exposure." *Plant Biology* **11**(1): 35-42.

-
- Dosskey MG, Linderman RG and Boersma L (1990). "Carbon-sink stimulation of photosynthesis in Douglas fir seedlings by some ectomycorrhizas." New Phytologist **115**(2): 269-274.
- Dreistadt SH (2008). "Integrated pest management for avocados". California, University of California Agriculture & Natural Resources.
- Du H, Liang Y, Pei K and Ma K (2011). "UV radiation responsive proteins in rice leaves: a proteomic analysis." Plant and Cell Physiology **52**(2): 306-316.
- Edreva A (2005). "Pathogenesis-related proteins: research progress in the last 15 years." General Applied Plant Physiology **31**: 105-124.
- Edwards JW and Coruzzi GM (1989). "Photorespiration and light act in concert to regulate the expression of the nuclear gene for chloroplast glutamine synthetase." Plant Cell **1**(2): 241-248.
- Egger C, Focke M, Bircher AJ, Scherer K, Mothes-Luksch N, Horak F and Valenta R (2008). "The allergen profile of beech and oak pollen." Clinical & Experimental Allergy **38**(10): 1688-1696.
- Ellenberg H (1996). "Vegetation Mitteleuropas mit den Alpen". Stuttgart, Eugen Ulmer Verlag.
- Ellenberg HH and Strutt GK (1988). "Vegetation Ecology of Central Europe", Cambridge University Press.
- Ernst D, Bodemann A, Schmelzer E, Langebartels C and Sandermann H (1996). "Beta-1,3-glucanase mRNA is locally, but not systemically induced in *Nicotiana tabacum* L cv BEL W3 after ozone fumigation." Journal of Plant Physiology **148**(1-2): 215-221.
- Ernst D, Schraudner M, Langebartels C and Sandermann H (1992). "Ozone-induced changes of mRNA levels of β -1,3-glucanase, chitinase and 'pathogenesis-related' protein 1b in tobacco plants." Plant Molecular Biology **20**(4): 673-682.
- Feng Y, Komatsu S, Furukawa T, Koshiba T and Kohno Y (2008). "Proteome analysis of proteins responsive to ambient and elevated ozone in rice seedlings." Agriculture, Ecosystems & Environment **125**(1-4): 255-265.
- Fleischman F, Winkler JB and Oßwald W (2009). "Effects of ozone and *Phytophthora citricola* on non-structural carbohydrates of European beech (*Fagus sylvatica*) saplings." Plant Soil **323**(1): 75-84.
- Fleischmann F, Schneider D, Matyssek R and Oßwald WF (2002). "Investigations on net CO₂ assimilation, transpiration and root growth of *Fagus sylvatica* infested with four different *Phytophthora* species." Plant Biology **4**(2): 144-152.
- Fraser MJ and Low RL (1993) "Fungal and Mitochondrial Nucleases." 171-207 DOI: 10.1101/087969426.25.171.
- Führs H, Hartwig M, Molina LEB, Heintz D, Van Dorsselaer A, Braun H-P and Horst WJ (2008). "Early manganese-toxicity response in *Vigna unguiculata* L. – a proteomic and transcriptomic study." Proteomics **8**(1): 149-159.
- Garcia RL, Long SP, Wall GW, Osborne CP, Kimball BA, Nie GY, Pinter PJ, Lamorte RL and Wechsung F (1998). "Photosynthesis and conductance of spring-wheat leaves: field response to continuous free-air atmospheric CO₂ enrichment." Plant, Cell & Environment **21**(7): 659-669.
- Garrett RH and Grisham CM (2008). "Biochemistry ". London, Brooks/Cole Publishing Company.
- GE-Healthcare (2004). "2-D electrophoresis principles and methods". 80-6429-60AC H.
- Goddijn OJM and van Dun K (1999). "Trehalose metabolism in plants." Trends in Plant Science **4**(8): 315-319.

-
- Gómez-Vidal S, Tena M, Lopez-Llorca LV and Salinas J (2008). "Protein extraction from *Phoenix dactylifera* L. leaves, a recalcitrant material, for two-dimensional electrophoresis." Electrophoresis **29**(2): 448-456.
- Görg A, Obermaier C, Boguth G and Weiss W (1999). "Recent developments in two-dimensional gel electrophoresis with immobilized pH gradients: wide pH gradients up to pH 12, longer separation distances and simplified procedures." Electrophoresis **20**(4-5): 712-717.
- Görg A, Postel W, Günther S and Weser J (1985). "Improved horizontal two-dimensional electrophoresis with hybrid isoelectric focusing in immobilized pH gradients in the first dimension and laying-on transfer to the second dimension." Electrophoresis **6**(12): 599-604.
- Goyal K, Walton LJ and Tunnacliffe A (2005). "LEA proteins prevent protein aggregation due to water stress." Biochemical Journal **388**(1): 151-157.
- Graham LE (2008). "The effects of elevated carbon dioxide concentration on leaf growth and development in *Populus*". Southampton, University of Southampton.
- Greenbaum D, Colangelo C, Williams K and Gerstein M (2003). "Comparing protein abundance and mRNA expression levels on a genomic scale." Genome Biology **4**(9).
- Grudkowska M and Zagdanska B (2004). "Multifunctional role of plant cysteine proteinases." Acta Biochimica Polonica **51**(3): 609-624.
- Hajheidari M, Abdollahian-Noghabi M, Askari H, Heidari M, Sadeghian SY, Ober ES and Hosseini Salekdeh G (2005). "Proteome analysis of sugar beet leaves under drought stress." Proteomics **5**(4): 950-960.
- Hayat S, Mori M, Pichtel J and Ahmad A (2009). "Nitric oxide in plant physiology". Weinheim, Wiley-VCH Verlag
- He XY, Fu SL, Chen W, Zhao TH, Xu S and Tuba Z (2007). "Changes in effects of ozone exposure on growth, photosynthesis, and respiration of *Ginkgo biloba* in Shenyang urban area." Photosynthetica **45**(4): 555-561.
- Heineke D, Kauder F, Frommer W, KÜHn C, Gillissen B, Ludewig F and Sonnewald U (1999). "Application of transgenic plants in understanding responses to atmospheric change." Plant, Cell & Environment **22**(6): 623-628.
- Hemavathi, Upadhyaya CP, Young KE, Akula N, Kim Hs, Heung JJ, Oh OM, Aswath CR, Chun SC, Kim DH and Park SW (2009). "Over-expression of strawberry d-galacturonic acid reductase in potato leads to accumulation of vitamin C with enhanced abiotic stress tolerance." Plant Science **177**(6): 659-667.
- Hesse H, Nikiforova V, Gakière B and Hoefgen R (2004). "Molecular analysis and control of cysteine biosynthesis: integration of nitrogen and sulphur metabolism." Journal of Experimental Botany **55**(401): 1283-1292.
- Heukeshoven J and Dernick R (1988). "Improved silver staining procedure for fast staining in PhastSystem Development Unit. I. Staining of sodium dodecyl sulfate gels." Electrophoresis **9**(1): 28-32.
- Heyen BJ, Alsheikh MK, Smith EA, Torvik CF, Seals DF and Randall SK (2002). "The calcium-binding activity of a vacuole-associated, dehydrin-like protein is regulated by phosphorylation." Plant Physiology **130**(2): 675-687.
- Hoekstra FA, Golovina EA and Buitink J (2001). "Mechanisms of plant desiccation tolerance." Trends in Plant Science **6**(9): 431-438.
- Horling F, Baier M and Dietz K-J (2001). "Redox-regulation of the expression of the peroxide-detoxifying chloroplast 2-cys peroxiredoxin in the liverwort *Riccia fluitans*." Planta **214**(2): 304-313.

-
- Horton TR and Bruns TD (2001). "The molecular revolution in ectomycorrhizal ecology: peeking into the black-box." Molecular Ecology **10**(8): 1855-1871.
- Hough AM and Derwent RG (1990). "Changes in the global concentration of tropospheric ozone due to human activities." Nature **344**(6267): 645-648.
- Hugouvieux V, Dutilleul C, Jourdain A, Reynaud F, Lopez V and Bourguignon J (2009). "Arabidopsis putative selenium-binding protein1 expression is tightly linked to cellular sulfur demand and can reduce sensitivity to stresses requiring glutathione for tolerance." Plant Physiology **151**(2): 768-781.
- InvestigadoresACG. (2011). from <http://www.investigadoresacg.org/databases/ecto/Cenococcum.html>.
- IPCC. (2011). from <http://www.ipcc.ch/>.
- Ishikawa T, Li Z-S, Lu Y-P and Rea PA (1997). "The GS-X pump in plant, yeast, and animal cells: structure, function, and gene expression." Bioscience Reports **17**(2): 189-207.
- James I.L. M, Michael D. M, Lewis H. Z and James A. B, Eds. (2007). "Plant Growth and Climate Change". Colchester, Blackwell Publishing Ltd.
- Jany J-L, Garbaye J and Martin F (2002). "*Cenococcum geophilum* populations show a high degree of genetic diversity in beech forests." New Phytologist **154**(3): 651-659.
- Jenkin ME and Hayman GD (1999). "Photochemical ozone creation potentials for oxygenated volatile organic compounds: sensitivity to variations in kinetic and mechanistic parameters." Atmospheric Environment **33**(8): 1275-1293.
- Jones JDG and Dangl JL (2006). "The plant immune system." Nature **444**(7117): 323-329.
- Jongen M, Jones MB, Hebeisen T, Blum H and Hendrey G (1995). "The effects of elevated CO₂ concentrations on the root growth of *Lolium perenne* and *Trifolium repens* grown in a FACE system." Global Change Biology **1**(5): 361-371.
- Jorge I, Navarro RM, Lenz C, Ariza D, Porrás C and Jorrián J (2005). "The holm oak leaf proteome: Analytical and biological variability in the protein expression level assessed by 2-DE and protein identification tandem mass spectrometry de novo sequencing and sequence similarity searching." Proteomics **5**(1): 222-234.
- Jorrián-Novo JV, Maldonado AM, Echevarría-Zomeño S, Villedor L, Castillejo MA, Curto M, Valero J, Sghaier B, Donoso G and Redondo I (2009). "Plant proteomics update (2007-2008): second-generation proteomic techniques, an appropriate experimental design, and data analysis to fulfill MIAPE standards, increase plant proteome coverage and expand biological knowledge." Journal of Proteomics **72**(3): 285-314.
- Jump AS, Hunt JM, Martínez-Izquierdo JA and Penuelas J (2006). "Natural selection and climate change: temperature-linked spatial and temporal trends in gene frequency in *Fagus sylvatica*." Molecular Ecology **15**(11): 3469-3480.
- Jung T (2004). "Phytophthora schädigt Buchenbestände in ganz Bayern", LWF.
- Kangasjärvi J, Jaspers P and Kollist H (2005). "Signalling and cell death in ozone-exposed plants." Plant, Cell & Environment **28**(8): 1021-1036.
- Kangasjärvi J, Talvinen J, Utriainen M and Karjalainen R (1994). "Plant defence systems induced by ozone." Plant, Cell & Environment **17**(7): 783-794.
- Kim YJ, Lee JH, Jung DY, Sathiyaraj G, Shim JS, In JG and Yang DC (2009). "Isolation and characterization of pathogenesis-related protein 5 (PgPR5) gene from *Panax ginseng*." Plant Pathology Journal **25**(4): 400-407.
- Kimball BA (1982). "Carbon dioxide and agricultural yield: an assemblage and analysis of 430 prior observations". Phoenix, Agricultural Research Service.

-
- Kimball BA, Kobayashi K and Bindi M (2002). "Responses of agricultural crops to free-air CO₂ enrichment". *Advances in Agronomy*, Academic Press. **77**: 293-368.
- Klose J (1975). "Protein mapping by combined isoelectric focusing and electrophoresis of mouse tissues." *Human Genetics* **26**(3): 231-243.
- Koji K, Daisuke T, Ryoichi A and Katsutoshi T (2003). "Correlation analysis of mRNA and protein abundances in human tissues." *Genome Letters* **2**: 139-148.
- Kontunen-Soppela S, Riikonen J, Ruhanen H, Brosché M, Somervuo P, Peltonen P, Kangasjärvi J, Auvinen P, Paulin L, Keinänen M, Oksanen E and Vapaavuori E (2010). "Differential gene expression in senescing leaves of two silver birch genotypes in response to elevated CO₂ and tropospheric ozone." *Plant, Cell & Environment* **33**(6): 1016-1028.
- Kovacs D, Kalmar E, Torok Z and Tompa P (2008). "Chaperone activity of ERD10 and ERD14, two disordered stress-related plant proteins." *Plant Physiology* **147**(1): 381-390.
- Kramer H, Gussone HA and Schober R (1988). "Waldwachstumslehre". Parey, Hamburg, Berlin, Blackwell Wissenschafts-Verlag.
- Kramer K (1995). "Phenotypic plasticity of the phenology of 7 European tree species in relation to climatic warming." *Plant, Cell & Environment* **18**(2): 93-104.
- Kronfuß G, Polle A, Tausz M, Havranek WM and Wieser G (1998). "Effects of ozone and mild drought stress on gas exchange, antioxidants and chloroplast pigments in current-year needles of young Norway spruce [*Picea abies* (L.) Karst.]." *Trees - Structure and Function* **12**(8): 482-489.
- Laemmli UK (1970). "Cleavage of structural proteins during the assembly of the head of bacteriophage T4." *Nature* **227**(5259): 680-685.
- Laisk A, Kull O and Moldau H (1989). "Ozone concentration in leaf intercellular air spaces is close to zero." *Plant Physiology* **90**(3): 1163-1167.
- Lambers H, Chapin III F and Pons T, Eds. (1998). "Plant Physiological Ecology". New York, Springer-Verlag.
- Langebartels C, Wohlgemuth H, Kschieschan S, Grün S and Sandermann H (2002). "Oxidative burst and cell death in ozone-exposed plants." *Plant Physiology and Biochemistry* **40**(6-8): 567-575.
- Langley JA and Magonigal JP (2010). "Ecosystem response to elevated CO₂ levels limited by nitrogen-induced plant species shift." *Nature* **466**(7302): 96-99.
- Larsson C and Albertsson E (1979). "Enzymes related to serine synthesis in spinach-chloroplast." *Physiologia Plantarum* **45**(1): 7-10.
- Lawson T, Oxborough K, Morison JIL and Baker NR (2002). "Responses of photosynthetic electron transport in stomatal guard cells and mesophyll cells in intact leaves to light, CO₂, and humidity." *Plant Physiology* **128**(1): 52-62.
- Leakey ADB, Ainsworth EA, Bernacchi CJ, Rogers A, Long SP and Ort DR (2009). "Elevated CO₂ effects on plant carbon, nitrogen, and water relations: six important lessons from FACE." *Journal of Experimental Botany* **60**(10): 2859-2876.
- Leakey ADB, Bernacchi CJ, Dohleman FG, Ort DR and Long SP (2004). "Will photosynthesis of maize (*Zea mays*) in the US corn belt increase in future [CO₂] rich atmospheres? An analysis of diurnal courses of CO₂ uptake under free-air concentration enrichment (FACE)." *Global Change Biology* **10**(6): 951-962.
- Leuschner C (2009). "Die Trockenheitsempfindlichkeit der Rotbuche vor dem Hintergrund des prognostizierten Klimawandels." *Jahrbuch der Akademie der Wissenschaften zu Göttingen*: 281-296.

-
- Leuschner C, Meier IC and Hertel D (2006). "On the niche breadth of *Fagus sylvatica*: soil nutrient status in 50 Central European beech stands on a broad range of bedrock types." Annals of Forest Science **63**(4): 355-368.
- Levin SA, Carpenter SR and Godfray HCJ (2009). "The Princeton guide to ecology". Princeton, New Jersey, Princeton University Press.
- Liu X, Kozovits AR, Grams TEE, Blaschke H, Rennenberg H and Matyssek R (2004). "Competition modifies effects of enhanced ozone/carbon dioxide concentrations on carbohydrate and biomass accumulation in juvenile Norway spruce and European beech." Tree Physiology **24**(9): 1045-1055.
- LoBuglio KF, Berbee ML and Taylor JW (1996). "Phylogenetic origins of the asexual mycorrhizal symbiont *Cenococcum geophilum* Fr and other mycorrhizal fungi among the ascomycetes." Molecular Phylogenetics and Evolution **6**(2): 287-294.
- LoBuglio KF, Rogers SO and Wang CJK (1991). "Variation in ribosomal DNA among isolates of the mycorrhizal fungus *Cenococcum geophilum*." Canadian Journal of Botany **69**(11): 2331-2343.
- Löster K and Kannicht C (2002). "2D-electrophoresis detection of glycosylation and influence on spot pattern". "Posttranslational modification of proteins: Tools for functional proteomics". Totowa, Springer Verlag. **194** 301-316.
- Luedemann G, Matyssek R, Fleischmann F and Grams TEE (2005). "Acclimation to ozone affects host/pathogen interaction and competitiveness for nitrogen in juvenile *Fagus sylvatica* and *Picea abies* trees infected with *Phytophthora citricola*." Plant Biology **7**(06): 640,649.
- Luethy-Krause B, Pfenninger I and Landolt W (1990). "Effects of ozone on organic acids in needles of Norway spruce and Scots pine." Trees - Structure and Function **4**(4): 198-204.
- Mallick P and Küster B (2010). "Proteomics: a pragmatic perspective." Nature Biotechnology **28**(7): 695-709.
- Marenco A, Gouget H, Nédélec P, Pagés J-P and Karcher F (1994). "Evidence of a long-term increase in tropospheric ozone from Pic du Midi data series: consequences: positive radiative forcing." Journal of Geophysical Research **99**(D8): 16617-16632.
- Marx DH and Bryan WC (1975). "Growth and ectomycorrhizal development of loblolly pine seedlings in fumigated soil infested with the fungal symbiont *Pisolithus tinctorius* " Forest Science **21**(3): 245-254.
- Matthiesen R (2006). "Mass spectrometry data analysis in proteomics". Totowa, Humana Press.
- Mechin V, Consoli L, Le Guilloux M and Damerval C (2003). "An efficient solubilization buffer for plant proteins focused in immobilized pH gradients." Proteomics **3**(7): 1299-1302.
- Mexal J and Reid C (1973). "The growth of selected mycorrhizal fungi in response to induced water stress." Canadian Journal of Botany **51**: 1579-1588.
- Miller JD, Arteca RN and Pell EJ (1999). "Senescence-associated gene expression during ozone-induced leaf senescence in *Arabidopsis*." Plant Physiology **120**(4): 1015-1024.
- Moeder W, del Pozo O, Navarre D, Martin G and Klessig D (2007). "Aconitase plays a role in regulating resistance to oxidative stress and cell death in *Arabidopsis* and *Nicotiana benthamiana*." Plant Molecular Biology **63**(2): 273-287.
- Molina R and Trappe J (1982). "Patterns of ectomycorrhizal host specificity and potential among Pacific northwest conifers and fungi." Forest Science **28**: 423-458.
- Molloy MP, Brzezinski EE, Hang J, McDowell MT and VanBogelen RA (2003). "Overcoming technical variation and biological variation in quantitative proteomics." Proteomics **3**(10): 1912-1919.

-
- Monteoliva L and Albar JP (2004). "Differential proteomics: an overview of gel and non-gel based approaches." Briefings in Functional Genomics & Proteomics **3**(3): 220-239.
- Moore BD, Cheng SH, Rice J and Seemann JR (1998). "Sucrose cycling, Rubisco expression, and prediction of photosynthetic acclimation to elevated atmospheric CO₂." Plant, Cell & Environment **21**(8): 905-915.
- Moore BD, Cheng SH, Sims D and Seemann JR (1999). "The biochemical and molecular basis for photosynthetic acclimation to elevated atmospheric CO₂." Plant, Cell & Environment **22**(6): 567-582.
- Morte A, Díaz G, Rodríguez P, Alarcón JJ and Sánchez-Blanco MJ (2001). "Growth and water relations in mycorrhizal and nonmycorrhizal *Pinus halepensis* plants in response to drought." Biologia Plantarum **44**(2): 263-267.
- Müller-Starck G, Baradat P and Bergmann F (1992). "Genetic variation within European tree species." New Forests **6**(1): 23-47.
- Müller-Starck G and Starke R (1993). "Inheritance of isoenzymes in European beech (*Fagus sylvatica* L.)." Journal of Heredity **84**(4): 291-296.
- NASA. (2004). from <http://www.science.nasa.gov/missions/aura/>.
- Noh YS and Amasino RM (1999). "Identification of a promoter region responsible for the senescence-specific expression of SAG12." Plant Molecular Biology **41**(2): 181-194.
- Norby R (1994). "Issues and perspectives for investigating root responses to elevated atmospheric carbon dioxide." Plant and Soil **165**(1): 9-20.
- Norby RJ, Wullschlegel SD, Gunderson CA, Johnson DW and Ceulemans R (1999). "Tree responses to rising CO₂ in field experiments: implications for the future forest." Plant, Cell & Environment **22**(6): 683-714.
- O'Farrell PH (1975). "High resolution two-dimensional electrophoresis of proteins." Journal of Biological Chemistry **250**(10): 4007-4021.
- Odanaka S, Bennett AB and Kanayama Y (2002). "Distinct physiological roles of fructokinase isozymes revealed by gene-specific suppression of Frk1 and Frk2 expression in tomato." Plant Physiology **129**(3): 1119-1126.
- Olbrich M, Betz G, Gerstner E, Langebartels C, Sandermann H and Ernst D (2005). "Transcriptome analysis of ozone-responsive genes in leaves of European beech (*Fagus sylvatica* L.)." Plant Biology **7**(6): 670-676.
- Olbrich M, Gerstner E, Welzl G, Winkler J and Ernst D (2009). "Transcript responses in leaves of ozone-treated beech saplings seasons at an outdoor free air model fumigation site over two growing seasons." Plant and Soil **323**(1): 61-74.
- Olbrich M, Knappe C, Wenig M, Gerstner E, Häberle K-H, Kitao M, Matyssek R, Stich S, Leuchner M, Werner H, Schlink K, Müller-Starck G, Welzl G, Scherb H, Ernst D, Heller W and Bahnweg G (2010). "Ozone fumigation (twice ambient) reduces leaf infestation following natural and artificial inoculation by the endophytic fungus *Apiognomonia errabunda* of adult European beech trees." Environmental Pollution **158**(4): 1043-1050.
- Overmyer K, Tuominen H, Kettunen R, Betz C, Langebartels C, Sandermann H and Kangasjärvi J (2000). "Ozone-sensitive *Arabidopsis* rcd1 mutant reveals opposite roles for ethylene and jasmonate signaling pathways in regulating superoxide-dependent cell death." Plant Cell **12**(10): 1849-1862.
- Pawlowski TA (2007). "Proteomics of European beech (*Fagus sylvatica* L.) seed dormancy breaking: influence of abscisic and gibberellic acids." Proteomics **7**(13): 2246-2257.
- Pell EJ, Schlagnhauser CD and Arteca RN (1997). "Ozone-induced oxidative stress: mechanisms of action and reaction." Physiologia Plantarum **100**(2): 264-273.

-
- Penque D (2009). "Two-dimensional gel electrophoresis and mass spectrometry for biomarker discovery." *Proteomics - Clinical Applications* **3**(2): 155-172.
- Perco P, Mühlberger I, Mayer G, Oberbauer R, Lukas A and Mayer B (2010). "Linking transcriptomic and proteomic data on the level of protein interaction networks." *Electrophoresis* **31**(11): 1780-1789.
- Pieterse CMJ and Dicke M (2007). "Plant interactions with microbes and insects: from molecular mechanisms to ecology." *Trends in Plant Science* **12**(12): 564-569.
- Pigott CD (1982). "Survival of mycorrhiza formed by *Cenococcum geophilum* Fr. in dry soils." *New Phytologist* **92**(4): 513-517.
- Poorter H, VanBerkel Y, Baxter R, DenHertog J, Dijkstra P, Gifford RM, Griffin KL, Roumet C, Roy J and Wong SC (1997). "The effect of elevated CO₂ on the chemical composition and construction costs of leaves of 27 C₃ species." *Plant Cell and Environment* **20**(4): 472-482.
- Porcel R, Azcón R and Ruiz-Lozano JM (2005). "Evaluation of the role of genes encoding for dehydrin proteins (LEA D-11) during drought stress in arbuscular mycorrhizal *Glycine max* and *Lactuca sativa* plants." *Journal of Experimental Botany* **56**(417): 1933-1942.
- Prentice IC, Farquhar GD, Fasham MJR, Goulden ML, Heimann M, Jaramillo VJ, S KH, Le Quéré C, Scholes RJ and Wallace DWR (2001). "The carbon cycle and atmospheric carbon dioxide". "Climate change 2001: the scientific basis. Contributions of working group I to the third assessment report of the intergovernmental panel on climate change". Cambridge, Cambridge University Press: 185-237.
- Pritsch K, Ernst D, Fleischmann F, Gayler S, Grams T, Göttlein A, Heller W, Koch N, Lang H, Matyssek R, Munch J, Olbrich M, Scherb H, Stich S, Winkler J and Schloter M (2008). "Plant and soil system responses to ozone after 3 years in a lysimeter study with juvenile beech (*Fagus sylvatica* L.)." *Water, Air, & Soil Pollution: Focus* **8**(2): 139-154.
- Rabilloud T, Adessi C, Giraudel A and Lunardi J (1997). "Improvement of the solubilization of proteins in two-dimensional electrophoresis with immobilized pH gradients." *Electrophoresis* **18**(3-4): 307-316.
- Rabilloud T, Valette C and Lawrence JJ (1994). "Sample application by in-gel rehydration improves the resolution of two-dimensional electrophoresis with immobilized pH gradients in the first dimension." *Electrophoresis* **15**(1): 1552-1558.
- Ranieri A, Giuntini D, Ferraro F, Nali C, Baldan B, Lorenzini G and Soldatini GF (2001). "Chronic ozone fumigation induces alterations in thylakoid functionality and composition in two poplar clones." *Plant Physiology and Biochemistry* **39**(11): 999-1008.
- Reich PB (1983). "Effects of low concentrations of O₃ on net photosynthesis, dark respiration, and chlorophyll contents in aging hybrid poplar leaves." *Plant Physiology* **73**(2): 291-296.
- Rincón A, Priha O, Lelu-Walter MA, Bonnet M, Sotta B and Le Tacon F (2005). "Shoot water status and ABA responses of transgenic hybrid larch *Larix kaempferi* × *L. decidua* to ectomycorrhizal fungi and osmotic stress." *Tree Physiology* **25**(9): 1101-1108.
- Roshchina VV and Roshchina VD (2003). "Ozone and Plant Cell". Dordrecht, Kluwer Academic Publisher.
- Rössler G and Neumann M. (2006). "Ertragskundliche Grundlagen zur Buchenbewirtschaftung." from http://www.waldwissen.net/themen/waldbau/waldwachstum/bfw_buche_ertragskunde_2006_DE?start=0.
- Ryang S, Woo S, Kwon S, Kim S, Lee S, Kim K and Lee D (2009). "Changes of net photosynthesis, antioxidant enzyme activities, and antioxidant contents of *Liriodendron tulipifera* under elevated ozone." *Photosynthetica* **47**(1): 19-25.

- Saleem A, Loponen J, Pihlaja K and Oksanen E (2001). "Effects of long-term open-field ozone exposure on leaf phenolics of European silver birch (*Betula pendula* Roth)." Journal of Chemical Ecology **27**(5): 1049-1062.
- Sander T, König S, Rothe GM, Janßen A and Weisgerber H (2000). "Genetic variation of European beech (*Fagus sylvatica* L.) along an altitudinal transect at mount Vogelsberg in Hesse, Germany." Molecular Ecology **9**(9): 1349-1361.
- Sang-Eun H, Sang-Ryeol P, Hawk-Bin K, Bu-Young Y, Gil-Bok L and Myung-Ok B (2005). "Genetic engineering of drought-resistant tobacco plants by introducing the trehalose phosphorylase (TP) gene from *Pleurotus sajor-caju*." Plant Cell, Tissue and Organ Culture **82**(2): 151-158.
- Scheel D (1998). "Resistance response physiology and signal transduction." Current Opinion in Plant Biology **1**(4): 305-310.
- Scheromm P, Plassard C and Salsac L (1990). "Effect of nitrate and ammonium nutrition on the metabolism of the ectomycorrhizal basidiomycete, *Hebeloma cylindrosporum* Romagn." New Phytologist **114**(2): 227-234.
- Schlink K (2009). "Identification and characterization of differentially expressed genes from *Fagus sylvatica* roots after infection with *Phytophthora citricola*." Plant Cell Reports **28**(5): 873-882.
- Schlink K (2010). "Down-regulation of defense genes and resource allocation into infected roots as factors for compatibility between *Fagus sylvatica* and *Phytophthora citricola*." Functional & Integrative Genomics **10**(2): 253-264.
- Schloter M, Winkler JB, Aneja M, Koch N, Fleischmann F, Pritsch K, Heller W, Stich S, Grams TE, Gottlein A, Matyssek R and Munch JC (2005). "Short term effects of ozone on the plant-rhizosphere-bulk soil system of young beech trees." Plant Biology **7**(6): 728-736.
- Schmidt G, Mann M, Ammann C, Benestad R, Bradley R, Rahmstorf S, Steig E, Archer D, Pierrehumbert R, Garidel Td, Bouldin J and Connolley W. (2004). "RealClimate. Climate science for climate scientists." from <http://www.realclimate.org/>.
- School of Biological Sciences. (2003). "Plant pathology." from http://bugs.bio.usyd.edu.au/learning/resources/PlantPathology/infection/plant_defenses/active_def.html#delayedActiveDef.
- Sharma YK and Davis KR (1994). "Ozone-induced expression of stress-related genes *Arabidopsis thaliana*." Plant Physiology **105**(4): 1089-1096.
- Shevchenko A, Vâlcu CM and Junqueira M (2009). "Tools for exploring the proteomesphere." Journal of Proteomics **72**(2): 137-144.
- Shi LB, Guttenberger M, Kottke I and Hampp R (2002). "The effect of drought on mycorrhizas of beech (*Fagus sylvatica* L.): changes in community structure, and the content of carbohydrates and nitrogen storage bodies of the fungi." Mycorrhiza **12**(6): 303-311.
- Shi SQ, Shi Z, Qi LW, Sun XM, Jiang ZP, Li CX, Xiao WF and Zhang SG (2009). "Molecular responses and expression analysis of genes in a xerophytic desert shrub *Haloxylon ammodendron* (Chenopodiaceae) to environmental stresses." African Journal of Biotechnology **8**(12): 2667-2676.
- Shinohara ML, LoBuglio KF and Rogers SO (1999). "Comparison of ribosomal DNA ITS regions among geographic isolates of *Cenococcum geophilum*." Current Genetics **35**(5): 527-535.
- Shinozaki K and Yamaguchi-Shinozaki K (1997). "Gene expression and signal transduction in water-stress response." Plant Physiology **115**(2): 327-334.
- Shinozaki K and Yamaguchi-Shinozaki K (2007). "Gene networks involved in drought stress response and tolerance." Journal of Experimental Botany **58**(2): 221-227.

-
- Sickmann A, Reinders J, Wagner Y, Joppich C, Zahedi R, Meyer HE, Schönfisch B, Perschil I, Chacinska A, Guiard B, Rehling P, Pfanner N and Meisinger C (2003). "The proteome of *Saccharomyces cerevisiae* mitochondria." Proceedings of the National Academy of Sciences **100**(23): 13207-13212.
- Singh SN (2009). "Climate change and crops". Berlin, Springer-Verlag.
- Sisler EC and Wood C (1988). "Interaction of ethylene and CO₂." Physiologia Plantarum **73**(3): 440-444.
- Smirnoff N (1998). "Plant resistance to environmental stress." Current Opinion in Biotechnology **9**(2): 214-219.
- Smith JJ and John P (1993). "Activation of 1-aminocyclopropane-1-carboxylate oxidase by bicarbonate/carbon dioxide." Phytochemistry **32**(6): 1381-1386.
- Smith SD, Huxman TE, Zitzer SF, Charlet TN, Housman DC, Coleman JS, Fenstermaker LK, Seemann JR and Nowak RS (2000). "Elevated CO₂ increases productivity and invasive species success in an arid ecosystem." Nature **408**(6808): 79-82.
- Solomon M, Belenghi B, Delledonne M, Menachem E and Levine A (1999). "The involvement of cysteine proteases and protease inhibitor genes in the regulation of programmed cell death in plants." Plant Cell **11**(3): 431-444.
- Solomon S, Qin D, Manning M, Chen Z, Marquis M, Averyt K, Tignor M and Miller H (2007). "Climate change 2007: the physical science basis". Cambridge, Cambridge University Press.
- Symington LS (2002). "Role of RAD52 epistasis group genes in homologous recombination and double-strand break repair." Microbiology and Molecular Biology Reviews **66**(4): 630.
- Tans P and Keeling R. "NOAA/ESRL." from <http://www.esrl.noaa.gov/gmd/ccgg/trends/>.
- Taub DR and Wang X (2008). "Why are nitrogen concentrations in plant tissues lower under elevated CO₂? A critical examination of the hypotheses." Journal of Integrative Plant Biology **50**(11): 1365-1374.
- Thalmair M, Bauw G, Thiel S, Dohring T, Langebartels C and Sandermann H (1996). "Ozone and ultraviolet B effects on the defense-related proteins beta-1,3-glucanase and chitinase in tobacco." Journal of Plant Physiology **148**(1-2): 222-228.
- Theodorou C (1978). "Soil moisture and the mycorrhizal association of *Pinus radiata* D. don." Soil Biology and Biochemistry **10**(1): 33-37.
- Thipyapong P and Steffens JC (1997). "Tomato polyphenol oxidase (differential response of the polyphenol oxidase F promoter to injuries and wound signals)." Plant Physiology **115**(2): 409-418.
- Tomkinson AE, Bardwell AJ, Bardwell L, Tappe NJ and Friedberg EC (1993). "Yeast DNA repair and recombination proteins Rad1 and Rad1O constitute a single-stranded-DNA endonuclease." Nature **362**(6423): 860-862.
- Tran L and Constabel C (2011). "The polyphenol oxidase gene family in poplar: phylogeny, differential expression and identification of a novel, vacuolar isoform." Planta: 1-15.
- Trappe JM (1964). "Mycorrhizal hosts and distribution of *Cenococcum graniforme*." Lloydia **27**(2): 100-107.
- Ünlü M, Morgan ME and Minden JS (1997). "Difference gel electrophoresis. A single gel method for detecting changes in protein extracts." Electrophoresis **18**(11): 2071-2077.
- Vâlcu CM, Junqueira M, Shevchenko A and Schlink K (2009). "Comparative proteomic analysis of responses to pathogen infection and wounding in *Fagus sylvatica*." Journal of Proteome Research **8**(8): 4077-4091.

-
- Vâlcu CM and Schlink K (2006a). "Efficient extraction of proteins from woody plant samples for two-dimensional electrophoresis." *Proteomics* **6**(14): 4166-4175.
- Vâlcu CM and Schlink K (2006b). "Reduction of proteins during sample preparation and two-dimensional gel electrophoresis of woody plant samples." *Proteomics* **6**(5): 1599-1605.
- Walters D (2010). "Plant Defense. Warding off attack by pathogens, pests and vertebrate herbivores". Edingburg, Blackwell Publishing.
- Wang W, Scali M, Vignani R, Spadafora A, Sensi E, Mazzuca S and Cresti M (2003). "Protein extraction for two-dimensional electrophoresis from olive leaf, a plant tissue containing high levels of interfering compounds." *Electrophoresis* **24**(14): 2369-2375.
- Wang W, Vignani R, Scali M and Cresti M (2006). "A universal and rapid protocol for protein extraction from recalcitrant plant tissues for proteomic analysis." *Electrophoresis* **27**(13): 2782-2786.
- Wang XZ, Lewis JD, Tissue DT, Seemann JR and Griffin KL (2001). "Effects of elevated atmospheric CO₂ concentration on leaf dark respiration of *Xanthium strumarium* in light and in darkness." *Proceedings of the National Academy of Sciences of the United States of America* **98**(5): 2479-2484.
- Webber AN, Nie GY and Long SP (1994). "Acclimation of photosynthetic proteins to rising atmospheric CO₂" *Photosynthesis Research* **39**(3): 413-425.
- Werres S (1995). "Influence of the *Phytophthora* isolate and the seed source on the development of beech (*Fagus sylvatica*) seedling blight." *European Journal of Forest Pathology* **25**(6-7): 381-390.
- Westermeier R (2006). "Preparation of plant samples for 2-D electrophoresis." *Proteomics*: 56-60.
- Westermeier R, Naven T and Höpker H-R, Eds. (2008). "Proteomics in practice: a guide to successful experimental design". Weinheim, Wiley-VCH.
- White BA (1990). "Amplification and direct sequencing of fungal ribosomal RNA genes for phylogenetics". "PCR Protocols: a guide to methods and applications". Innis MA. New York, Academic Press: 315-322.
- Wingler A, Wallenda T and Hampp R (1996). "Mycorrhiza formation on Norway spruce (*Picea abies*) roots affects the pathway of anaplerotic CO₂ fixation." *Physiologia Plantarum* **96**(4): 699-705.
- Winkler J, Lang H, Graf W, Reth S and Munch J (2009). "Experimental setup of field lysimeters for studying effects of elevated ozone and below-ground pathogen infection on a plant-soil-system of juvenile beech (*Fagus sylvatica* L.)." *Plant and Soil* **323**(1): 7-19.
- Wolf HU and Braun H (1996). "Beiträge der Forstpflanzenzüchtung zur Erhaltung und Erhöhung der genetischen Vielfalt". "Biodiversität und nachhaltige Forstwirtschaft". Müller-Starck G. Landsberg Ecomed: 60-77.
- Wullschleger SD, Tschaplinski TJ and Norby RJ (2002). "Plant water relations at elevated CO₂-implications for water-limited environments." *Plant, Cell & Environment* **25**(2): 319-331.
- Xu G, Li CY and Yao YN (2009). "Proteomics analysis of drought stress-responsive proteins in *Hippophae rhamnoides* L." *Plant Molecular Biology Reporter* **27**(2): 153-161.
- Yan W and Chen SS (2005). "Mass spectrometry-based quantitative proteomic profiling." *Briefings in Functional Genomics & Proteomics* **4**(1): 27-38.
- Yuan S and Lin HH (2008). "Role of salicylic acid in plant abiotic stress." *Zeitschrift für Naturforschung* **63**(5-6): 313-320.
- Zhou W, Eudes F and Laroche A (2006). "Identification of differentially regulated proteins in response to a compatible interaction between the pathogen *Fusarium graminearum* and its host, *Triticum aestivum*." *Proteomics* **6**(16): 4599-4609.

-
- Zhu JK (2002). "Salt and drought stress signal transduction in plants." Annual Review of Plant Biology **53**: 247-273.
- Ziska LH and Bunce JA (2007). "Predicting the impact of changing CO₂ on crop yields: some thoughts on food." New Phytologist **175**(4): 607-618.

6 Appendix

Tab. 7 - Frequently used chemicals and equipments for protein extraction, separation and visualization.

Frequently used chemicals	Company	Product code
2-mercaptoethanol	Sigma-Aldrich	M7154
Acetic acid	Roth	3738.5
Aceton	Merck	1.00014.2500
Acetonitrile (ACN)	Sigma-Aldrich	Chromasolv 34881
Acrylamide 40% solution	GE Healthcare	17130301
Amberlite	GE Healthcare	17132601
Ammonium bicarbonate	Sigma	A6141
Ammonium persulfate	Sigma-Aldrich	A3678
Brilliant blue G	Sigma-Aldrich	B0770
Bromophenol blue	Merck	8122
CHAPS	GE Healthcare	17-1314-01
Cleaning solution, strip holder	GE Healthcare	80645278
CyDye DIGE Fluor, minimal labeling kit	GE Healthcare	25-8010-65
DeStreak rehydration solution	GE Healthcare	17600318
Dimethylformamide (DMF)	GE Healthcare	80203980
Dithiothreitol (DTT)	GE Healthcare	17131802
Drystrips pH 4-7, 24 cm	GE Healthcare	17600246
Ethanol p.a.	Roth	9065.5
Ethylenediaminetetraacetic acid (EDTA)	Fluka	03609
Formaldehyde solution	Sigma-Aldrich	F8775
Formic acid	Prolabo	Normapur 20 318.297
Glutaraldehyde solution	Sigma-Aldrich	G6257
Glycerol 87%	GE Healthcare	17132501
Glycine	GE Healthcare	17132301
Hydrochloric acid	Sigma-Aldrich	258148
Immobiline DryStrip Cover Fluid	GE Healthcare	17133501
Iodoacetamide	Sigma-Aldrich	57670
Methanol	Sigma-Aldrich	32,241-5
N,N,N',N'-tetramethylethylenediamine (TEMED)	Sigma-Aldrich	T9281
N,N'-methylene-bisacrylamide 2% solution	GE Healthcare	17130601
Natriumacetat-trihydrat	Roth	6779.1
Novex NuPAGE SDS-PAGE Gel System	Invitrogen	n.s.
NuPAGE® MOPS SDS Running Buffer	Invitrogen	NP0001
n-octyl β D-glucopiranoside (OG)	Sigma-Aldrich	3757
Paperwicks	GE Healthcare	80649914
Pharmalyte 3-10	GE Healthcare	17045601

Tab. 7 continued.

Frequently used chemicals	Company	Product code
Phenol solution	Sigma-Aldrich	P4557
Polyvinylpyrrolidone (PVPP)	Sigma-Aldrich	P-6755
Potassium chloride (KCL)	J.T.Baker	231-211-8
Protein quantitation kit RC DC Protein Assay	BIO-RAD	500-0120
Protein quantitation Kit: Coomassie (Bradford)	Thermo Scientific	23200
Sample cups	GE Healthcare	80-6498-95
Silver nitrate	Sigma-Aldrich	S6506
Sodium carbonate	Roth	A135.2
Sodium dodecylsulfate (SDS)	GE Healthcare	17-1313-01
Sodium hydroxide solution	Sigma-Aldrich	72068
Sodium thiosulfate	Sigma-Aldrich	21,726-3
Sucrose	Sigma-Aldrich	S-5016
Technical ethanol	JT Baker	80.982.500
Thiourea	Sigma-Aldrich	T-8656
Trichloroacetic acid (TCA)	Roth	8789.1
Tris	GE Healthcare	17132101
Tris(2-carboxyethyl)phosphine hydrochloride (TCEP)	Sigma-Aldrich	C4706
Trypsin	Sigma-Aldrich	T6567
Urea	GE Healthcare	17131901

Frequently used equipments	Company	Product code
ESI amaZon EDT iontrap mass spectrometer	Bruker	n.s.
Ettan DALTsix electrophoresis chamber	GE Healthcare	n.s.
Ettan IPGphor 2 isoelectric focusing unit	GE Healthcare	n.s.
Hermle centrifuge Z323K	Hermle	n.s.
ImageScanner II	GE Healthcare	n.s.
Nanospray LCQ Deca XP ion trap mass spectrometer	Thermo-Finnigan	n.s.
PB303 precision balance	Mettler Toledo	n.s.
Retsch MM300 dismembrator	Retsch	n.s.
SPD 121 P speedvac	Thermo Savant	n.s.
Typhoon 9410 Variable mode imager	GE Healthcare	n.s.
XCell SureLock™ electrophoresis Cell	Invitrogen	n.s.
Ultrospec 3100 pro	GE Healthcare	n.s.

Tab. 8 – Mass spectrometric information of proteins identified upon twice ambient elevated ozone fumigation (Lysimeterexperiment).

Spot ID	Accession number	Identified protein	Exp.		Theor.		Number of identified peptides		Number of unique peptides	
			pl	Mw	pl	Mw	Peptide sequence		Peptide sequence	
More than 2 unique peptides										
elD:0031	P43309	Polyphenol oxidase	4,86	23	6,39	56,29	2	K.VISTLVS RPK.Q K.FDVYINDEDDSPSGPDK.X	2	K.VISTLVS RPK.Q K.FDVYINDEDDSPSGPDK.X
elD:0053	B7TWE7	Fag s 1 pollen allergen*	5,72	20	4,87	17,35	3	K.SSEIEGNGGPGTIK.K K.SSEIEGNGGPGTIK.K K.ITFGEQSQFK.Y	2	K.SSEIEGNGGPGTIK.K K.ITFGEQSQFK.Y
elD:0101	Q9ZUC1	Quinone oxidoreductase-like protein At1g23740	5,93	48	8,46	40,99	3	K.TIGSLAEYTAVEEK.V K.VVAAALNPVDSK.R K.LDSNVTVPEVK.E	3	K.TIGSLAEYTAVEEK.V K.VVAAALNPVDSK.R K.LDSNVTVPEVK.E
elD:0165	Q40459	Oxygen-evolving enhancer protein 1	5,24	38	5,12	26,66	7	K.DGIDYAAVTVQLP GGER.V R.GDEEELAK.E R.GDEEELAKENVK.N R.GDEEELAKENVK.N K.NSPPEFQNTK.L R.LTYDEIQSK.T R.GGSTGYENAIALPAGGR.G	6	K.DGIDYAAVTVQLP GGER.V R.GDEEELAK.E R.GDEEELAKENVK.N R.GDEEELAKENVK.N K.NSPPEFQNTK.L R.LTYDEIQSK.T R.GGSTGYENAIALPAGGR.G
elD:0173	P27774	Phosphoribulokinase	5,33	55	5,22	39,18	6	K.FYGEVTQQMLK.H K.IRDLFEQLIASK.A R.LDELIYVESHLNISTK.F R.LDELIYVESHLNISTK.F R.DLFEQLIASK.A K.FFYGPDAYFGHEVSVLEM*DGQFDR.L	5	K.FYGEVTQQMLK.H K.IRDLFEQLIASK.A R.LDELIYVESHLNISTK.F R.DLFEQLIASK.A K.FFYGPDAYFGHEVSVLEM*DGQFDR.L
elD:0174	Q40281	RuBisCO activase	5,36	55	8,20	48,07	2	K.GLAFDESDDQDITR.G K.M*GINPIM*M*SAGELESGNAGEPAK.L	2	K.GLAFDESDDQDITR.G K.M*GINPIM*M*SAGELESGNAGEPAK.L
elD:0290	B7TWE7	Fag s 1 pollen allergen*	6,16	20	4,87	17,35	4	K.GDHEIKEEQVK.A K.IVASPDGGSVLK.S K.SSEIEGNGGPGTIK.K K.ITFGEQSQFK.Y	4	K.GDHEIKEEQVK.A K.IVASPDGGSVLK.S K.SSEIEGNGGPGTIK.K K.ITFGEQSQFK.Y
elD:0350	P26291	Cytochrome b6-f complex iron-sulfur subunit	5,61	22	6,07	19,07	3	K.DALGNDIVASEWLK.T K.VVFPVWVETDFR.T -GDPTYLVVEK.-	3	K.DALGNDIVASEWLK.T K.VVFPVWVETDFR.T -GDPTYLVVEK.-
elD:0356	P16096	Fructose-bisphosphate aldolase	6,51	53	5,80	37,70	4	R.LASIGLENTEANR.Q R.GILAMDES NATC#GK.R K.IVDVLVEQK.I -GLVPLVGSNNESWC#QGLDGLASR.-	4	R.LASIGLENTEANR.Q R.GILAMDES NATC#GK.R K.IVDVLVEQK.I -GLVPLVGSNNESWC#QGLDGLASR.-
elD:0526	O23264	Putative selenium-binding protein	6,20	69	5,37	54,06	4	K.DTGFVGC#ALTSNM*VR.F K.GFNLQHVSDGLYGR.H K.TM*ISTSWGAPAAFTK.G K.QLDLGNTGLLPLEIR.F	4	K.DTGFVGC#ALTSNM*VR.F K.GFNLQHVSDGLYGR.H K.TM*ISTSWGAPAAFTK.G K.QLDLGNTGLLPLEIR.F

Tab. 8 continued.

Spot ID	Accession number	Identified protein	Exp.		Theor.		Number of identified peptides	Number of unique peptides
			pI	Mw	pI	Mw	Peptide sequence	Peptide sequence
ID:0160	Q6YZX6	Putative aconitate hydratase	6,41	101	5,67	98,08	4	3
							K.TGEDADTLGLTGHHER.Y K.ISEIRPGQDVTVTDSGK.S K.ISEIRPGQDVTVTDSGK.S K.TAGQGTIILAGAEGSGSSR.D	K.TGEDADTLGLTGHHER.Y K.ISEIRPGQDVTVTDSGK.S K.TAGQGTIILAGAEGSGSSR.D
	Q9SIB9	Aconitate hydratase 2	6,41	101	5,86	99,74	3	2
							R.IATM*ASENPFK.A R.SENAVQANM*ELEFQR.N R.SENAVQANM*ELEFQR.N	R.IATM*ASENPFK.A R.SENAVQANM*ELEFQR.N
ID:0170	049954	Glycine dehydrogenase [decarboxylating]	6,53	99	5,94	105,57	5	5
							R.GVNGTVAHEFIVDLR.G K.NTAGIEPEDVAKR.L K.NTAGIEPEDVAK.R K.IAIIANANYM*AK.R K.HLAPYLPSPVPTGGIPAPDK.S	R.GVNGTVAHEFIVDLR.G K.NTAGIEPEDVAKR.L K.NTAGIEPEDVAK.R K.IAIIANANYM*AK.R K.HLAPYLPSPVPTGGIPAPDK.S
ID:0262	P35100	ATP-dependent Clp protease ATP-binding subunit clpC homolog, chloroplastic	5,86	91	5,69	94,93	6=	4=
							R.IGFDLDYDEK.E K.NTLIMTSNVGSSVIEK.G K.NTLIMTSNVGSSVIEK.G K.ALAAYYFGSEEMIR.L R.LDMSEFM*ER.H R.LDM*SEFMER.H	R.IGFDLDYDEK.E K.NTLIMTSNVGSSVIEK.G K.ALAAYYFGSEEMIR.L R.LDM*SEFMER.H
	P31542	ATP-dependent Clp protease ATP-binding subunit clpA homolog CD4B, chloroplastic	5,86	91	5,86	10,22	5	4
							K.AIDLIDEAGSR.V K.VPEPTVDETIQILK.G K.VITLDMGLLVAGTK.Y K.VITLDM*GLLVAGTK.Y R.HAQLPEEAR.E	K.AIDLIDEAGSR.V K.VPEPTVDETIQILK.G K.VITLDMGLLVAGTK.Y R.HAQLPEEAR.E
ID:0295	Q43848	Transketolase	6,23	88	5,53	72,93	4	3
							K.KYKEAAELK.S K.VTTTIGFGSPNK.A K.ALPTYTPESPADATR.X K.ALPTYTPESPADATR.X	K.KYKEAAELK.S K.VTTTIGFGSPNK.A K.ALPTYTPESPADATR.X
ID:0296	Q43848	Transketolase	6,16	88	5,53	72,93	3	3
							-XGNTGYDEIR.- K.ALPTYTPESPADATR.X R.NLSQQC#LNALAK.G	-XGNTGYDEIR.- K.ALPTYTPESPADATR.X R.NLSQQC#LNALAK.G
ID:0445	Q9FMP3	Dihydropyrimidinase *	6,15	74	9,19	63,03	6	5
							-JWENNELK.- K.YVEMPPFGYLFNGIDK.G K.YVEM*PPFGYLFNGIDK.G K.GKVEVTIAGGR.I K.VEVTIAGGR.I K.GDANYISSLK.A	-JWENNELK.- K.YVEMPPFGYLFNGIDK.G K.GKVEVTIAGGR.I K.VEVTIAGGR.I K.GDANYISSLK.A
ID:0450	Q9FMP3	Dihydropyrimidinase *	6,05	74	9,19	63,03	2	2
							K.YVEM*PPFGYLFNGIDK.G K.VEVTIAGGR.I	K.YVEM*PPFGYLFNGIDK.G K.VEVTIAGGR.I
ID:0462	004130	D-3-phosphoglycerate dehydrogenase	5,96	74	5,28	61,20	2	2
							K.FASAI SDSGEIK.V R.LAVQLVAGSGVK.T	K.FASAI SDSGEIK.V R.LAVQLVAGSGVK.T

Tab. 8 continued.

Spot ID	Accession number	Identified protein	Exp.		Theor.		Number of identified peptides	Number of unique peptides
			pI	Mw	pI	Mw	Peptide sequence	Peptide sequence
ID:0562	P34106	Alanine aminotransferase 2	6,50	66	5,82	52,68	14=	10=
							K.AKHYSLTTGGLGAYSDSR.G	K.AKHYSLTTGGLGAYSDSR.G
							K.AKHYSLTTGGLGAYSDSR.G	K.AKHYSLTTGGLGAYSDSR.G
							K.ALDYESLNENVK.K	K.ALDYESLNENVK.K
							K.IIFTNVGNPHALGQR.P	K.IIFTNVGNPHALGQR.P
							K.ALDYESLNENVK.K	K.ALDYESLNENVK.K
							R.NEVAEFIER.R	R.NEVAEFIER.R
							K.HYLSLTTGGLGAYSDSR.G	K.HYLSLTTGGLGAYSDSR.G
							R.RDGYPSPDELIFLTDGASK.G	R.RDGYPSPDELIFLTDGASK.G
							-.GVM*QILNTIIR.-	-.GVM*QILNTIIR.-
							K.GVM*QILNTIIR.G	K.GVM*QILNTIIR.G
							R.DGYPSPDELIFLTDGASK.G	R.DGYPSPDELIFLTDGASK.G
							R.DGYPSPDELIFLTDGASK.G	R.DGYPSPDELIFLTDGASK.G
							R.DGYPSPDELIFLTDGASK.G	R.DGYPSPDELIFLTDGASK.G
							R.QVVALC#QAPFLDDPNVGLLFPADAIK.A	R.QVVALC#QAPFLDDPNVGLLFPADAIK.A
ID:0565	P34106	Alanine aminotransferase 2	6,48	66	5,82	52,68	16=	10=
							K.IIFTNVGNPHALGQR.P	K.IIFTNVGNPHALGQR.P
							K.AKHYSLTTGGLGAYSDSR.G	K.AKHYSLTTGGLGAYSDSR.G
							K.ALDYESLNENVK.K	K.ALDYESLNENVK.K
							K.ALDYESLNENVK.K	K.ALDYESLNENVK.K
							K.IIFTNVGNPHALGQR.P	K.IIFTNVGNPHALGQR.P
							K.ALDYESLNENVK.K	K.ALDYESLNENVK.K
							R.NEVAEFIER.R	R.NEVAEFIER.R
							R.NEVAEFIER.R	R.NEVAEFIER.R
							K.HYLSLTTGGLGAYSDSR.G	K.HYLSLTTGGLGAYSDSR.G
							R.RDGYPSPDELIFLTDGASK.G	R.RDGYPSPDELIFLTDGASK.G
							K.GVM*QILNTIIR.G	K.GVM*QILNTIIR.G
							R.DGYPSPDELIFLTDGASK.G	R.DGYPSPDELIFLTDGASK.G
							R.DGYPSPDELIFLTDGASK.G	R.DGYPSPDELIFLTDGASK.G
							R.DGYPSPDELIFLTDGASK.G	R.DGYPSPDELIFLTDGASK.G
							R.QVVALC#QAPFLDDPNVGLLFPADAIK.A	R.QVVALC#QAPFLDDPNVGLLFPADAIK.A
							R.QVVALC#QAPFLDDPNVGLLFPADAIK.A	R.QVVALC#QAPFLDDPNVGLLFPADAIK.A
ID:0651	Q40281	RuBisCO activase	5,54	58	8,20	48,08	3=	2=
							K.SFQC#ELVFAK.M	K.SFQC#ELVFAK.M
							K.MC#C#LFINDLDAGAGR.L	K.MC#C#LFINDLDAGAGR.L
							K.M*C#C#LFINDLDAGAGR.L	K.M*C#C#LFINDLDAGAGR.L
ID:0673	P15102	Glutamine synthetase leaf isozyme, chloroplastic	5,83	57	5,50	41,58	6	6
							R.GGNNILVIC#DAYTPQGEPIPTNK.R	R.GGNNILVIC#DAYTPQGEPIPTNK.R
							R.GGNNILVIC#DAYTPQGEPIPTNK.R	R.GGNNILVIC#DAYTPQGEPIPTNK.R
							R.LESLLNDITPFTEK.I	R.LESLLNDITPFTEK.I
							K.IIAEYIWIGGTGIDL.R.S	K.IIAEYIWIGGTGIDL.R.S
							K.VVDEVPWYIGIEQYLLQTDVK.W	K.VVDEVPWYIGIEQYLLQTDVK.W
							R.AAEVFSNK.K	R.AAEVFSNK.K
ID:0724	Q40281	RuBisCO activase	5,08	56	8,20	48,07	4	3
							K.GLAFDESDDQDITR.G	K.GLAFDESDDQDITR.G
							K.SFQC#ELVFAK.M	K.SFQC#ELVFAK.M
							K.M*C#C#LFINDLDAGAGR.L	K.M*C#C#LFINDLDAGAGR.L
							K.MC#C#LFINDLDAGAGR.L	K.MC#C#LFINDLDAGAGR.L

Tab. 8 continued.

Spot ID	Accession number	Identified protein	Exp.		Theor.		Number of identified peptides	Number of unique peptides
			pl	Mw	pl	Mw	Peptide sequence	Peptide sequence
ID:0778	P46283	Sedoheptulose-1,7-bisphosphatase	5,16	53	6,17	42,41	15=	3=
							R.LMVC#M*GEAIR.T	R.LMVC#M*GEAIR.T
							R.LMVC#MGEAIR.T	
							K.LLFEALTYSHFC#K.Y	
							K.LLFEALTYSHFC#K.Y	
							K.LLFEALTYSHFC#K.Y	
							K.LLFEALTYSHFC#K.Y	K.LLFEALTYSHFC#K.Y
							K.LLFEALTYSHFC#K.Y	
							K.LLFEALTYSHFC#K.Y	
							K.TASC#GGTAC#VNTFGDEQLAVDLLANK.L	
							K.TASC#GGTAC#VNTFGDEQLAVDLLANK.L	
							K.TASC#GGTAC#VNTFGDEQLAVDLLANK.L	
							K.TASC#GGTAC#VNTFGDEQLAVDLLANK.L	K.TASC#GGTAC#VNTFGDEQLAVDLLANK.L
ID:0779	O20252	Sedoheptulose-1,7-bisphosphatase	5,28	52	5,87	42,08	2=	2=
							R.LMVC#MGEAIR.T	R.LMVC#MGEAIR.T
ID:0845	Q9SN86	Malate dehydrogenase	5,82	48	5,69	34,08	4=	4=
							K.VQDFTGASELSALK.G	K.VQDFTGASELSALK.G
ID:0860	Q9SID0	Probable fructokinase-1	5,12	48	5,31	35,28	4=	4=
							K.VQDFTGASELSALK.G	K.VQDFTGASELSALK.G
							K.GVDVVVIPAGVPR.K	K.GVDVVVIPAGVPR.K
							R.DDLFNINAGIVK.T	R.DDLFNINAGIVK.T
							K.VAILGAAGGIGQPLALLI.K.M	K.VAILGAAGGIGQPLALLI.K.M
							K.VQDFTGASELSALK.G	K.VQDFTGASELSALK.G
	Q9LNE3	Probable fructokinase-2	5,12	48	4,93	35,89	3	3
							K.IVDDQSIIEDEQR.L	K.IVDDQSIIEDEQR.L
							K.LLLVTLGENGCH.R.Y	K.LLLVTLGENGCH.R.Y
							-.DAGVLLSYDPNLR.-	-.DAGVLLSYDPNLR.-
							K.VFHYGSISLIVEPC#R.S	K.VFHYGSISLIVEPC#R.S
							-.DAGVLLSYDPNLR.-	-.DAGVLLSYDPNLR.-
							-.DAGVLLSYDPNLR.-	-.DAGVLLSYDPNLR.-
ID:0907	A1Y2Z0	Galacturonic acid reductase*	6,11	45	6,32	35,49	5	4
							K.DIHITAFSPLANGTK.W	K.DIHITAFSPLANGTK.W
							R.IVECDILEEIAK.A	R.IVECDILEEIAK.A
							R.HFDTAFAYR.S	R.HFDTAFAYR.S
							K.KLEELLSFAK.I	K.KLEELLSFAK.I
ID:0993	Q8LAS8	S-formylglutathione hydrolase	6,46	40	5,91	31,66	3=	3=
							R.AASSEGVALIVPDTSPR.G	R.AASSEGVALIVPDTSPR.G
							K.ADWEEDATSLISK.Y	K.ADWEEDATSLISK.Y
							K.AFTNYLGGNK.A	K.AFTNYLGGNK.A
ID:0999	P15102	Glutamine synthetase, leaf isoenzyme chloroplastic	6,26	39	5,50	41,58	3	3
							R.LESLNLDITPFTEK.I	R.LESLNLDITPFTEK.I
							K.VVDEVPWYGIQEYTLQTDVK.W	K.VVDEVPWYGIQEYTLQTDVK.W
ID:1162	Q03662	Probable glutathione S-transferase	5,67	31	6,77	25,67	5	5
							K.VPVLVHNGK.A	K.VPVLVHNGK.A
							R.FWANFYDQK.I	R.FWANFYDQK.I
							K.GIPYEVVEEDLTNK.S	K.GIPYEVVEEDLTNK.S
							R.ETAIEDLSQVLR.V	R.ETAIEDLSQVLR.V
							-.JLPSFYVIFGSK.-	-.JLPSFYVIFGSK.-

Tab. 8 continued.

Spot ID	Accession number	Identified protein	Exp.		Theor.		Number of identified peptides		Number of unique peptides	
			pI	Mw	pI	Mw	Peptide sequence	Peptide sequence		
ID:1250	Q9FT52	ATP synthase subunit d	5,46	26	5,09	19,45	2= R.AFDEVNSTLQTK.F K.FDALLVELK.E	2= R.AFDEVNSTLQTK.F K.FDALLVELK.E		
ID:1307	P26291	Cytochrome b6-f complex iron-sulfur subunit	5,64	22	6,07	19,07	4 K.DALGNDIVASEWLK.T K.VVFPWVETDFR.T R.GDPTYLVVEKDR.T -.GDPTYLVVEK.-	4 K.DALGNDIVASEWLK.T K.VVFPWVETDFR.T R.GDPTYLVVEKDR.T -.GDPTYLVVEK.-		
ID:1340	B7TWE7	Fag s 1 pollen allergen ⁺	6,05	19	4,87	17,35	4 K.SSEIEGNGGPGTIK.K K.SSEIEGNGGPGTIK.K K.KITFEGESQFK.Y K.ITFEGESQFK.Y	3 K.SSEIEGNGGPGTIK.K K.KITFEGESQFK.Y K.ITFEGESQFK.Y		
ID:1348	B7TWE7	Fag s 1 pollen allergen ⁺	5,97	20	4,87	17,35	3 K.SSEIEGNGGPGTIK.K K.SSEIEGNGGPGTIK.K K.ITFEGESQFK.Y	2 K.SSEIEGNGGPGTIK.K K.ITFEGESQFK.Y		
One unique peptide										
elD:0124	A7LAB9	Cysteine protease Cp ⁺	4,82	38	5,08	23,65	2 K.YNGGLTDEAYPYTAK.D K.YNGGLTDEAYPYTAK.D	1 K.YNGGLTDEAYPYTAK.D		
ID:0434	Q9XF61	Protein disulfide-isomerase	5,12	77	4,84	54,87	3 R.EADGIVDYLLK.K K.HDFIVVEFYAPWC#GHC#K.K K.QLATEFEVQGFPTIK.I	0 R.EADGIVDYLLK.K K.HDFIVVEFYAPWC#GHC#K.K K.QLATEFEVQGFPTIK.I		
elD:0353 ^{pp1}	Q9ZT66	Endo-1,3;1,4-beta-D-glucanase	5,71	31	7,23	28,78	1 K.APIAVLGAENDHLSPPALK.Q	1 K.APIAVLGAENDHLSPPALK.Q		
ID:1174 ^{pp1}	Q9ZT66	Endo-1,3;1,4-beta-D-glucanase	5,20	31	7,23	28,78	1 K.EANQDVLDFWFAK.H	1 K.EANQDVLDFWFAK.H		
ID:0812 ^{pp1}	Q9LZG0	Adenosine kinase 2	5,30	51	5,14	37,85	1= K.DNVEIYAGGATQNSIR.V	1= K.DNVEIYAGGATQNSIR.V		
ID:1372 ^{pp1}	P80499	Cytochrome c oxidase subunit 5B	4,87	20	4,96	3,10	1= R.PILDINFPVPGPGTK.E	1= R.PILDINFPVPGPGTK.E		
ID:1014 ^{pp1}	Q68BK5	Peptidyl-prolyl cis-trans isomerase ^e	5,68	39	6,64	44,66	1 R.LGEHNIDVLEGEQFINAAK.I	1 R.LGEHNIDVLEGEQFINAAK.I		
ID:1166 ^{pp1}	Q03662	Probable glutathione S-transferase	5,54	31	6,77	25,67	1= R.ETAIEDLSQVLR.V	1= R.ETAIEDLSQVLR.V		
elD:0846 ^{pp1}	D8L7V9	Epoxide hydrolase 3 ⁺	5,82	49	5,88	43,06	1= K.SGFQATALQVPPYR.S	1= K.SGFQATALQVPPYR.S		
ID:0626 ^{pp1}	Q43848	Transketolase	5,99	62	5,53	72,93	1 K.ALPTYTPESPADATR.X	1 K.ALPTYTPESPADATR.X		
ID:0863 ^{pp1}	Q68BK5	Peptidyl-prolyl cis-trans isomerase ^e	6,45	47	6,64	44,66	1 R.LGEHNIDVLEGEQFINAAK.I	1 R.LGEHNIDVLEGEQFINAAK.I		
ID:1067 ^{pp1}	Q68BK5	Peptidyl-prolyl cis-trans isomerase ^e	6,04	36	6,64	44,66	1 -.LGEHNIDVLEGEQFINAAK.-	1 -.LGEHNIDVLEGEQFINAAK.-		
Multiple proteins in a spot										
elD:0242	Q49434	Allantoate deiminase	6,02	69	5,09	46,49	5= R.LLAGSEVLVK.A K.NLM*GLSGLSVR.E K.QIDELATFSDTPAPSVTR.I K.DQDDLSSVFLR.K K.YDGVIGVLGAIEAINSLK.R	5= R.LLAGSEVLVK.A K.NLM*GLSGLSVR.E K.QIDELATFSDTPAPSVTR.I K.DQDDLSSVFLR.K K.YDGVIGVLGAIEAINSLK.R		
	Q9LEI9	Enolase 2	6,02	69	5,92	47,91	2 R.IEEELGAAAVYAGSK.Y K.VNQIGTVTESIEAVK.M	2 R.IEEELGAAAVYAGSK.Y K.VNQIGTVTESIEAVK.M		
	P48350	Catalase isozyme 1	6,02	69	6,96	57,07	2= R.LGPNYM*QLPVNAPK.C R.FPINNAIVTGR.R	2= R.LGPNYM*QLPVNAPK.C R.FPINNAIVTGR.R		

Tab. 8 continued.

Spot ID	Accession number	Identified protein	Exp.		Theor.		Number of identified peptides	Number of unique peptides
			pl	Mw	pl	Mw	Peptide sequence	Peptide sequence
elD:0690	Q43467	Elongation factor Tu	5,56	58	5,29	44,54	13	5
							-VATIM*NDKDEESK.- R.VATIMNDKDEESK.M K.M*VVELIM*PVAC#EQGMR.F K.MVVELIM*PVAC#EQGM*R.F K.M*VVELIMPVAC#EQGM*R.F K.MVVELIM*PVAC#EQGMR.F -FEAIVVVK.- K.ILDDAM*AGDNVGLLR.G -FEAIVVVK.- K.ILDDAM*AGDNVGLLR.G K.MVVELIMPVAC#EQGM*R.F K.ILDDAM*AGDNVGLLR.G K.ILDDAMAGDNVGLLR.G	-VATIM*NDKDEESK.- R.VATIMNDKDEESK.M K.MVVELIM*PVAC#EQGM*R.F -FEAIVVVK.- K.ILDDAM*AGDNVGLLR.G
	P15102	Glutamine synthetase leaf isozyme	5,56	58	5,50	41,58	7	5
							R.GGNNILVIC#DAYTPQGEPIPTNKR.H R.GGNNILVIC#DAYTPQGEPIPTNK.R R.GGNNILVIC#DAYTPQGEPIPTNK.R R.LESLNLDITPFTEK.I K.IIAEYIWIGGTGIDL.R.S R.LESLNLDITPFTEK.I K.VVDEVPWYGIQEYTLTQTDVK.W	R.GGNNILVIC#DAYTPQGEPIPTNKR.H R.GGNNILVIC#DAYTPQGEPIPTNK.R R.GGNNILVIC#DAYTPQGEPIPTNK.R K.IIAEYIWIGGTGIDL.R.S R.LESLNLDITPFTEK.I K.VVDEVPWYGIQEYTLTQTDVK.W
	Q42711	Monodehydroascorbate reductase	5,56	58	5,29	47,42	5	4
							K.GTVATGFTADSNGEVK.E K.GTVATGFTADSNGEVK.E K.IFGAFLEGGTPEENK.A K.TSVPGVYAVGDVATFPLK.L K.TVEEYDYLPHYFSR.S	K.GTVATGFTADSNGEVK.E K.IFGAFLEGGTPEENK.A K.TSVPGVYAVGDVATFPLK.L K.TVEEYDYLPHYFSR.S
	Q39639	Glycerol-3-phosphate acyltransferase	5,56	58	5,01	41,25	4	4
							K.NAVFQSGNPR.A R.ADEIVLSNM*AM*AFDR.M R.EPFDYYM*FGQNYIR.P R.TFLNATTEELLAGIR.K	K.NAVFQSGNPR.A R.ADEIVLSNM*AM*AFDR.M R.EPFDYYM*FGQNYIR.P R.TFLNATTEELLAGIR.K
	Q42961	Phosphoglycerate kinase	5,56	58	5,59	42,58	3	3
							K.TFNEALET.K.T K.GVTTHIGGGDSVAAVEK.V K.GVSLLLPTDVVIADK.F	K.TFNEALET.K.T K.GVTTHIGGGDSVAAVEK.V K.GVSLLLPTDVVIADK.F
	Q10DV7	Actin-1	5,56	58	5,30	41,81	4	3
							K.DAYVGDEAQS.K.R K.DAYVGDEAQS.K.R R.GYSFTT.AER.E R.VAPEEHPVLLTEAPLNPK.A	K.DAYVGDEAQS.K.R R.GYSFTT.AER.E R.VAPEEHPVLLTEAPLNPK.A
	Q92T91	Elongation factor Tu	5,56	58	5,93	44,10	2=	2=
							R.HYAHVDC#PGHADV.K.N R.QVGVP.SLVC#FLNK.V	R.HYAHVDC#PGHADV.K.N R.QVGVP.SLVC#FLNK.V
	P02580	Actin-3	5,56	58	5,23	41,61	2=	2=
							K.GEYDESGPSIVHR.K K.EITALAPSSM*K.I	K.GEYDESGPSIVHR.K K.EITALAPSSM*K.I
ID:0169	O49954	Glycine dehydrogenase	6,44	100	5,94	105,57	3	3
							K.NTAGIEPEDVAKR.L K.NTAGIEPEDVAKR.R K.HLAPYLPSPVPTGGIPAPDK.S	K.NTAGIEPEDVAKR.L K.NTAGIEPEDVAKR.R K.HLAPYLPSPVPTGGIPAPDK.S
	Q6VZX6	Putative aconitate hydratase	6,44	100	5,67	98,08	2	2
							K.TGEDADTLGLTGH.R.Y K.ISEIRPGQDVTVTDSGK.S	K.TGEDADTLGLTGH.R.Y K.ISEIRPGQDVTVTDSGK.S

Tab. 8 continued.

Spot ID	Accession number	Identified protein	Exp.		Theor.		Number of identified peptides		Number of unique peptides	
			pl	Mw	pl	Mw	Peptide sequence	Peptide sequence		
ID:0654	P15102	Glutamine synthetase leaf isozyme	5,41	60	5,50	41,58	5		5	
							R.GGNNILVIC#DAYTPQGEPIPTNK.R	R.GGNNILVIC#DAYTPQGEPIPTNK.R		
							K.WNYDGSSTGQAPGEDSEVILYPQAIK.D	K.WNYDGSSTGQAPGEDSEVILYPQAIK.D		
							R.LESLNLDITPFTEK.I	R.LESLNLDITPFTEK.I		
							K.IIAEYIWIGGTGIDL.R.S	K.IIAEYIWIGGTGIDL.R.S		
							K.VVDEVPWYIGIEQEYTLQTDVK.W	K.VVDEVPWYIGIEQEYTLQTDVK.W		
	Q43467	Elongation factor Tu	5,41	60	5,29	44,54	3		2	
							-.FEAIVVVLK.-	-.FEAIVVVLK.-		
							K.ILDDAM*AGDNVGLLLR.G			
							K.ILDDAMAGDNVGLLLR.G	K.ILDDAMAGDNVGLLLR.G		
	Q40281	RuBisCO activase	5,41	60	8,20	48,08	7		3	
							K.GLAFDTSDDQDITR.G			
							K.GLAFDTSDDQDITR.G			
							K.GLAFDTSDDQDITR.G			
							K.GLAFDTSDDQDITR.G	K.GLAFDTSDDQDITR.G		
							K.SFQC#ELVFAK.M	K.SFQC#ELVFAK.M		
							K.SFQC#ELVFAK.M			
							K.MGISPIM*MSAGELESGNAGEPAK.L	K.MGISPIM*MSAGELESGNAGEPAK.L		
	P16096	Fructose-bisphosphate aldolase	5,41	60	5,80	37,70	2=		2=	
							R.TAAYYQQGAR.F	R.TAAYYQQGAR.F		
							R.GILAM*DESNATC#GK.R	R.GILAM*DESNATC#GK.R		
	P46258	Actin-3	5,41	60	5,31	41,63	2=		2=	
							K.DAYVGDEAQS.K.R	K.DAYVGDEAQS.K.R		
							K.AGFAGDDAPR.A	K.AGFAGDDAPR.A		
ID:0699	Q42962	Phosphoglycerate kinase	6,40	56	5,69	42,36	4		3	
							K.KLASLADLYVNDAFGTAHR.A	K.KLASLADLYVNDAFGTAHR.A		
							K.LASLADLYVNDAFGTAHR.A	K.LASLADLYVNDAFGTAHR.A		
							R.FYKEEEKNDPEFAK.K	R.FYKEEEKNDPEFAK.K		
							R.FYKEEEKNDPEFAK.K			
	B9SJL8	Protease C56, putative*	6,40	56	5,60	41,67	3		2	
							K.ALGGTITGSDK.R			
							K.ALGGTITGSDK.R	K.ALGGTITGSDK.R		
							K.KPVASIC#HGQQLSAAAVLK.G	K.KPVASIC#HGQQLSAAAVLK.G		
	Q9S283	Uncharacterized oxidoreductase At4g09670	6,40	56	5,61	39,56	7		2	
							R.AITLAPNATIAAIGSR.S	R.AITLAPNATIAAIGSR.S		
							K.FASANNFPPDVK.I			
							K.FASANNFPPDVK.I			
							K.FASANNFPPDVK.I			
							K.FASANNFPPDVK.I			
							K.FASANNFPPDVK.I			
							K.FASANNFPPDVK.I	K.FASANNFPPDVK.I		
	Q42961	Phosphoglycerate kinase	6,40	56	5,59	42,58	4		2	
							K.GVSLLLPTDVIADK.F	K.GVSLLLPTDVIADK.F		
							K.TFNEALETTK.T			
							K.TFNEALETTK.T	K.TFNEALETTK.T		
							K.TFNEALETTK.T			
ID:0703	P42495	Probable cinnamyl alcohol dehydrogenase 1	5,95	56	5,33	39,13	3		3	
							R.AMGHHVTVISSDK.K	R.AMGHHVTVISSDK.K		
							R.FVVDVAGSK.L	R.FVVDVAGSK.L		
							K.SITGSFVGSIK.E	K.SITGSFVGSIK.E		
	Q42961	Phosphoglycerate kinase	5,95	56	5,59	42,58	2		2	
							K.GVTTHIGGDSVAAVEK.V	K.GVTTHIGGDSVAAVEK.V		
							K.AQGISVGSLSVEEDKLDLATTUAK.A	K.AQGISVGSLSVEEDKLDLATTUAK.A		
	P31657	Probable cinnamyl alcohol dehydrogenase	5,95	56	5,96	39,03	2=		1=	
							R.GGILGLGGVGHM*GVK.I			
							R.GGILGLGGVGHM*GVK.I	R.GGILGLGGVGHM*GVK.I		
	Q68BK5	Peptidyl-prolyl cis-trans isomerase*	5,95	56	6,64	44,66	2		2	
							R.LGEHNI DVLENEQFINAAK.I	R.LGEHNI DVLENEQFINAAK.I		
							K.VC#NYVNWIIQQTIAAN.-	K.VC#NYVNWIIQQTIAAN.-		
	P50746	Probable cinnamyl alcohol dehydrogenase	5,95	56	5,66	38,68	2		2	
							-.NTGPEDVYIK.-	-.NTGPEDVYIK.-		
							K.DPSGILSPYTYTLR.N	K.DPSGILSPYTYTLR.N		

Tab. 8 continued.

Spot ID	Accession number	Identified protein	Exp.		Theor.		Number of identified peptides		Number of unique peptides		
			pl	Mw	pl	Mw	Peptide sequence	Peptide sequence			
ID:0725	Q40281	RuBisCO activase	5,14	56	8,20	48,08	5	4			
							K.GLAFDESDDQQDITR.G K.SFQC#ELVFAK.M K.M*C#C#LFINDLDAGAGR.L K.MC#C#LFINDLDAGAGR.L -.MGINPIMMSAGELESGNAGEPAK.-	K.GLAFDESDDQQDITR.G K.SFQC#ELVFAK.M K.MC#C#LFINDLDAGAGR.L -.MGINPIMMSAGELESGNAGEPAK.-			
	P27774	Phosphoribulokinase	5,14	56	5,22	39,18	3	3			
							K.FYGEVTQQMLK.H R.LDELIYVESHLNISTK.F K.FFYGPDAYFGHEVSVLEMDGQFDR.L	K.FYGEVTQQMLK.H R.LDELIYVESHLNISTK.F K.FFYGPDAYFGHEVSVLEMDGQFDR.L			
ID:0801	Q01908	ATP synthase gamma chain 1	6,15	50	6,16	35,71	2	2			
							R.M*SAM*SNASDNASDLK.K R.M*SAM*SNASDNASDLK.K	R.M*SAM*SNASDNASDLK.K R.M*SAM*SNASDNASDLK.K			
	P49249	IN2-2 protein	6,15	50	8,88	33,83	2	2			
							R.VPIEVTIGELK.K R.VPIEVTIGELK.L	R.VPIEVTIGELK.K R.VPIEVTIGELK.L			
ID:0828	Q68BK5	Peptidyl-prolyl cis-trans isomerase ^a	6,21	49	6,64	44,66	1	1			
							R.LGEHNIDVLEGNEQFINAAK.I	R.LGEHNIDVLEGNEQFINAAK.I			
	Q9LIU0	Clavamate synthase-like protein At3g21360	6,21	49	5,70	37,21	1	1			
							R.VLGEDDDPSSPIGR.G	R.VLGEDDDPSSPIGR.G			
ID:0849	Q43317	Cysteine synthase	5,46	48	6,26	34,34	16=	8=			
							-.YLKDQNPDIK.- R.IGYSM*IAADAEK.G R.IGYSM*IAADAEK.G K.VHYETTGPPEIWK.G K.LIITM*PASM*SLER.R R.IGYSMIAADAEK.G R.IGYSMIAADAEK.G K.VDAFVSGIGTGGTITGAGK.Y K.LIITM*PASM*SLER.R K.VDAFVSGIGTGGTITGAGK.Y K.TPNAYLQQFENPANPK.V K.LIITMPASM*SLER.R K.GLITPAGESILIEPTSGNTGIGLAFM*AAAK.G K.GLITPAGESILIEPTSGNTGIGLAFM*AAAK.G K.DVTELI GNTPLVYLNR.V K.GLITPAGESILIEPTSGNTGIGLAFMAAAK.G	-.YLKDQNPDIK.- R.IGYSM*IAADAEK.G R.IGYSM*IAADAEK.G K.VHYETTGPPEIWK.G K.LIITM*PASM*SLER.R R.IGYSMIAADAEK.G R.IGYSMIAADAEK.G K.VDAFVSGIGTGGTITGAGK.Y K.TPNAYLQQFENPANPK.V K.LIITMPASM*SLER.R K.DVTELI GNTPLVYLNR.V K.GLITPAGESILIEPTSGNTGIGLAFMAAAK.G			
							R.LGEHNIDVLEGNEQFINAAK.I -.LGEHNIDVLEGNEQFINAAK.-	R.LGEHNIDVLEGNEQFINAAK.I -.LGEHNIDVLEGNEQFINAAK.-			
		Q68BK5	Peptidyl-prolyl cis-trans isomerase ^a	5,46	48	6,64	44,66	2	2		
								R.LGEHNIDVLEGNEQFINAAK.I -.LGEHNIDVLEGNEQFINAAK.-	R.LGEHNIDVLEGNEQFINAAK.I -.LGEHNIDVLEGNEQFINAAK.-		
		Q9ZUC1	Quinone oxidoreductase-like protein At1g23740	5,46	48	8,46	40,99	2	2		
								K.VVAAALNPVDSK.R K.TIGSLAEYTAVEEK.V	K.VVAAALNPVDSK.R K.TIGSLAEYTAVEEK.V		
		A4UHT7	Salutaridine reductase	5,78	48	4,82	34,05	1	1		
								R.IVNVSSGLGQLK.Y	R.IVNVSSGLGQLK.Y		
		Q9SN86	Malate dehydrogenase	5,78	48	5,69	34,08	1=	1=		
							K.VQDFTGASELSALK.G	K.VQDFTGASELSALK.G			

Tab. 8 continued.

Spot ID	Accession number	Identified protein	Exp.		Theor.		Number of identified peptides	Number of unique peptides
			pl	Mw	pl	Mw	Peptide sequence	Peptide sequence
ID:0861	Q9LNE3	Probable fructokinase-2	5,20	48	4,93	35,89	4 K.FANAC#GAIITTK.K K.IVDDQSILEDEQR.L -DAGVLLSYDPNLR.- -GAI PALPTESEALALK.-	4 K.FANAC#GAIITTK.K K.IVDDQSILEDEQR.L -DAGVLLSYDPNLR.- -GAI PALPTESEALALK.-
	Q9SID0	Probable fructokinase-1	5,20	48	5,31	35,28	4= K.APGGAPANVAIAVTR.L R.TALAFVTLR.A -DAGVLLSYDPNLR.- K.LGDDEFQHM*LAGILR.Q	4= K.APGGAPANVAIAVTR.L R.TALAFVTLR.A -DAGVLLSYDPNLR.- K.LGDDEFQHM*LAGILR.Q
	Q68BK5	Peptidyl-prolyl cis-trans isomerase ^o	5,20	48	6,64	44,66	2 R.LGEHNIDVLEGEQFINAQK.I K.IITHPNFNGNTLDNDIM*LIK.L	2 R.LGEHNIDVLEGEQFINAQK.I K.IITHPNFNGNTLDNDIM*LIK.L
ID:0954	Q68BK5	Peptidyl-prolyl cis-trans isomerase ^o	5,80	41	6,64	44,66	1 R.LGEHNIDVLEGEQFINAQK.I	1 R.LGEHNIDVLEGEQFINAQK.I
	Q40143	Cysteine proteinase 3	5,80	41	5,27	23,34	1= R.GTNEC#GIEDDVVAGLPSSK.N	1= R.GTNEC#GIEDDVVAGLPSSK.N
elD:0176	Q68BK5	Peptidyl-prolyl cis-trans isomerase ^o	6,44	30	6,64	44,66	2 R.LGEHNIDVLEGEQFINAQK.I R.LGEHNIDVLEGEQFINAQK.I	1 R.LGEHNIDVLEGEQFINAQK.I
	P34106	Alanine aminotransferase 2	6,44	30	5,82	52,68	1= R.DGYPSDPELI FLTDGASK.G	1= R.DGYPSDPELI FLTDGASK.G
	O22077	RuBisCO small chain	6,44	30	8,41	14,42	1= R.SPGYDGR.Y	1= R.SPGYDGR.Y
elD:0522	O23264	Putative selenium-binding protein	6,11	68	5,37	54,06	4 K.GSPIVAEGEDGK.T K.DTGFVGC#ALTSNM*VR.F K.TM*ISTSWGAPAAFTK.G K.QLDLGNTGLLPLEIR.F	4 K.GSPIVAEGEDGK.T K.DTGFVGC#ALTSNM*VR.F K.TM*ISTSWGAPAAFTK.G K.QLDLGNTGLLPLEIR.F
	O49434	Allantoate deiminase	6,11	68	5,09	46,49	3= K.LPAVATGSHIDAI PYSYGK.Y K.QIDELATFS DTPAPSVTR.I K.YDGVIGVLGAI EAINSLK.R	3= K.LPAVATGSHIDAI PYSYGK.Y K.QIDELATFS DTPAPSVTR.I K.YDGVIGVLGAI EAINSLK.R
	P29677	mitochondrial-processing peptidase subunit alpha	6,11	68	5,71	54,68	6= R.EVEAIGGNVEASSYK.E R.EVEAIGGNVEASSYK.E R.EVEAIGGNVEASSYK.E K.TYVPEM*VELLIDSVR.N K.SVPPLDFPLAGVTVPPLPDYVEPSK.T K.SVPPLDFPLAGVTVPPLPDYVEPSK.T	3= R.EVEAIGGNVEASSYK.E K.TYVPEM*VELLIDSVR.N K.SVPPLDFPLAGVTVPPLPDYVEPSK.T
	P48350	Catalase isozyme 1	6,11	68	6,96	57,07	2= R.LGPNYM*QLPVNAPK.C -FPIINNAIVTGR.-	2= R.LGPNYM*QLPVNAPK.C -FPIINNAIVTGR.-

Tab. 8 continued.

Spot ID	Accession number	Identified protein	Exp.		Theor.		Number of identified peptides		Number of unique peptides	
			pl	Mw	pl	Mw	Peptide sequence	Peptide sequence		
ID:0675	P29344	30S ribosomal protein S1	5,24	60	4,99	40,43	12=	5=		
							-FVEVDEEQSR.-			-FVEVDEEQSR.-
							-FVEVDEEQSR.-			
							-FVEVDEEQSR.-			
							-FVEVDEEQSR.-			
							-KLFEDAYER.-			-KLFEDAYER.-
							K.SSAYLPVQEASIH.R			K.SSAYLPVQEASIH.R
							K.YDFNAEIGTK.V			K.YDFNAEIGTK.V
							K.YDFNAEIGTK.V			
							K.IDANGALVDITAK.S			K.IDANGALVDITAK.S
							K.IDANGALVDITAK.S			
							K.IDANGALVDITAK.S			
							K.IDANGALVDITAK.S			K.IDANGALVDITAK.S
							K.IDANGALVDITAK.S			
	P15102	Glutamine synthetase leaf isozyme	5,24	60	5,50	41,58	4	4		
							R.GGNNILVIC#DAYTPQGEPIPTNK.R			R.GGNNILVIC#DAYTPQGEPIPTNK.R
							K.WNYDGSSTGQAPGEDSEVILYPQAIK.D			K.WNYDGSSTGQAPGEDSEVILYPQAIK.D
							R.LESLNLDITPFTEK.I			R.LESLNLDITPFTEK.I
							K.VVDEVPWYGIQEYLLQTDVK.W			K.VVDEVPWYGIQEYLLQTDVK.W
	Q40281	RuBisCO activase	5,24	60	8,20	48,08	5	3		
							K.GLAFDTSDDQQDITR.G			K.GLAFDTSDDQQDITR.G
							K.GLAFDTSDDQQDITR.G			
							K.GLAFDTSDDQQDITR.G			
							K.SFQC#ELVFAK.M			K.SFQC#ELVFAK.M
							K.IPLILGVWGGK.G			K.IPLILGVWGGK.G
ID:0711	Q43467	Elongation factor Tu	5,40	58	5,29	44,54	5	3		
							K.M*VVELIM*PVAC#EQGMR.F			K.M*VVELIM*PVAC#EQGMR.F
							K.MVVELIM*PVAC#EQGM*R.F			
							K.FEAIYVVLK.K			K.FEAIYVVLK.K
							K.ILDDAM*AGDNVGLLLR.G			
							K.ILDDAMAGDNVGLLLR.G			K.ILDDAMAGDNVGLLLR.G
	P15102	Glutamine synthetase leaf isozyme	5,40	58	5,50	41,58	5	5		
							R.GGNNILVIC#DAYTPQGEPIPTNK.R			R.GGNNILVIC#DAYTPQGEPIPTNK.R
							K.WNYDGSSTGQAPGEDSEVILYPQAIK.D			K.WNYDGSSTGQAPGEDSEVILYPQAIK.D
							R.LESLNLDITPFTEK.I			R.LESLNLDITPFTEK.I
							K.IIAEYIWIGGTGIDL.R.S			K.IIAEYIWIGGTGIDL.R.S
							K.VVDEVPWYGIQEYLLQTDVK.W			K.VVDEVPWYGIQEYLLQTDVK.W
	Q10DV7	Actin-1	5,40	58	5,30	41,81	5	4		
							K.DAYVGDEAQS.K.R			K.DAYVGDEAQS.K.R
							K.DAYVGDEAQS.K.R			
							K.AGFAGDDAPR.A			K.AGFAGDDAPR.A
							R.GYSFTTAE.R.E			R.GYSFTTAE.R.E
							R.VAPEEHPVLLTEAPLNPK.A			R.VAPEEHPVLLTEAPLNPK.A
	Q39639	Glycerol-3-phosphate acyltransferase	5,40	58	5,01	41,25	3	3		
							K.NAVFQSGNPR.A			K.NAVFQSGNPR.A
							R.ADEIVLSNM*AM*AFDR.M			R.ADEIVLSNM*AM*AFDR.M
							R.TFLNATTEELLGIR.K			R.TFLNATTEELLGIR.K
	Q42711	Monodehydroascorbate reductase	5,40	58	5,29	47,42	4	3		
							K.GTVATGFTADSNGEVK.E			K.GTVATGFTADSNGEVK.E
							K.GTVATGFTADSNGEVK.E			
							K.TSVPGVYAVGDVATFPLK.L			K.TSVPGVYAVGDVATFPLK.L
							K.TVEEYDYLPHYFSR.S			K.TVEEYDYLPHYFSR.S
	Q40281	RuBisCO activase	5,40	58	8,20	48,08	5	2		
							K.GLAFDTSDDQQDITR.G			K.GLAFDTSDDQQDITR.G
							K.M*GISPIM*M*SAGELESGNAGEPAK.L			
							K.GLAFDTSDDQQDITR.G			
							K.GLAFDTSDDQQDITR.G			
							K.MGISPIM*M*SAGELESGNAGEPAK.L			K.MGISPIM*M*SAGELESGNAGEPAK.L
	Q42522	Glutamate-1-semialdehyde 2,1-aminomutase 2	5,40	58	5,70	46,45	2	2		
							R.M*VNSGTEAC#M*GVLR.L			R.M*VNSGTEAC#M*GVLR.L
							K.AGSGVATLGLPDSGPVK.G			K.AGSGVATLGLPDSGPVK.G

Tab. 8 continued.

Spot ID	Accession number	Identified protein	Exp.		Theor.		Number of identified peptides		Number of unique peptides			
			pl	Mw	pl	Mw	Peptide sequence		Peptide sequence			
ID:1208	Q6L8G4	Keratin-associated protein 5-11	5,82	29	8,16	14,61	2		1			
							R.VSTSTVSNEGGGDFIR.F R.VSTSTVSNEGGGDFIR.F		R.VSTSTVSNEGGGDFIR.F			
	Q8P5Z8	UPF0189 protein XCC3184	5,82	29	6,23	19,81	1		1			
							R.M*LGGGGADGAIHR.A		R.M*LGGGGADGAIHR.A			
ID:1208	Q87JZ5	UPF0189 protein VPA0103	5,82	29	5,02	18,19	1		1			
							K.TDAIVNPANER.M		K.TDAIVNPANER.M			
	P09886	Small heat shock protein	5,82	29	5,15	21,29	1		1			
						-DNLHLNR.-		-DNLHLNR.-				
elD:0175	P46423	Glutathione S-transferase	6,43	30	5,88	23,68	1		1			
							K.YIAC#EYADK.G		K.YIAC#EYADK.G			
elD:0175	O82531	Proteasome subunit beta type-1	6,43	30	6,30	24,62	1		1			
							R.M*SSGYNILTR.E		R.M*SSGYNILTR.E			
elD:0685	Q40281	RuBisCO activase	5,55	56	8,20	48,08	3		3			
							K.GLAFDTSDDQQDITR.G K.SFQC#ELVFAK.M K.IPLILGVWGGK.G		K.GLAFDTSDDQQDITR.G K.SFQC#ELVFAK.M K.IPLILGVWGGK.G			
	Q68BK5	Peptidyl-prolyl cis-trans isomerase ^o	5,55	56	6,64	44,66	1		1			
							R.LGEHNIDVLEGNEQFIINAAK.I		R.LGEHNIDVLEGNEQFIINAAK.I			
elD:0861	Q40281	RuBisCO activase	5,33	60	8,20	48,08	16		7			
							K.GLAFDTSDDQQDITR.G K.GLAFDTSDDQQDITR.G K.GLAFDTSDDQQDITR.G		K.GLAFDTSDDQQDITR.G			
							K.M*GISPIM*M*SAGELESGNAGEPAK.L					
							K.GLAFDTSDDQQDITR.G					
							-MGISPIM*M*SAGELESGNAGEPAK.-		-MGISPIM*M*SAGELESGNAGEPAK.-			
							K.GLAFDTSDDQQDITR.G					
							K.SFQC#ELVFAK.M		K.SFQC#ELVFAK.M			
							K.SFQC#ELVFAK.M					
							K.M*GISPIM*M*SAGELESGNAGEPAK.L		K.M*GISPIM*M*SAGELESGNAGEPAK.L			
							K.SFQC#ELVFAK.M					
							K.NFMSLPNIK.I		K.NFMSLPNIK.I			
							-NFMSLPNIK.-		-NFMSLPNIK.-			
							K.IPLILGVWGGK.G					
							K.IPLILGVWGGK.G		K.IPLILGVWGGK.G			
elD:0861	P15102	Glutamine synthetase leaf isozyme	5,33	60	5,50	41,58	5		5			
							R.AAEVFSNK.K R.GGNNILVIC#DAYTPQGEPIPTNK.R K.WNYDGSSTGQAPGEDSEVILYPQAIK.F.D R.LESLNLDITPFTEK.I K.VVDEVPWYGIQEYTLQTDVK.W		R.AAEVFSNK.K R.GGNNILVIC#DAYTPQGEPIPTNK.R K.WNYDGSSTGQAPGEDSEVILYPQAIK.F.D R.LESLNLDITPFTEK.I K.VVDEVPWYGIQEYTLQTDVK.W			
ID:0615	O80433	Citrate synthase	6,55	62	6,95	52,66	5		4			
							R.VPVVAAVYR.R K.VQLGNISVDMVLGGMR.G K.VQLGNISVDMVLGGM*R.G R.YWEPTYEDSLNIAR.V K.PGGEPLPEGLLWLLLTGK.V		R.VPVVAAVYR.R K.VQLGNISVDMVLGGM*R.G R.YWEPTYEDSLNIAR.V K.PGGEPLPEGLLWLLLTGK.V			
	P49298	Citrate synthase	6,55	62	6,26	50,30	3		3			
									R.SIGIGSQUIWDR.A K.SVTMDWLESYC#K.K -ALGLPLERPK.-		R.SIGIGSQUIWDR.A K.SVTMDWLESYC#K.K -ALGLPLERPK.-	
	Q68BK5	Peptidyl-prolyl cis-trans isomerase ^o	6,55	62	6,64	44,66	1		1			
						R.LGEHNIDVLEGNEQFIINAAK.I		R.LGEHNIDVLEGNEQFIINAAK.I				

Tab. 8 continued.

Spot ID	Accession number	Identified protein	Exp.		Theor.		Number of identified peptides		Number of unique peptides	
			pI	Mw	pI	Mw	Peptide sequence	Peptide sequence		
ID:0871	Q9ZUC1	Quinone oxidoreductase-like protein At1g23740	5,62	48	8,46	40,99	1		1	
	Q43317	Cysteine synthase	5,62	48	6,26	34,34	1	K.VVAAALNPVDSK.R	1	K.VVAAALNPVDSK.R
elD:0291	Q01402	ribulokinase	6,17	19	6,88	18,57	4	R.IGYSM*IADAEAK.G	4	R.IGYSM*IADAEAK.G
	Q22077	RuBisCO small chain	6,17	19	8,41	14,42	2=	R.KLIGSTDPLQADPGTIR.G R.GLVGEIISR.F K.LIGSTDPLQADPGTIR.G K.EGEVC#QWTPAQAPWLR.E K.LPM*FGC#TDATQVLAELQEASK.T K.LPMFGC#TDATQVLAELQEASK.T	1=	R.KLIGSTDPLQADPGTIR.G R.GLVGEIISR.F K.LIGSTDPLQADPGTIR.G K.EGEVC#QWTPAQAPWLR.E K.LPM*FGC#TDATQVLAELQEASK.T
elD:0299	Q40281	RuBisCO activase	5,21	56	8,20	48,08	6	K.GLAFDESDDQQDITR.G K.SFQC#ELVFAK.M K.M*CH#LFINDLDAGAGR.L K.M*GINPIMMSAGELESGNAGEPAK.L K.MC#CH#LFINDLDAGAGR.L K.MGINPIMMSAGELESGNAGEPAK.L	4	K.GLAFDESDDQQDITR.G K.SFQC#ELVFAK.M K.M*GINPIMMSAGELESGNAGEPAK.L K.MC#CH#LFINDLDAGAGR.L
	P27774	Phosphoribulokinase	5,21	56	5,22	39,18	5	K.FYGEVTQQMLK.H K.IRDLFEQLIASK.A R.LDELIVESHLSNISTK.F K.HSDFPGSNNGTGLFQTIIVGLK.I R.DLFEQLIASK.A	5	K.FYGEVTQQMLK.H K.IRDLFEQLIASK.A R.LDELIVESHLSNISTK.F K.HSDFPGSNNGTGLFQTIIVGLK.I R.DLFEQLIASK.A
ID:0486		No data output from MS	5,44	74				No MS data acquired		
ID:0885		No data output from MS	6,04	46				No MS data acquired		

Tab. 9 - Mass spectrometric information of proteins identified upon elevated CO₂ treatment.

Spot ID	TP	Accession number	Identified protein	Experimental		Theoretical		MS/MS data				
				pI	Mw	pI	Mw	Protein Score	Peptide Score	NP	Protein coverage %	Peptide sequence
eID:0180	t ₅	B9T876	Minor allergen Alt a, putative*	6,61	25,00	6,10	21,75	162	84,13	1	20.0	GGSPYGAGTFAGDGSR
		Q05994	RuBisCO large chain	6,61	25,00	5,99	49,15	129	66,49	1	2.2	VALEACVQAR
		B9T876	Minor allergen Alt a, putative*	6,61	25,00	6,10	21,75	113	85,47	1	13.4	GAASVEGVEAK
		P46423	Glutathione S-transferase	6,61	25,00	5,88	23,68	58	58,36	1	1.7	VLDVYENR
eID:0181	t ₅	B9N5B8	Predicted protein*	6,61	25,00	5,55	10,03	52	51,98	1	1.9	VVTVSIPR
		B9T876	Minor allergen Alt a, putative*	6,61	24,00	6,10	21,75	1758	137,81	1	38.8	GGSPYGAGTFAGDGSR
		B9T876	Minor allergen Alt a, putative*	6,61	24,00	6,10	21,75	634	91,75	1	14.6	GAASVEGVEAK
		Q05994	RuBisCO large chain	6,61	24,00	5,99	49,15	106	69,59	1	2.2	VALEACVQAR
eID:0189	t ₅	P27522	Chlorophyll a-b binding protein 8	6,61	24,00	8,67	26,13	97	77,70	1	3.6	YAMLGAVGAI APEILGK
		Q40281	RuBisCO	5,12	48,00	8,20	48,08	3560	137,24	0	21.5	MCCLFINDLDAGAGR
ID:0436	t ₅	Q07209	RuBisCO	6,64	58,00	6,09	51,65	79	61,81	1	2.5	VALEACVQAR
ID:0678	t ₅	Q43317	Cysteine synthase	5,33	42,00	6,26	34,34	803	123,85	1	19.0	EGLLVGISSGAAAAAIK
		B9N5B8	Predicted protein*	5,33	42,00	5,55	10,03	56	56,00	1	1.9	VVTVSIPR
		P09975	Protein ycf2	5,33	42,00	9,88	259,91	55	54,56	1	2.6	MAALTEQRYLQK
ID:0699	t ₅	Q39366	Putative lactoylglutathione lyase	5,16	39,00	5,19	31,65	138	73,82	1	6.4	GPTPEPLCQVMLR
		P09975	Protein ycf2	5,16	39,00	9,88	259,91	68	53,19	1	2.6	MAALTEQRYLQK
ID:1010	t ₅	B9N5B8	Predicted protein*	4,81	23,00	5,55	10,03	55	55,40	1	1.9	VVTVSIPR
		P09975	Protein ycf2	4,81	23,00	9,88	259,91	55	55,38	1	2.6	MAALTEQRYLQK
		Q40089	ATP synthase subunit delta'	4,81	23,00	4,85	18,76	52	52,15	1	2.2	LSSASTDLEK
eID:0403	t ₈	P09975	Protein ycf2	6,76	40,00	9,88	259,91	52	52,42	1	2.6	MAALTEQRYLQK
		D8R9K8	Putative uncharacterized protein*	6,76	40,00	9,10	44,36	51	50,78	1	1.9	VVTVSIPR

TP, sampling time point
pI, isoelectric point
Mw, molecular weight
NP, number of unique peptides

Tab. 10 - *C. geophilum* facing drought stress. List of proteins identified by MS (raw data). Protein ID colored in blue represent significant different proteins after statistical analysis. MW, molecular weight.

Sum of all MW [kDa]		Spectral counts for each protein																	
Protein ID	MW [kDa]	Control samples									Drought stressed samples								
		CT1 R1	CT1 R2	CT1 R3	CT2 R1	CT2 R2	CT2 R3	CT3 R1	CT3 R2	CT3 R3	ST1 R1	ST1 R2	ST1 R3	ST2 R1	ST2 R2	ST2 R3	ST3 R1	ST3 R2	ST3 R3
Cg-lib123_irc144	106	181	157	216	197	244	322	193	310	177	156	267	197	378	245	335	343	283	224
Cg-lib123_irc164	294	208	160	234	330	400	451	176	159	158	159	205	194	405	429	482	154	152	142
Cg-lib6_c375	229	91	106	92	133	105	152	138	129	119	100	127	88	187	204	108	158	131	124
Cg-lib123_c373	198	132	151	128	151	126	128	78	57	78	123	125	164	128	130	137	101	98	117
Cg-lib123_irc259	163	118	146	121	189	101	80	130	122	114	132	120	96	67	181	29	173	164	172
Cg-lib123_irc138	212	129	116	123	113	165	144	93	101	86	115	118	76	132	123	120	94	94	91
Cg-lib123_irc88	115	153	119	130	80	126	132	111	97	84	103	153	104	100	144	69	93	90	122
Cg-lib6_c1225	91	99	108	99	102	110	132	84	78	71	89	113	87	134	133	74	91	77	72
Cg-lib123_irc61	209	106	134	110	144	129	151	34	28	25	157	84	155	92	216	15	69	67	75
Cg-lib123_irc188	173	84	77	90	100	77	105	82	103	81	72	92	43	114	113	10	109	98	96
Cg-lib6_irc45	122	58	72	60	78	90	77	99	73	58	39	39	29	65	108	57	153	142	99
Cg-lib123_irc51	141	37	15	12	108	110	182	86	69	64	37	14	35	116	110	44	114	97	101
Cg-lib123_irc181	146	62	45	58	138	148	144	63	55	50	77	58	36	65	65	38	76	93	71
Cg-lib123_c316	222	40	37	40	120	59	100	64	57	33	45	44	43	101	107	121	134	120	98
Cg-lib123_c348	63	47	108	83	65	72	131	1	16	22	85	15	30	112	68	38	116	84	124
Cg-lib123_irc201	136	49	42	44	56	47	52	78	73	63	53	72	40	49	52	2	126	140	95
Cg-lib123_c1104	189	65	72	66	70	99	75	47	44	44	67	71	67	86	107	24	60	62	61
Cg-lib123_c666	154	31	50	56	67	48	56	51	60	51	49	64	31	80	76	15	51	78	55
Cg-lib123_irc215	258	30	16	14	69	25	53	35	55	39	37	38	25	50	56	45	34	52	40
Cg-lib123_irc287	174	40	51	39	102	55	30	31	42	36	34	37	30	31	69	2	64	56	47
Cg-lib6_c412	269	62	40	112	62	81	63	21	15	25	50	63	70	76	57	52	12	8	8
Cg-lib123_c762	236	36	41	39	54	53	59	34	39	29	35	47	28	64	49	41	52	42	35
Cg-lib6_irc147	198	37	33	41	34	28	50	24	26	21	43	30	46	46	71	68	30	31	36
Cg-lib123_irc218	142	39	27	19	54	54	45	33	34	32	32	30	44	47	79	8	29	46	31
Cg-lib123_c399	182	21	12	16	63	50	28	48	57	39	11	24	25	36	23	27	61	53	39
Cg-lib6_irc48	89	44	39	37	71	68	79	10	9	0	58	46	6	67	32	5	58	44	26
Cg-lib123_c3844	52	22	35	32	48	46	50	44	44	33	32	36	16	18	71	6	46	59	39
Cg-lib6_c213	110	24	24	29	49	68	45	50	48	25	29	15	24	25	63	23	82	55	33
Cg-lib6_c529	192	9	16	19	59	42	46	56	60	43	10	12	6	61	52	73	38	26	10
Cg-lib123_c390	160	14	16	22	57	34	46	30	33	33	14	17	33	17	42	55	51	40	29
Cg-lib123_c306	246	17	11	7	43	2	55	25	26	16	16	21	27	36	49	58	16	45	38
Cg-lib123_c680	148	15	8	14	69	48	52	31	31	27	25	13	24	34	12	45	62	44	
Cg-lib6_c5089	34	31	25	28	46	56	63	39	29	31	24	24	29	56	61	31	31	31	19
Cg-lib6_c288	306	17	28	22	52	10	34	18	17	16	14	26	12	56	32	28	31	38	26
Cg-lib123_c352	159	35	10	11	62	65	46	4	9	10	11	9	25	38	61	1	13	21	4
Cg-lib6_c2084	130	18	18	13	34	27	24	47	47	30	26	17	13	26	34	1	52	50	37
Cg-lib123_irc10	82	29	26	46	30	37	48	3	0	0	30	30	0	61	45	6	47	53	24
Cg-lib123_irc22	57	17	36	25	63	19	18	2	2	2	39	39	18	37	89	11	11	5	9
Cg-lib123_c4719	61	33	29	18	35	10	34	26	20	15	43	22	22	43	32	30	20	20	12
Cg-lib123_c319	147	19	26	28	40	34	34	17	10	9	25	26	19	39	47	28	18	27	19
Cg-lib123_irc282	112	45	16	34	51	46	37	22	10	11	20	19	7	50	34	0	12	7	5
Cg-lib6_c202	99	15	20	20	32	30	36	6	5	5	16	13	13	26	21	26	1	1	4
Cg-lib123_irc65	99	16	14	26	33	27	33	19	21	23	19	21	11	25	32	27	39	31	29
Cg-lib123_c781	100	19	16	14	35	29	16	30	17	21	11	14	20	37	33	10	36	29	28
Cg-lib6_c307	157	10	1	5	45	27	17	20	23	30	3	6	11	30	17	3	42	42	25
Cg-lib123_c664	209	3	5	4	20	18	21	13	8	16	4	7	5	18	22	21	24	17	24
Cg-lib123_c2288	88	21	10	11	35	46	35	20	23	20	10	15	21	54	53	12	25	29	23
Cg-lib123_c677	142	13	16	19	31	26	38	27	25	31	18	19	8	23	29	17	30	24	24
Cg-lib123_irc98	78	28	25	19	37	22	15	0	25	35	23	23	18	31	35	9	28	32	27
Cg-lib123_irc1293	71	10	13	6	44	16	12	0	0	0	30	14	8	8	36	13	75	121	90
Cg-lib123_c443	214	15	21	14	34	5	33	6	4	7	17	24	12	39	27	29	22	19	18
Cg-lib123_c519	95	10	14	11	27	26	21	5	5	6	8	11	26	26	24	71	20	16	6
Cg-lib6_c2492	113	19	16	15	73	35	44	1	0	0	18	12	15	46	50	26	2	3	5
Cg-lib123_c2191	81	29	21	52	63	27	36	0	0	0	23	31	28	29	20	27	4	2	6
Cg-lib123_c381	170	23	13	10	32	38	9	17	15	20	12	11	23	13	12	4	25	24	20
Cg-lib123_c714	174	15	22	16	39	15	28	7	3	4	16	17	14	33	25	37	20	8	4

Tab. 10 – continued.

Sum of all MW [kDa]		Spectral counts for each protein																	
Protein ID	MW [kDa]	Control samples									Drought stressed samples								
		CT1 R1	CT1 R2	CT1 R3	CT2 R1	CT2 R2	CT2 R3	CT3 R1	CT3 R2	CT3 R3	ST1 R1	ST1 R2	ST1 R3	ST2 R1	ST2 R2	ST2 R3	ST3 R1	ST3 R2	ST3 R3
Cg-lib123_irc40	82	28	19	29	22	17	15	11	13	13	14	32	28	20	20	0	17	15	15
Cg-lib123_irc83	112	9	1	6	55	30	40	2	8	5	17	8	16	46	31	0	6	1	0
Cg-lib123_irc69	94	2	52	7	20	29	16	1	2	1	15	1	3	15	5	20	3	6	0
Cg-lib123_c578	231	12	12	15	33	7	33	4	1	4	13	19	12	32	31	17	11	14	10
Cg-lib123_c388	175	8	7	5	19	25	12	15	11	16	10	12	8	16	19	7	28	25	21
Cg-lib123_c1248	160	21	23	14	14	21	23	15	8	8	17	17	16	19	23	9	13	15	19
Cg-lib123_c512	109	8	10	7	35	38	16	7	5	5	9	4	10	21	23	37	7	7	4
Cg-lib123_irc132	94	24	8	17	7	10	45	11	1	3	18	6	2	19	15	10	5	7	7
Cg-lib123_c11790	66	9	4	3	33	21	26	15	15	10	6	7	13	27	16	0	13	15	14
Cg-lib123_irc275	54	1	7	6	22	10	12	0	1	3	10	1	0	19	17	9	42	32	31
Cg-lib6_irc26	154	2	2	2	10	10	5	7	10	11	3	4	2	11	19	0	39	43	25
Cg-lib6_c548	131	7	10	5	19	37	20	6	8	5	9	2	5	19	13	12	16	3	0
Cg-lib123_c1044	144	12	9	6	21	15	28	4	3	7	18	14	14	18	36	7	16	9	11
Cg-lib123_irc202	60	6	12	12	21	13	40	0	6	4	7	11	3	17	26	13	6	16	10
Cg-lib6_c1005	50	6	16	9	19	19	26	5	4	1	9	11	1	21	27	42	5	5	4
Cg-lib123_irc16	82	6	4	6	9	14	15	2	1	0	30	5	2	10	12	0	6	5	8
Cg-lib123_c493	102	8	13	8	17	25	18	8	1	2	4	14	10	6	35	12	19	4	4
Cg-lib123_irc143	59	14	17	24	15	13	17	0	1	0	17	17	7	14	8	13	6	5	3
Cg-lib123_irc375	92	8	2	2	27	23	13	10	9	5	6	11	19	33	18	0	7	14	4
Cg-lib123_c895	114	4	9	12	12	12	12	7	9	6	11	9	15	7	14	6	11	8	7
Cg-lib123_c692	176	10	4	6	16	14	7	3	4	3	3	4	9	16	10	0	11	14	10
Cg-lib123_c311	161	4	4	1	21	19	19	7	2	7	4	5	4	24	23	0	25	20	8
Cg-lib123_c470	241	10	9	9	9	4	15	7	11	6	9	11	9	18	16	17	12	14	11
Cg-lib6_irc17	91	9	6	0	28	11	14	4	6	5	5	7	1	16	20	1	3	7	5
Cg-lib123_irc243	87	5	7	8	17	17	16	0	5	15	10	6	8	21	8	8	1	2	3
Cg-lib123_c759	151	1	2	5	18	11	19	14	16	14	3	0	3	16	3	0	26	24	23
Cg-lib123_c553	136	3	0	3	11	11	9	15	13	14	4	10	3	13	23	1	19	22	6
Cg-lib6_irc118	115	8	7	11	15	10	20	6	4	14	9	1	4	8	28	4	5	18	16
Cg-lib123_c417	131	1	4	5	16	14	13	6	10	6	2	5	2	13	34	0	15	17	7
F05GI4S01D042P	42	1	2	1	19	2	9	8	9	3	1	2	0	8	8	13	24	17	18
Cg-lib123_c2265	71	16	13	36	19	10	0	0	0	0	20	22	21	15	7	16	1	1	0
Cg-lib6_irc270	78	14	12	7	21	21	16	8	7	5	13	4	9	15	14	39	7	8	6
Cg-lib6_c654	42	5	5	2	10	17	7	0	0	2	5	0	1	0	23	0	16	17	19
Cg-lib123_irc206	60	3	15	3	27	18	12	0	2	6	10	2	0	21	4	6	10	4	5
Cg-lib6_c2495	60	1	2	1	7	8	13	5	3	2	7	5	2	8	10	0	4	2	1
Cg-lib123_irc120	88	7	4	5	13	16	15	2	7	8	4	11	4	15	38	0	10	2	0
Cg-lib123_irc195	129	6	1	6	12	16	9	2	3	6	5	0	1	6	6	2	10	9	11
Cg-lib123_c395	90	8	11	10	15	13	13	6	3	2	10	11	8	21	20	24	7	7	6
Cg-lib123_c441	143	1	3	6	31	3	5	9	10	7	0	1	7	7	2	0	19	11	8
Cg-lib123_c473	115	5	10	4	14	21	23	0	8	1	10	5	7	22	16	0	13	5	1
Cg-lib123_c864	116	2	4	0	11	8	10	5	10	4	3	3	2	6	14	0	19	8	3
F05GI4S01C0JAH	38	0	0	0	0	0	0	0	0	0	7	6	17	17	89	11	10	8	
Cg-lib123_irc140	58	4	28	0	28	18	11	0	2	0	14	3	0	12	30	3	3	2	4
Cg-lib6_c468	167	7	5	7	14	16	14	4	4	4	6	6	8	17	16	6	8	6	7
Cg-lib123_c591	137	2	8	9	9	12	18	6	11	3	9	5	2	16	15	3	13	7	1
Cg-lib123_c434	166	4	2	8	16	3	9	3	3	6	2	4	3	8	5	0	12	13	14
Cg-lib123_irc11446	31	8	11	5	5	16	10	0	5	8	10	5	4	25	8	15	8	8	7
Cg-lib123_c1606	107	0	8	4	20	20	25	2	0	2	3	5	2	8	11	11	2	2	1
Cg-lib123_c1121	99	4	3	6	14	18	20	7	5	2	4	2	7	13	15	0	11	5	3
Cg-lib123_c588	70	3	1	0	10	7	13	8	13	6	2	3	0	20	6	13	15	19	11
Cg-lib123_irc203	52	2	10	8	10	33	12	0	0	1	8	1	1	11	23	14	6	7	2
Cg-lib123_c2084	127	1	10	2	33	14	31	1	1	0	5	4	0	18	21	6	2	1	0
F05GI4S01B9MDI	35	2	6	28	6	16	20	0	0	0	8	7	2	23	20	20	0	0	0
Cg-lib123_c7765	101	2	13	4	23	11	16	1	4	1	5	10	1	19	9	5	2	0	0
Cg-lib123_c672	109	6	6	4	15	17	4	6	5	4	11	7	5	11	8	0	5	6	9
F05GI4S01BD0JX	39	7	7	6	10	12	9	8	1	0	9	11	7	26	14	2	11	10	7
Cg-lib123_c1723	184	4	13	8	10	1	12	2	0	5	2	11	6	13	13	9	7	8	9

Tab. 10 – continued.

Sum of all MW [kDa]		Spectral counts for each protein																	
913061		Control samples									Drought stressed samples								
Protein ID	MW [kDa]	CT1	CT1	CT1	CT2	CT2	CT2	CT3	CT3	CT3	ST1	ST1	ST1	ST2	ST2	ST2	ST3	ST3	ST3
		R1	R2	R3	R1	R2	R3	R1	R2	R3	R1	R2	R3	R1	R2	R3	R1	R2	R3
Cg-lib123_c1366	183	7	7	6	5	9	6	7	5	6	7	6	7	8	13	1	9	9	6
Cg-lib123_irc299	67	4	11	3	9	10	2	1	1	0	4	1	0	8	19	4	7	0	1
Cg-lib123_c1566	149	7	1	2	18	10	3	5	5	10	0	3	4	11	2	0	12	6	8
Cg-lib123_c4489	56	3	2	4	22	4	6	1	3	2	2	1	0	15	9	20	8	6	5
Cg-lib123_c1508	118	0	4	9	10	7	11	5	9	5	1	1	1	9	12	2	6	8	5
Cg-lib123_irc231	119	8	7	3	16	16	8	5	5	6	3	6	5	9	9	0	4	7	7
Cg-lib6_c3204	109	2	0	0	14	12	12	6	6	3	2	3	4	9	7	1	8	4	12
Cg-lib123_c705	123	5	4	5	14	10	5	2	3	2	2	9	4	7	22	5	8	6	0
Cg-lib6_c596	94	3	8	12	11	12	8	6	6	2	8	7	7	2	12	0	7	4	3
Cg-lib6_irc215	58	1	12	6	17	9	9	0	7	10	8	2	3	15	1	16	1	0	1
Cg-lib123_c4697	152	1	3	2	10	4	16	1	0	1	6	4	5	15	16	15	3	4	5
Cg-lib123_irc170	155	6	5	7	10	2	7	0	0	3	10	8	8	9	8	11	12	8	6
Cg-lib123_c4133	48	7	5	8	13	14	8	4	5	5	7	6	7	15	14	7	6	8	0
Cg-lib123_irc14	74	0	2	1	12	22	3	0	2	3	0	0	0	2	14	8	0	14	1
Cg-lib123_c920	138	2	1	0	8	3	7	6	6	5	2	2	1	6	13	0	7	11	4
Cg-lib6_c451	128	6	5	2	3	3	4	11	8	4	5	3	1	2	7	5	14	9	3
Cg-lib123_c487	93	5	4	4	17	31	5	0	0	0	5	5	2	22	20	0	4	3	3
Cg-lib123_c3778	53	0	0	0	4	4	1	0	0	0	4	0	0	25	17	45	3	1	0
Cg-lib123_c615	207	5	4	5	8	3	6	1	0	2	4	5	4	9	8	12	4	5	8
Cg-lib123_c870	138	7	8	1	21	6	6	3	5	0	5	6	2	5	9	5	9	4	10
Cg-lib123_c1804	128	4	1	1	5	6	5	8	2	12	1	0	7	6	1	0	13	1	11
Cg-lib123_irc36	90	3	3	5	3	12	13	4	1	1	4	1	0	9	15	5	6	4	1
Cg-lib6_c2592	56	1	0	0	5	3	4	0	0	0	0	0	0	17	16	9	2	0	0
Cg-lib123_irc356	90	0	0	0	2	0	0	0	0	0	1	3	1	16	31	27	3	4	1
Cg-lib6_c355	106	1	3	2	7	6	2	3	2	1	3	2	4	7	12	1	12	8	2
Cg-lib123_c6618	130	3	7	4	11	6	9	0	2	0	2	5	4	12	5	4	5	3	4
Cg-lib6_c648	81	8	6	8	9	5	9	5	4	5	9	8	14	3	8	0	5	6	6
Cg-lib123_irc94	186	8	2	10	12	14	24	0	0	0	6	0	6	14	18	5	0	1	1
Cg-lib123_c673	86	7	9	5	6	10	5	6	4	3	7	5	6	7	7	19	6	4	4
Cg-lib123_c1197	103	2	8	5	14	9	18	0	0	0	4	3	1	7	11	8	1	1	1
Cg-lib123_c4234	65	2	3	3	6	1	7	5	4	7	3	2	3	6	1	3	5	9	3
Cg-lib123_c592	133	1	1	0	9	7	5	9	9	3	0	0	2	2	1	8	19	11	4
Cg-lib123_c926	132	5	12	5	16	5	8	1	3	3	3	4	3	12	6	8	3	2	4
Cg-lib123_c1226	187	8	8	8	10	7	9	1	0	0	6	3	1	4	6	5	2	1	3
Cg-lib6_c433	174	3	2	1	9	6	9	3	2	3	1	2	2	8	12	4	6	6	3
Cg-lib123_c742	120	3	2	0	2	1	2	1	4	0	1	4	1	3	6	3	13	3	0
Cg-lib123_irc103	104	2	0	2	7	13	17	3	7	4	6	0	4	9	12	0	6	6	3
Cg-lib123_c6619	71	10	1	3	8	0	13	0	2	3	6	7	7	10	14	10	1	5	6
Cg-lib6_c434	95	3	6	5	12	10	6	2	0	0	4	4	4	5	16	0	5	1	0
Cg-lib123_c1281	93	3	0	0	16	9	4	0	0	1	0	0	8	9	5	0	6	1	2
Cg-lib6_irc123	307	2	5	6	12	3	12	0	0	1	3	3	1	11	9	11	5	6	5
Cg-lib6_c3167	39	1	2	2	7	3	3	6	9	6	0	6	3	6	5	2	8	10	6
Cg-lib6_irc59	210	1	0	0	13	8	0	0	0	0	0	1	10	10	11	0	21	10	8
Cg-lib123_c816	143	3	2	2	5	4	5	6	6	5	3	4	4	3	6	2	10	11	4
Cg-lib123_c972	184	3	0	1	8	4	5	8	6	6	2	2	2	4	9	0	11	9	6
Cg-lib6_c214	136	2	0	0	4	4	2	7	5	7	1	0	2	0	1	0	12	11	12
Cg-lib123_irc155	125	0	1	1	4	6	5	3	1	0	2	0	1	10	11	0	5	6	0
Cg-lib123_c3507	89	1	0	0	11	5	4	0	0	0	3	4	1	9	11	7	5	3	6
Cg-lib6_c882	200	4	0	3	2	6	6	1	3	6	4	2	4	2	4	0	7	6	5
Cg-lib123_c1235	106	1	0	0	6	1	7	3	3	4	1	1	0	7	5	18	7	4	3
Cg-lib123_irc117	72	5	3	2	5	4	4	0	1	4	6	2	0	5	14	8	10	5	4
Cg-lib123_c507	72	0	0	0	0	0	0	0	0	0	12	12	9	19	9	0	10	10	1
Cg-lib123_c607	103	2	0	3	6	3	6	1	3	2	4	0	0	6	3	0	9	7	5
Cg-lib123_c716	150	2	2	0	5	5	10	5	3	7	3	0	0	1	4	0	15	7	7
Cg-lib123_c4420	161	2	2	0	2	1	3	0	2	2	2	3	0	9	3	4	4	7	7
Cg-lib6_irc128	135	2	2	0	6	4	5	5	7	5	3	1	0	12	18	0	5	13	9
Cg-lib123_c1062	113	7	4	3	8	8	3	2	2	1	3	4	6	4	7	1	9	5	9

Tab. 10 – continued.

Sum of all MW [kDa]		Spectral counts for each protein																	
453112		Control samples									Drought stressed samples								
Protein ID	MW [kDa]	CT1	CT1	CT1	CT2	CT2	CT2	CT3	CT3	CT3	ST1	ST1	ST1	ST2	ST2	ST2	ST3	ST3	ST3
		R1	R2	R3	R1	R2	R3	R1	R2	R3	R1	R2	R3	R1	R2	R3	R1	R2	R3
Cg-lib123_c1234	151	1	0	0	6	10	3	4	5	1	0	0	3	9	3	0	9	7	4
Cg-lib6_c2408	55	0	2	0	2	9	3	0	0	0	1	0	0	3	3	4	0	3	3
Cg-lib6_lrc109	80	2	4	3	8	5	8	0	0	0	2	3	2	7	9	7	5	5	3
Cg-lib6_c2398	49	4	14	5	10	17	9	4	3	1	9	4	3	7	10	1	2	4	3
Cg-lib123_c1442	144	3	0	5	6	5	12	5	4	4	4	0	2	11	7	1	13	5	0
Cg-lib123_c4899	47	1	3	3	11	6	8	0	0	0	3	5	4	9	8	8	4	4	3
Cg-lib6_lrc166	183	3	0	0	2	1	4	4	3	2	1	0	1	7	4	7	10	4	3
Cg-lib6_c436	150	3	1	3	6	3	2	8	9	12	1	2	1	0	4	0	8	13	7
Cg-lib123_c2723	146	8	8	5	13	8	16	0	0	0	7	6	0	13	23	2	0	2	0
F05GI4S01D5CK7	40	4	5	5	9	3	7	3	1	3	4	5	4	7	8	13	3	3	3
Cg-lib6_c1376	171	2	3	3	12	1	7	0	0	0	2	2	5	7	5	10	2	2	4
Cg-lib123_lrc44	85	3	24	0	19	16	4	0	0	0	7	0	0	5	1	2	1	0	0
Cg-lib6_c1748	62	1	0	0	6	14	0	0	0	0	0	0	1	6	34	0	0	0	0
Cg-lib123_lrc80	151	2	0	1	5	7	8	3	9	6	2	0	0	10	6	0	9	10	5
Cg-lib123_lrc281	70	3	0	0	5	9	2	0	2	0	1	3	2	10	8	0	10	0	2
Cg-lib123_c330	120	3	5	4	0	0	1	5	5	3	4	4	3	3	1	0	6	8	3
Cg-lib6_c2285	115	5	0	0	5	0	0	3	1	2	0	0	5	4	0	0	14	19	24
Cg-lib6_c183	96	0	0	1	1	3	0	3	7	6	1	0	2	4	6	0	11	10	6
Cg-lib123_c559	63	0	0	4	7	10	4	0	0	0	2	0	1	0	17	0	3	15	5
Cg-lib123_c780	127	3	5	6	6	4	5	3	4	6	1	5	2	6	6	0	4	4	4
Cg-lib123_c2120	199	3	4	4	5	2	7	3	3	1	3	4	5	6	2	3	6	3	1
Cg-lib123_lrc182	82	6	6	18	8	7	5	0	0	0	9	7	1	9	8	1	1	1	3
Cg-lib123_c412	55	0	2	3	6	2	2	0	2	1	0	2	4	6	7	0	5	3	6
Cg-lib123_c1547	131	0	1	0	11	7	7	7	3	4	0	0	0	3	2	0	5	7	4
Cg-lib6_c239	90	4	3	4	14	14	6	2	0	0	3	2	3	19	4	0	1	0	0
Cg-lib123_lrc145	71	3	10	6	25	3	0	0	0	0	4	3	1	4	0	0	0	0	0
Cg-lib123_lrc89	53	4	2	4	3	5	4	0	2	1	2	1	0	5	4	0	6	7	5
Cg-lib123_c3068	98	0	1	2	7	5	10	2	1	2	2	0	0	5	5	3	2	2	2
Cg-lib123_c889	173	0	0	0	6	7	3	0	0	0	1	0	0	12	12	6	5	0	12
Cg-lib123_c6340	137	7	2	4	7	2	5	4	1	3	6	4	8	4	3	6	4	6	5
Cg-lib6_c1274	106	5	3	4	5	4	6	1	1	1	3	2	2	3	7	6	0	1	3
Cg-lib6_c4231	47	3	1	5	12	6	6	0	0	0	4	1	2	9	8	1	1	2	0
Cg-lib123_c843	74	0	12	0	18	3	2	0	0	0	6	1	1	3	0	0	0	1	0
Cg-lib123_c1546	153	1	3	3	3	4	7	2	0	0	4	1	1	11	18	0	3	0	0
Cg-lib123_c1429	145	3	4	4	5	3	5	0	2	3	3	3	4	4	5	3	1	2	2
Cg-lib123_c424	68	9	4	6	10	5	7	3	3	2	7	6	6	5	10	0	3	4	3
Cg-lib6_c445	193	0	0	0	1	4	0	3	0	1	0	1	0	7	3	13	1	0	0
Cg-lib123_c1332	124	5	4	3	7	12	6	2	0	0	2	3	4	6	6	8	2	1	0
Cg-lib123_c426	68	0	11	2	8	5	0	0	0	0	3	2	0	8	0	2	0	0	1
F05GI4S01ARRO2	36	3	1	1	2	1	7	0	1	2	1	3	4	2	3	4	1	2	1
Cg-lib123_c1589	165	1	0	1	11	7	5	7	2	4	0	0	1	1	7	0	3	2	4
Cg-lib123_c450	99	4	0	0	8	13	4	0	0	0	0	1	0	20	1	2	5	0	1
Cg-lib6_lrc81	129	0	3	0	5	9	0	2	0	1	3	0	3	24	14	0	0	0	0
Cg-lib6_c791	129	0	0	0	11	3	4	2	3	2	0	0	1	6	10	0	3	0	4
Cg-lib6_c371	83	0	13	1	2	2	2	0	0	2	3	0	1	1	4	0	6	6	7
Cg-lib123_c325	89	0	0	1	9	10	13	0	2	0	4	0	0	11	4	3	1	0	0
Cg-lib123_c2686	118	4	1	3	3	4	5	6	4	2	2	0	2	4	3	2	10	6	1
Cg-lib123_c8040	84	4	2	0	5	7	2	3	3	6	1	1	3	4	5	0	8	11	8
Cg-lib123_c7944	45	5	5	4	6	4	4	0	1	1	4	4	3	8	9	11	1	0	0
Cg-lib6_c766	206	0	3	0	0	0	5	1	0	2	0	4	1	4	3	7	5	1	2
Cg-lib6_c351	110	1	1	2	4	5	3	4	2	1	2	2	1	6	5	0	6	1	0
Cg-lib123_lrc333	130	3	2	2	5	6	9	1	0	0	4	2	2	9	2	0	4	0	1
F05GI4S01BJYOL	36	0	0	0	2	0	4	8	8	7	0	0	0	6	1	0	10	14	5
Cg-lib123_c1475	171	4	2	4	8	3	5	4	5	4	4	2	2	3	3	0	4	3	5
Cg-lib123_lrc362	156	8	8	8	4	5	3	0	1	2	7	4	2	4	3	0	2	1	0
Cg-lib123_lrc327	85	2	0	5	9	7	7	1	1	2	2	1	0	2	3	0	3	2	2
Cg-lib123_lrc185	129	2	9	0	11	3	1	0	0	0	7	0	0	5	1	5	1	0	0

Tab. 10 – continued.

Sum of all MW [kDa]		Spectral counts for each protein																	
223470		Control samples									Drought stressed samples								
Protein ID	MW [kDa]	CT1 R1	CT1 R2	CT1 R3	CT2 R1	CT2 R2	CT2 R3	CT3 R1	CT3 R2	CT3 R3	ST1 R1	ST1 R2	ST1 R3	ST2 R1	ST2 R2	ST2 R3	ST3 R1	ST3 R2	ST3 R3
Cg-lib6_c2120	40	5	5	4	9	6	6	1	1	3	4	3	3	6	2	0	0	0	0
Cg-lib123_c773	151	1	0	0	7	0	0	3	0	0	0	1	0	0	1	0	9	10	11
Cg-lib123_c1988	112	3	4	7	5	5	6	4	2	3	5	4	4	4	8	9	2	0	0
Cg-lib123_c477	258	0	0	5	2	9	3	0	0	0	4	0	1	1	5	0	3	0	1
Cg-lib123_c634	129	3	4	2	1	3	2	4	3	3	1	3	1	0	9	0	4	4	2
Cg-lib123_irc180	82	3	2	3	3	6	5	0	0	0	4	0	2	3	3	0	2	0	1
Cg-lib123_irc106	93	1	3	2	6	7	18	0	0	0	1	0	0	9	3	7	0	0	0
Cg-lib123_c807	110	0	2	3	9	10	6	2	1	2	3	3	0	5	10	0	2	2	2
Cg-lib123_c632	111	1	2	4	11	4	1	0	0	0	1	4	0	8	6	1	0	0	0
Cg-lib6_c1558	59	0	0	0	4	2	2	1	2	2	2	0	0	2	0	1	4	2	0
Cg-lib123_c764	148	0	0	0	2	0	1	3	2	0	0	0	0	2	0	6	6	5	5
Cg-lib123_c1097	154	0	0	0	2	0	1	2	2	6	0	0	1	4	1	0	6	11	10
Cg-lib123_c1219	226	1	0	2	3	1	4	0	0	0	1	0	1	0	4	0	0	0	1
Cg-lib123_c1209	107	0	1	0	5	7	11	0	1	0	0	1	1	2	16	1	3	1	1
Cg-lib123_c6185	40	1	4	5	3	4	6	3	2	0	1	8	1	4	4	0	1	0	0
Cg-lib123_irc134	90	3	0	1	5	4	3	2	2	0	1	2	0	7	5	0	3	4	1
F05GI4S01EK1B8	40	5	2	5	4	3	6	1	0	1	5	2	4	3	7	5	1	2	0
Cg-lib123_c320	99	1	0	1	11	2	2	1	1	3	2	5	0	5	3	0	1	2	1
Cg-lib123_c1484	154	1	0	0	4	6	0	2	3	0	0	0	1	2	2	0	9	3	4
Cg-lib123_c1425	158	0	4	2	11	8	5	0	0	0	1	7	1	6	4	4	0	1	0
Cg-lib123_c10979	63	3	3	4	4	2	3	1	0	1	4	3	4	3	4	5	1	0	0
Cg-lib123_c882	101	6	5	7	6	4	3	2	1	2	4	3	0	5	9	0	5	2	2
Cg-lib123_c3132	108	1	5	1	9	0	1	1	1	1	0	1	1	2	1	2	8	0	5
Cg-lib6_c1198	66	0	0	3	6	6	4	5	1	0	2	2	4	7	9	1	3	0	0
Cg-lib123_irc254	103	3	0	0	7	9	10	0	0	0	5	0	3	8	8	1	1	1	0
Cg-lib123_c337	149	0	0	1	10	1	0	3	2	2	0	0	0	0	4	0	4	3	4
Cg-lib123_c1639	111	0	6	0	2	8	6	0	0	0	3	0	0	17	4	5	3	3	3
Cg-lib123_irc8560	54	0	0	0	1	3	2	0	1	4	0	0	0	1	5	0	0	3	2
Cg-lib123_c2276	67	2	3	1	3	2	3	4	3	3	5	2	2	4	3	0	6	2	2
Cg-lib123_c754	139	0	0	0	4	0	2	6	7	3	0	1	0	3	1	0	6	6	2
Cg-lib6_c369	70	0	14	2	14	0	1	0	0	0	6	0	0	6	0	1	0	0	2
Cg-lib6_c743	102	4	2	3	3	6	5	4	6	1	2	0	1	3	5	0	5	2	0
Cg-lib123_c1482	138	1	0	0	2	5	2	5	5	2	2	0	0	0	0	0	6	5	4
Cg-lib6_c768	81	1	3	3	7	5	0	0	1	2	0	0	0	0	6	0	1	5	3
Cg-lib6_c4207	84	0	4	1	10	1	6	0	0	0	0	2	0	9	5	2	0	1	0
Cg-lib123_c952	53	1	0	0	0	2	1	0	1	0	0	1	1	5	0	1	3	1	4
Cg-lib123_irc221	63	0	0	1	7	4	4	0	1	1	0	1	0	1	2	1	0	4	5
Cg-lib6_c2994	62	3	2	3	7	7	10	0	0	0	5	4	2	9	7	6	0	0	0
Cg-lib123_c718	92	5	2	5	10	5	4	1	1	1	2	6	0	4	9	0	2	3	2
Cg-lib6_c292	194	0	0	1	2	0	3	3	2	3	1	3	0	5	2	4	4	6	4
Cg-lib123_c623	217	2	1	3	5	0	4	0	0	0	5	2	3	4	4	5	2	3	4
Cg-lib123_c1349	148	0	0	0	1	1	1	2	4	4	1	2	0	4	4	0	6	6	6
F05GI4S01A2NKP	40	0	1	3	0	3	4	0	1	0	1	0	2	5	5	6	5	5	4
Cg-lib123_c326	102	1	0	2	5	4	7	0	0	0	3	0	0	4	4	0	0	0	0
Cg-lib123_c3325	104	0	0	0	1	6	3	1	0	0	0	1	0	0	9	0	3	0	0
Cg-lib123_c9914	94	4	3	5	5	1	4	1	1	2	2	4	3	4	5	4	1	1	1
Cg-lib6_c1220	169	0	1	1	2	2	4	0	0	1	2	1	4	6	3	4	3	3	0
Cg-lib6_c1749	71	0	0	0	7	11	0	0	0	0	0	0	0	9	7	0	1	0	0
Cg-lib123_c360	91	1	0	0	5	5	4	0	1	1	2	1	1	7	8	0	0	0	0
Cg-lib123_c3496	131	2	4	0	16	0	3	1	0	0	2	3	0	10	7	3	0	0	0
Cg-lib123_c878	176	3	2	1	4	3	5	1	1	2	4	0	1	0	0	0	2	2	1
Cg-lib123_c1762	89	0	0	2	5	5	7	0	1	0	4	0	1	4	4	0	2	1	1
Cg-lib6_c6355	76	0	0	0	5	3	4	0	0	1	1	0	0	2	5	6	0	0	0
Cg-lib123_c8444	57	0	0	1	6	5	2	2	0	0	0	0	0	6	9	0	13	0	0
Cg-lib6_c241	130	1	1	0	3	4	2	4	3	2	1	1	1	2	6	1	5	4	5
Cg-lib6_c3083	161	3	2	2	3	0	3	0	0	0	3	3	2	4	4	7	0	2	1
Cg-lib123_c3037	203	1	5	2	4	4	4	3	3	2	2	4	4	6	3	0	3	4	0

Tab. 10 – continued.

Sum of all MW [kDa]		Spectral counts for each protein																	
108575		Control samples									Drought stressed samples								
Protein ID	MW [kDa]	CT1 R1	CT1 R2	CT1 R3	CT2 R1	CT2 R2	CT2 R3	CT3 R1	CT3 R2	CT3 R3	ST1 R1	ST1 R2	ST1 R3	ST2 R1	ST2 R2	ST2 R3	ST3 R1	ST3 R2	ST3 R3
Cg-lib123_irc371	86	2	0	1	1	5	2	0	1	1	1	1	0	4	11	0	4	0	3
Cg-lib6_c464	38	0	0	1	0	2	1	0	0	0	3	1	0	3	10	1	1	10	6
Cg-lib123_irc168	93	0	2	2	1	1	2	0	1	1	0	2	2	1	0	0	1	1	0
Cg-lib123_c2657	79	0	1	0	4	1	1	1	0	0	1	3	0	4	3	4	4	4	1
Cg-lib6_c5867	41	4	3	3	2	0	3	3	6	2	4	2	0	2	0	0	5	3	4
Cg-lib123_c1449	138	1	0	0	6	3	2	2	0	2	0	0	0	1	6	0	3	3	6
Cg-lib123_c567	88	3	0	0	5	1	2	1	1	0	3	3	0	4	2	0	0	1	3
Cg-lib6_c1422	181	0	0	0	5	0	3	2	1	0	0	1	0	10	4	3	1	2	3
Cg-lib123_c359	86	0	0	0	4	3	3	0	0	0	0	1	0	3	2	0	0	0	0
Cg-lib123_c2996	117	0	0	1	3	4	6	0	0	0	0	0	0	2	6	0	3	0	0
Cg-lib123_c947	124	1	0	1	0	0	1	2	0	2	1	0	0	4	0	0	4	7	6
Cg-lib123_c446	138	0	0	0	2	1	3	0	0	3	0	0	0	0	0	0	9	1	1
Cg-lib123_c1717	86	3	3	0	2	1	2	1	0	3	2	4	0	2	4	0	0	0	2
F05GI4S01D48F3	35	1	1	0	4	0	3	0	0	1	0	3	1	3	5	1	0	0	0
Cg-lib123_c3467	126	2	2	3	5	1	1	0	1	2	0	1	2	1	2	0	2	2	2
F05GI4S01ARHON	42	2	2	0	2	0	4	1	1	0	2	2	1	1	3	2	1	1	3
Cg-lib123_c1623	224	0	1	1	0	0	1	1	1	0	1	0	0	1	1	3	0	1	1
Cg-lib123_irc63	72	1	0	4	4	3	1	0	0	1	0	1	8	3	1	7	1	0	0
Cg-lib123_c5416	94	1	0	0	4	0	3	2	0	1	1	2	0	3	7	1	1	4	8
Cg-lib123_irc212	70	0	0	1	2	3	2	0	0	2	1	0	0	2	2	0	5	6	4
Cg-lib123_c1045	128	0	3	5	3	5	3	4	2	0	3	0	2	2	3	0	5	0	0
Cg-lib123_c1225	141	2	0	2	4	1	2	2	3	3	0	0	0	0	5	0	5	4	3
F05GI4S01DBIVM	18	1	2	1	5	0	4	0	0	0	3	2	1	6	5	10	0	2	1
Cg-lib123_c2309	142	0	1	2	2	2	0	2	0	0	0	0	1	1	2	0	0	0	0
Cg-lib123_c436	77	2	1	1	2	4	2	1	0	3	1	5	0	5	0	0	3	1	5
Cg-lib123_c1521	236	2	0	0	3	2	1	1	0	0	3	0	0	0	7	0	3	1	4
Cg-lib6_c2437	63	2	2	4	2	2	3	3	0	1	1	3	4	2	2	3	1	3	5
Cg-lib123_c2352	128	2	2	4	1	2	2	2	1	2	0	2	2	3	3	1	2	3	2
Cg-lib123_c2494	162	1	3	2	4	0	2	0	0	0	2	0	0	4	5	2	0	1	1
Cg-lib123_c6706	81	2	1	1	1	0	6	0	0	1	2	1	3	4	3	6	0	1	2
Cg-lib123_irc66	441	0	0	0	2	0	0	0	0	0	2	2	0	6	2	0	0	0	0
Cg-lib123_c1523	121	0	0	0	0	0	2	3	2	1	1	1	0	3	1	4	2	2	4
Cg-lib123_c397	67	1	2	2	6	0	3	0	1	0	0	0	0	0	0	0	4	9	4
Cg-lib123_c2688	107	0	4	2	2	1	1	3	2	3	4	4	1	1	1	1	0	0	2
Cg-lib123_c931	93	1	0	0	6	5	2	0	3	7	1	1	0	3	2	0	0	1	1
Cg-lib123_c747	125	0	0	0	3	0	5	3	2	2	0	0	1	4	3	0	2	10	0
Cg-lib123_c1676	110	1	4	1	6	1	6	0	0	0	1	3	2	7	6	12	0	0	0
Cg-lib6_c827	83	0	0	0	3	0	5	0	1	0	0	1	0	4	3	6	0	2	2
Cg-lib123_irc82	73	2	0	0	5	1	8	1	1	1	1	0	0	5	2	0	2	1	0
Cg-lib123_c850	129	0	0	0	5	3	3	4	3	1	0	0	1	6	4	0	0	2	3
F05GI4S01EQTP0	35	0	0	0	6	4	13	0	0	0	0	0	0	5	1	0	0	0	0
Cg-lib123_c886	194	0	0	0	13	13	4	0	0	0	0	0	0	13	0	0	0	0	0
Cg-lib123_c2252	135	2	3	2	1	0	1	2	0	0	1	1	3	3	4	4	6	2	2
Cg-lib123_irc297	86	0	1	3	4	3	4	2	1	1	1	1	0	6	10	0	2	0	0
Cg-lib6_irc160	97	2	0	0	2	2	0	4	3	3	2	1	0	3	1	0	4	7	4
Cg-lib123_c1637	148	0	0	0	1	7	0	0	0	1	1	0	1	2	6	0	2	0	2
Cg-lib6_irc194	66	0	0	0	2	0	0	0	0	0	0	0	0	15	11	3	1	0	1
Cg-lib123_c2870	246	0	0	0	1	1	1	0	0	0	1	0	1	1	4	3	3	2	1
Cg-lib123_c2563	112	2	2	0	4	8	4	1	0	0	3	2	2	6	6	0	1	0	1
Cg-lib123_c2071	116	0	0	0	2	2	2	0	1	1	0	0	0	7	3	0	4	3	3
Cg-lib123_c2551	92	2	1	1	1	0	2	1	0	2	3	2	3	2	2	2	1	1	1
Cg-lib123_c3208	61	2	0	2	4	6	4	0	1	0	1	0	2	6	3	0	1	0	0
Cg-lib123_c1597	132	0	4	2	5	5	4	3	3	0	3	0	1	3	3	0	2	0	0
F05GI4S01C9LOJ	41	0	0	0	5	1	3	2	1	5	0	0	0	2	0	2	5	2	
Cg-lib123_c678	115	0	0	0	3	1	0	4	0	0	0	1	0	2	9	2	3	1	0
Cg-lib123_c3955	102	0	0	0	5	0	1	0	0	0	0	1	0	3	2	6	2	0	1
Cg-lib123_c573	132	0	2	0	2	3	4	0	0	2	0	0	0	6	5	0	6	0	1

Tab. 10 – continued.

Protein ID	MW [kDa]	Spectral counts for each protein																	
		Control samples									Drought stressed samples								
		CT1 R1	CT1 R2	CT1 R3	CT2 R1	CT2 R2	CT2 R3	CT3 R1	CT3 R2	CT3 R3	ST1 R1	ST1 R2	ST1 R3	ST2 R1	ST2 R2	ST2 R3	ST3 R1	ST3 R2	ST3 R3
Cg-lib123_c321	64	0	0	0	0	1	0	0	0	0	0	0	0	0	2	10	0	0	2
Cg-lib123_c3250	85	0	0	0	7	9	6	0	0	0	0	0	5	7	0	0	0	0	
Cg-lib6_c627	63	1	0	0	5	6	0	1	0	0	0	1	0	3	0	0	0	1	1
Cg-lib123_c2445	222	0	1	1	3	1	2	0	0	0	0	0	1	0	2	2	0	0	0
Cg-lib6_c6097	67	0	2	0	4	1	4	0	0	0	0	2	1	5	6	3	0	0	0
Cg-lib123_c1078	97	0	1	1	5	0	0	1	1	1	0	3	0	0	0	4	2	3	
Cg-lib123_c564	91	0	0	0	3	0	2	0	0	0	0	1	1	3	5	5	0	1	0
Cg-lib123_irc248	142	0	3	0	1	1	2	1	0	0	2	0	0	0	0	3	0	0	
Cg-lib6_c401	59	0	0	1	5	3	3	0	1	0	2	0	0	2	5	1	0	0	0
Cg-lib123_c1969	209	1	0	0	3	2	2	3	1	1	1	2	0	1	1	1	1	0	0
Cg-lib123_c5793	76	1	0	1	0	0	2	0	1	0	1	1	2	2	1	2	3	2	0
Cg-lib6_c1444	106	2	0	1	1	7	0	1	2	1	1	0	1	1	2	0	2	4	7
Cg-lib6_c483	54	0	0	1	7	7	3	0	0	0	0	1	1	6	2	0	9	0	0
Cg-lib123_c1330	109	1	0	1	10	7	8	0	0	0	0	0	0	4	0	0	0	0	0
F05GI4S01CO5FL	36	0	0	0	0	0	0	0	0	0	0	0	0	3	8	12	2	1	1
Cg-lib123_c826	123	0	0	1	1	0	1	2	2	3	1	3	4	1	3	0	2	3	2
Cg-lib123_c7153	76	0	4	0	6	0	2	0	0	0	0	0	0	4	1	4	1	2	1
Cg-lib123_irc157	72	0	1	0	6	7	0	0	0	1	0	0	0	1	0	1	0	0	1
Cg-lib6_c275	79	0	0	0	3	2	2	0	0	0	1	0	0	4	4	0	0	0	1
Cg-lib123_irc43	61	0	0	0	10	3	0	1	0	0	1	0	0	5	5	0	0	0	0
Cg-lib6_c514	119	0	0	0	0	0	0	1	2	0	0	0	0	1	0	2	4	3	3
Cg-lib123_c1935	178	1	0	0	2	3	1	1	0	0	1	0	1	7	5	5	1	0	2
Cg-lib6_c772	66	0	0	0	2	0	3	0	0	0	0	0	0	5	0	0	0	0	0
Cg-lib123_c8286	51	1	0	0	3	0	2	0	0	0	2	1	0	2	2	1	2	4	3
Cg-lib6_c6153	76	0	0	0	1	0	0	3	2	2	0	0	0	0	0	0	7	2	3
Cg-lib123_c884	163	1	0	1	2	0	5	1	1	2	0	1	2	1	2	0	1	0	0
Cg-lib123_c2163	96	0	1	0	2	1	2	2	3	0	0	0	0	4	4	0	4	1	0
Cg-lib123_c1092	134	0	1	0	8	0	0	1	0	0	0	2	0	4	0	0	1	0	0
Cg-lib123_c2197	79	0	0	0	4	2	0	0	0	0	0	0	1	5	1	0	8	4	0
Cg-lib123_c1314	38	0	1	0	4	4	1	0	0	0	0	0	0	2	0	2	0	0	0
F05GI4S01CNP7T	39	0	1	0	5	1	1	0	0	0	0	2	0	3	3	0	2	0	0
F05GI4S01BVXMO	33	0	0	0	2	3	0	0	0	2	0	0	2	0	0	0	0	2	0
F05GI4S01A8U4A	39	0	0	0	0	0	0	0	1	0	1	0	0	3	2	4	4	2	3
Cg-lib6_c930	131	0	1	0	3	2	2	1	0	0	1	2	0	5	3	0	4	0	0
Cg-lib123_c2085	93	0	0	1	1	5	3	1	0	0	0	0	0	3	2	0	1	0	0
Cg-lib6_c904	158	0	0	1	0	0	1	1	1	2	0	0	0	2	4	0	2	1	1
Cg-lib123_c5771	56	2	3	2	2	0	1	0	0	0	0	1	0	1	0	0	1	0	0
Cg-lib123_c1355	105	0	0	0	2	3	1	0	0	2	0	0	0	1	2	0	1	1	6
Cg-lib123_c513	174	0	0	0	7	0	2	0	0	1	0	0	0	1	1	0	1	1	1
Cg-lib123_c1588	96	0	0	0	2	1	0	1	0	2	0	0	1	0	0	0	5	2	5
Cg-lib123_c1522	193	0	0	0	2	1	3	0	2	1	0	0	0	0	0	0	3	5	
F05GI4S01CJ5WF	41	0	0	0	6	9	2	0	0	0	0	0	2	4	6	0	1	0	0
Cg-lib123_c624	135	0	0	0	1	5	3	0	0	0	0	0	0	1	10	0	0	0	0
Cg-lib123_c372	131	0	0	0	1	0	1	0	0	1	0	0	0	1	0	0	5	1	0
Cg-lib123_c2823	88	1	0	0	4	1	1	2	0	0	1	2	2	4	0	4	3	1	0
Cg-lib6_c1648	108	2	0	0	0	0	0	2	1	2	0	0	0	1	0	0	3	2	2
F05GI4S01BDLNI	38	1	0	0	6	0	1	0	4	0	1	1	0	2	0	0	1	3	2
Cg-lib123_c1043	186	0	0	0	3	4	3	0	0	0	1	0	1	7	5	2	0	0	0
F05GI4S01CPCGF	27	0	0	1	3	0	1	1	0	0	1	2	1	2	5	4	0	1	2
Cg-lib123_c1440	132	0	1	0	0	0	0	2	0	0	1	2	2	0	3	0	0	0	1
Cg-lib123_c8224	46	1	0	0	1	3	0	0	0	0	0	0	0	4	2	0	0	1	1
Cg-lib6_c478	168	0	0	0	1	1	0	0	0	0	0	0	0	0	0	1	4	3	2
F05GI4S01CD4RX	31	1	0	0	3	0	0	0	0	0	0	0	0	4	0	0	1	0	0
Cg-lib123_c1699	200	0	0	1	3	1	0	0	0	3	0	0	0	2	2	0	0	0	2
F05GI4S01BEVE0	41	1	3	0	2	1	0	0	1	0	3	2	1	2	4	0	0	0	1
Cg-lib123_c7143	51	0	0	0	4	1	5	1	1	3	0	0	0	3	0	0	1	1	2
Cg-lib123_c9767	50	1	0	1	3	2	5	0	0	0	2	1	0	5	5	5	1	0	0

Tab. 10 – continued.

Sum of all MW [kDa]		Spectral counts for each protein																	
22805		Control samples									Drought stressed samples								
Protein ID	MW [kDa]	CT1 R1	CT1 R2	CT1 R3	CT2 R1	CT2 R2	CT2 R3	CT3 R1	CT3 R2	CT3 R3	ST1 R1	ST1 R2	ST1 R3	ST2 R1	ST2 R2	ST2 R3	ST3 R1	ST3 R2	ST3 R3
Cg-lib123_c5054	41	0	0	0	0	2	4	2	3	1	0	0	1	3	2	0	0	0	1
Cg-lib123_c1708	106	0	0	0	0	0	0	2	0	1	0	0	0	1	2	1	7	6	4
Cg-lib123_c2581	263	1	0	0	2	0	0	0	0	0	2	1	0	1	2	0	0	0	1
Cg-lib123_c602	110	0	0	1	0	1	0	2	0	0	0	0	0	4	0	1	0	1	1
Cg-lib6_c2170	49	0	0	0	2	0	0	4	1	0	0	0	0	3	0	10	0	0	0
Cg-lib6_c2898	93	0	1	1	1	0	1	0	0	1	0	0	1	1	1	0	2	1	0
Cg-lib123_c1579	75	1	0	0	0	4	1	0	1	0	0	1	1	1	0	0	0	1	0
Cg-lib6_c4338	47	2	1	0	4	1	2	0	0	0	2	1	1	8	3	1	0	0	0
F05GI4S01BFUA9	43	0	0	0	2	1	2	0	0	0	0	0	0	2	1	1	1	0	1
Cg-lib123_lrc86	140	0	0	0	3	0	0	0	0	0	0	0	0	5	0	1	0	1	1
Cg-lib6_c6383	65	1	0	1	0	1	2	1	1	2	1	0	1	0	2	0	1	1	2
Cg-lib6_c982	65	1	1	1	3	0	0	4	1	1	0	0	0	1	1	0	0	0	0
Cg-lib123_c2375	78	1	0	0	3	0	1	0	1	0	0	0	0	4	5	2	0	0	0
Cg-lib123_c887	119	0	0	0	0	0	0	2	1	0	0	0	0	2	3	0	1	2	2
Cg-lib6_c220	109	0	0	0	0	4	1	0	0	3	0	0	0	5	0	0	0	3	0
Cg-lib123_c357	84	0	0	0	2	4	0	0	0	0	0	4	0	0	1	0	0	0	0
Cg-lib123_c1060	158	0	0	0	0	0	0	1	4	5	0	0	0	0	0	4	2	3	3
Cg-lib123_c2967	67	0	0	0	0	2	2	0	0	2	0	0	2	1	0	1	1	2	2
Cg-lib123_c1058	152	0	0	1	2	3	1	0	1	0	0	0	0	1	0	0	1	0	1
Cg-lib123_c3750	123	1	0	0	3	1	1	0	0	0	1	0	0	2	2	3	0	0	0
Cg-lib123_c1569	129	0	0	0	5	4	0	2	0	1	0	0	0	7	0	0	0	1	1
Cg-lib123_c6261	38	0	0	1	1	0	2	0	0	0	0	0	0	2	0	4	1	1	1
Cg-lib123_c6922	39	4	0	0	0	1	1	0	2	1	0	0	0	1	1	0	3	1	2
Cg-lib123_c1823	126	0	0	0	5	4	0	0	0	1	0	0	0	5	1	0	3	1	1
Cg-lib123_c5923	59	0	0	3	5	3	5	0	0	0	0	1	0	2	0	0	0	0	0
Cg-lib123_c2418	106	0	0	0	3	1	1	1	0	1	1	5	6	1	3	0	0	0	0
Cg-lib123_lrc200	86	0	3	0	3	0	0	0	0	0	1	0	0	0	1	0	0	0	0
Cg-lib123_c1179	139	0	0	0	3	0	1	0	2	3	1	0	0	1	0	0	3	3	2
Cg-lib123_c1108	133	0	0	0	1	2	0	1	0	1	0	0	0	0	0	2	3	1	1
Cg-lib123_c5264	103	0	0	0	0	1	3	0	0	0	0	0	0	0	0	0	0	0	0
Cg-lib123_lrc208	96	0	0	0	0	1	0	0	0	0	0	0	1	2	3	2	0	1	0
Cg-lib123_c1017	127	1	0	0	4	2	0	1	2	0	0	1	0	2	2	1	0	0	1
Cg-lib6_c592	133	0	1	0	0	0	0	0	0	0	0	0	1	2	0	4	1	0	0
Cg-lib123_c1748	128	0	0	1	0	0	0	1	0	0	0	0	0	3	1	0	5	3	1
Cg-lib123_c3124	115	0	0	0	0	0	0	5	2	4	0	0	0	1	0	0	3	1	0
Cg-lib123_c2935	160	0	0	0	2	0	1	0	0	0	0	0	0	3	1	0	0	4	3
Cg-lib6_c659	58	0	0	0	7	3	0	0	0	0	0	0	0	5	0	0	0	0	0
Cg-lib123_c951	292	0	0	0	1	2	0	2	0	1	0	0	0	0	1	2	0	2	2
Cg-lib123_c865	109	0	1	0	0	1	0	0	0	1	0	0	0	2	2	0	3	0	2
Cg-lib123_c3685	42	1	0	0	3	2	3	0	0	1	2	2	1	0	0	0	3	1	2
Cg-lib6_c496	98	0	0	0	0	0	0	0	0	0	0	0	0	1	3	0	0	0	0
Cg-lib123_c2270	136	0	1	0	0	3	1	0	0	0	1	0	0	3	1	0	0	1	0
F05GI4S01C7AF1	14	1	1	1	0	0	0	1	2	0	0	0	0	1	1	0	0	2	1
Cg-lib123_c1581	153	0	0	0	3	1	0	1	0	0	1	0	0	1	1	0	2	1	0
Cg-lib123_c3591	52	0	1	0	3	0	1	0	0	0	0	1	0	2	2	1	3	1	2
Cg-lib123_c1098	157	0	0	0	0	2	0	1	0	2	0	0	0	1	0	0	0	1	1
Cg-lib6_c569	116	0	1	0	1	0	1	0	0	2	0	0	0	3	0	0	1	0	1
Cg-lib123_c1311	86	0	0	0	5	1	2	0	0	0	0	1	0	4	2	0	0	0	0
Cg-lib123_c1077	107	0	0	0	2	2	1	0	0	0	0	0	0	1	6	0	1	0	0
Cg-lib123_c516	94	0	1	1	1	0	0	1	1	0	2	1	0	0	2	0	1	0	1
Cg-lib123_c1166	217	0	0	0	2	0	0	1	2	1	0	0	0	2	0	1	0	0	2
Cg-lib123_c1210	90	2	3	0	1	4	1	0	0	0	2	0	2	0	1	0	0	0	0
Cg-lib123_c2165	48	0	0	0	0	0	1	0	0	0	0	0	2	0	1	0	0	1	2
Cg-lib123_c5274	63	0	1	2	3	0	3	0	0	0	0	0	0	1	0	0	0	0	0
Cg-lib6_c702	116	0	0	0	3	4	1	0	0	0	0	0	0	3	3	0	0	0	0
Cg-lib123_c565	128	0	0	0	2	1	2	0	0	0	0	0	0	3	5	0	0	0	0
Cg-lib123_c7735	69	0	1	1	0	2	0	1	2	1	0	0	1	2	2	0	2	1	1

Tab. 10 – continued.

Sum of all MW [kDa]		Spectral counts for each protein																	
8428		Control samples									Drought stressed samples								
Protein ID	MW [kDa]	CT1 R1	CT1 R2	CT1 R3	CT2 R1	CT2 R2	CT2 R3	CT3 R1	CT3 R2	CT3 R3	ST1 R1	ST1 R2	ST1 R3	ST2 R1	ST2 R2	ST2 R3	ST3 R1	ST3 R2	ST3 R3
Cg-lib123_c2721	91	0	0	0	2	3	2	0	0	0	0	0	2	0	2	0	0	0	0
F05GI4S01CQE0Z	36	0	0	0	2	0	2	0	0	0	0	0	2	0	3	0	0	0	0
Cg-lib123_c713	119	0	1	1	0	0	3	0	0	0	0	0	0	0	1	0	0	0	0
Cg-lib6_c327	97	0	0	0	0	7	1	0	0	0	0	0	0	0	1	0	0	0	0
Cg-lib6_c2683	78	0	0	0	5	5	4	0	0	0	0	0	2	2	0	1	0	0	0
Cg-lib123_c4288	62	0	0	0	0	0	1	0	0	0	1	0	0	3	0	0	1	3	0
Cg-lib123_c3765	49	0	0	0	3	2	1	1	0	0	0	1	1	1	0	1	1	0	0
Cg-lib123_c342	68	0	1	1	2	0	0	0	0	0	0	0	0	2	0	1	2	0	0
Cg-lib123_c1237	184	1	0	0	1	2	0	0	0	0	2	0	4	1	0	0	0	0	0
Cg-lib123_c832	177	0	0	0	0	0	0	0	0	0	0	0	0	0	0	2	0	2	0
Cg-lib123_c10122	62	0	0	0	6	0	1	0	0	0	1	0	0	0	0	0	0	0	0
Cg-lib123_c504	119	0	0	0	2	5	4	0	0	0	0	0	2	2	0	0	0	0	0
Cg-lib6_c3230	69	0	0	0	0	0	0	2	0	1	0	0	3	0	0	1	1	0	0
Cg-lib123_c661	127	0	1	0	0	0	2	1	0	0	0	0	0	1	2	1	2	0	0
F05GI4S01C7HW7	38	0	0	0	1	2	0	0	0	0	0	0	1	3	0	0	0	0	0
Cg-lib123_c5768	93	0	0	0	0	0	0	0	0	0	0	0	3	0	0	2	3	1	0
Cg-lib123_c1971	184	0	1	1	6	0	2	0	0	0	1	0	2	0	0	0	0	0	0
Cg-lib123_lrc223	64	0	0	0	0	0	0	0	0	0	0	0	1	4	1	0	0	0	0
Cg-lib123_c3660	115	0	0	0	1	0	1	0	0	0	0	0	1	0	3	0	0	0	0
Cg-lib123_lrc205	56	0	0	0	2	0	0	0	0	0	0	0	1	1	0	0	1	0	0
Cg-lib123_c1354	183	0	0	0	0	0	0	0	0	0	0	0	0	0	1	2	2	2	0
Cg-lib123_c323	87	0	0	0	0	3	2	0	0	0	0	0	3	1	0	0	0	0	0
Cg-lib6_c1385	178	1	0	0	0	1	0	1	2	1	0	0	0	0	0	1	3	1	0
Cg-lib123_c1325	161	0	0	0	1	3	2	0	1	0	0	0	0	0	1	0	0	0	0
Cg-lib123_c3633	178	0	0	0	0	0	0	1	0	0	0	0	1	0	0	3	3	2	0
Cg-lib123_c3195	93	0	0	1	4	0	0	0	0	0	2	0	3	0	0	0	1	0	0
Cg-lib123_lrc62	106	0	0	0	1	0	0	0	0	1	0	0	0	2	0	5	0	0	0
Cg-lib123_c905	77	0	0	0	4	3	1	0	0	0	0	0	5	0	0	1	0	0	0
F05GI4S01EFSNT	33	0	0	0	1	2	1	0	1	0	0	0	0	1	0	2	2	1	0
F05GI4S01DJRM9	36	0	0	0	2	0	1	0	0	0	0	0	3	2	0	0	2	0	0
Cg-lib123_c534	147	0	0	0	0	0	0	0	0	1	0	0	0	0	0	2	1	1	0
Cg-lib6_c4184	106	0	3	0	3	0	0	0	1	0	0	0	0	0	0	1	0	0	0
Cg-lib123_c479	87	0	0	0	1	3	1	0	0	0	0	0	1	3	0	0	0	0	0
Cg-lib6_c4267	63	1	0	0	1	0	0	0	0	1	0	0	0	0	1	0	2	1	0
Cg-lib123_c2329	245	0	0	0	0	3	1	0	0	0	0	0	1	0	1	2	0	0	0
Cg-lib123_lrc224	72	0	0	1	1	2	0	0	0	0	0	0	2	4	0	1	0	0	0
Cg-lib123_c2406	74	0	0	0	1	0	2	1	0	0	0	0	0	0	0	0	0	0	0
F05GI4S01AM2V4	34	0	0	0	1	0	0	0	0	0	0	0	1	2	0	1	1	2	0
Cg-lib123_c5508	106	0	0	0	2	1	0	1	0	0	0	0	2	0	0	0	0	0	0
Cg-lib6_c366	204	0	0	1	0	0	2	0	0	0	0	0	1	0	0	0	0	0	0
Cg-lib123_c1472	152	1	0	0	1	3	0	0	0	0	0	0	2	2	0	0	0	0	0
Cg-lib6_c3098	70	0	0	0	3	1	0	0	0	0	0	1	0	0	0	0	0	2	0
Cg-lib6_c562	121	0	0	0	0	0	0	0	0	0	0	0	0	0	0	4	1	2	0
Cg-lib123_c11086	63	0	0	0	3	0	0	0	0	0	0	0	0	0	0	0	0	0	0
Cg-lib6_c589	68	0	0	0	0	5	0	0	0	0	0	0	2	0	0	0	0	0	0
Cg-lib6_c1345	115	0	0	0	2	0	1	0	0	0	0	0	1	1	2	0	1	0	0
Cg-lib123_c1645	85	0	0	0	3	0	1	0	0	0	0	1	0	0	1	0	0	0	0
Cg-lib6_c1406	187	0	0	0	1	2	0	0	0	0	0	0	2	0	0	1	0	0	0
Cg-lib123_c1143	161	0	0	0	1	8	1	0	0	0	0	0	0	1	0	0	0	0	0
Cg-lib123_c3567	84	0	1	0	0	0	0	0	0	0	0	2	0	0	0	2	2	3	0
Cg-lib123_c2652	110	0	1	0	1	0	0	2	0	0	0	0	3	0	0	0	0	0	0
Cg-lib123_c2195	218	0	0	0	2	1	0	0	0	0	0	0	0	1	0	0	0	0	0
F05GI4S01ET7HY	40	0	0	0	2	0	0	0	0	0	0	0	0	0	0	0	1	0	0
Cg-lib123_c5814	145	1	0	0	2	0	0	0	0	0	1	0	1	0	0	0	0	0	0
Cg-lib123_c1373	82	0	0	0	3	1	0	0	0	0	0	0	3	1	0	0	0	0	0
Cg-lib123_c717	65	0	0	0	0	0	0	0	0	0	0	0	0	4	0	0	0	0	0
Cg-lib123_c10320	54	0	0	0	1	0	0	0	0	1	0	0	0	0	2	1	1	2	0

Tab. 10 – continued.

Sum of all MW [kDa]		Spectral counts for each protein																	
1225		Control samples									Drought stressed samples								
Protein ID	MW [kDa]	CT1 R1	CT1 R2	CT1 R3	CT2 R1	CT2 R2	CT2 R3	CT3 R1	CT3 R2	CT3 R3	ST1 R1	ST1 R2	ST1 R3	ST2 R1	ST2 R2	ST2 R3	ST3 R1	ST3 R2	ST3 R3
Cg-lib123_lrc108	73	0	0	0	0	1	0	0	0	0	0	4	0	0	0	0	1	0	0
Cg-lib6_lrc148	225	0	0	0	0	0	0	0	0	0	0	0	0	1	0	0	1	0	2
F05GI4S01AQ271	37	0	1	0	1	0	0	0	0	0	0	0	0	2	0	0	1	0	0
Cg-lib6_c2334	47	0	0	0	0	0	0	0	0	0	0	0	0	2	0	0	0	0	0
Cg-lib6_c1359	124	0	0	0	0	0	0	0	0	0	0	0	0	2	0	0	1	0	0
Cg-lib123_c11145	60	0	0	0	0	0	0	0	0	0	0	0	0	0	0	0	4	0	0
F05GI4S01DDNCI	34	0	0	1	0	0	0	0	0	0	0	0	0	1	0	1	2	0	1
F05GI4S01C00Q6	38	0	0	0	2	1	1	0	0	0	0	0	0	1	0	0	0	0	0
Cg-lib123_c2977	216	0	0	0	1	0	0	0	0	0	0	0	0	0	0	0	3	0	0
Cg-lib6_c1282	128	0	0	0	2	0	0	0	0	0	0	0	0	0	0	0	0	0	0
Cg-lib6_c2498	72	0	0	0	0	0	1	0	0	0	0	0	0	3	0	0	0	0	0
Cg-lib123_c1228	112	0	0	0	0	0	0	0	0	0	0	0	0	0	0	0	2	0	0
Cg-lib123_c4414	59	0	0	0	0	0	0	2	0	0	0	0	0	0	0	0	0	0	0

Lebenslauf Dipl. Biol. René Kerner

geboren am 27.12.1978
in Caracas, Venezuela
Staatsangehörigkeit: Deutsch



Ausbildung

- 08.2007 – heute* **Doktorarbeit**, TU-München und Helmholtz Zentrum München
- 10.1999 – 08.2006* **Studium der Biologie**, TU-München
- 02.1998 – 07.1999* **Deutsches Fachabitur**, Studienkolleg, München
- 10.1986 – 07.1996* **Venezolanische Schule** (Abiturabschluss), Colegio San José / Maracay, Venezuela

Labortechniken

Proteinextraktion, -aufreinigung, -trennung und -quantifizierung, amplified fragment length polymorphism (AFLP), RNA-microarrays, Real-Time-PCR, Hochleistungsflüssigkeitschromatographie (HPLC), Elektronenmikroskopie.

Auszeichnungen

- 05.2009* Stipendierte Posterpräsentation für die Tagung: “Plant Abiotic Stress. From signaling to development”, Tartu, Estland

Fortbildungen

- 03.2009 Arbeitstagung „**Protein Analysis of Tissues**“, Helmholtz Zentrum München
- 05.2009 Fortbildung zur „**Fachkraft für Molekulare Medizin**“, Gläsernes Labor, Campus Berlin-Buch, Berlin
- 06.2007 – 08.2007 **Microarray** Praktikum, Helmholtz Zentrum München
- 03.2004 – 09.2004 Fortbildung zum **Forschungstaucher**, TU-München

Publikationen

Abril N, Gion J-M, **Kerner R**, Müller-Starck G, Cerrillo RMN, Plomion C, Renaut J, Valledor L and Jorrin-Novo JV (2011). Proteomics research on forest trees, the most recalcitrant and orphan plant species. *Phytochemistry* 72(10): 1219-1242

Kerner R, Winkler J, Dupuy J, Jürgensen M, Lindermayr C, Ernst D and Müller-Starck G (2011). Changes in the proteome of juvenile European beech following three years exposure to free-air elevated ozone. *iForest - Biogeosciences and Forestry* 4(1): 69-76

Vorträge und Posterpräsentationen

- 05.2011 **Vortrag:** Reaktionen freistehender juveniler Buchen nach dreijähriger Ozonbegasung: eine integrative Studie. 1. Jahrestagung der Sektion „Forstgenetik/Forstpflanzenzüchtung“, Teisendorf, Deutschland
09. 2010 **Vortrag:** Genetische Reaktionen und Proteinexpression unter Einwirkung von troposphärischem Ozon auf Jungpflanzen der Buche (*Fagus sylvatica* L.). Forstwissenschaftliche Tagung, Göttingen, Deutschland
- 03.2010 **Vortrag:** Long-term impact of ozone on transcript and protein expression profiles of European beech saplings (*Fagus sylvatica* L.), SFB 607 Symposium, Freising, Deutschland
- 03.2010 **Vortrag:** Responses of juvenile European beech (*Fagus sylvatica* L.) to long-term ozone exposure: Linking transcriptomic and proteomic data. IUFRO-conference". Adaptation of forest ecosystems to air pollution and climate change", Antalya, Türkei
- 09.2009 **Posterpräsentation:** Long-term impact of ozone on transcriptom and proteom of European beech saplings (*Fagus sylvatica* L.). Jahrestagung der Gesellschaft für Ökologie, Bayreuth, Deutschland